CO-ORDINATED REGULATION OF AUTOPHAGY BY MTORC1 AND PROTEIN PHOSPHATASE 2A

A Dissertation

Presented to the Faculty of the Weill Cornell Graduate School

of Medical Sciences

in Partial Fulfillment of the Requirements for the Degree of

Doctor of Philosophy

by

Pui-Mun Wong

August 2015

CO-ORDINATED REGULATION OF AUTOPHAGY BY MTORC1 AND PROTEIN PHOSPHATASE 2A

Pui-Mun Wong, Ph.D.

Cornell University 2015

Autophagy is a cellular catabolic process critical for cell viability and homeostasis. As a membrane trafficking pathway, it is closely related to endocytosis and shares many points of convergence with endocytosis. In the first part of this dissertation, I find that although the two pathways are closely related, autophagosome fusion with lysosomes is governed by a distinct molecular mechanism from endosomal fusion with lysosomes.

In recent years, the discovery of autophagy-essential-genes has accelerated research into the molecular mechanisms governing autophagy. For example, inhibition of mammalian target of rapamycin (mTOR) complex-1 (mTORC1) activates autophagy by relieving its inhibitory effects on autophagy essential gene, ULK1- a mTORC1 substrate whose dephosphorylation is required for autophagy induction.

Puzzlingly, I observe that amino acid starvation triggers more rapid autophagy than pharmacological inhibition of mTORC1, although they both block mTORC1 activity with similar kinetics. Here I find that in addition to mTORC1 inactivation, starvation also causes a stimulation in phosphatase activity toward ULK1. In the second part of this dissertation, I identify the starvation-stimulated phosphatase for ULK1 as the

PP2A-B55α complex and attempt to elucidate the mechanism of phosphatase stimulation during starvation.

I find that treatment of cells with starvation but not mTORC1 inhibitors triggers dissociation of PP2A from its inhibitor Alpha4. Furthermore, pancreatic ductal adenocarcinoma cells (PDACs), whose growth depends on high basal autophagy, possess stronger basal phosphatase activity toward ULK1 and require ULK1 for sustained anchorage-independent growth. Taken together, these results suggest that concurrent mTORC1 inactivation and PP2A-B55α stimulation fuel ULK1-dependent autophagy.

BIOBRAPHICAL SKETCH

Pui-Mun Wong was born in Singapore, Singapore. She attended Hwa Chong Junior College and subsequently enrolled in the National University of Singapore (NUS) where she majored in Life Sciences. During her stay at NUS, she joined the Special Program in Science where her interest for scientific research was ignited attending seminars and discussions with like-minded individuals and mentors from various fields. As an initial foray into the scientific method, she joined the Molecular Genetics Laboratory under Dr. Chan Woon Khiong where she developed a passion for cell and molecular biology studying the plasticity of human embryonic stem cells (hESCs) at a transcriptomic level. In her final year at NUS, she focused on the characterization of natural antisense transcription in hESCs as part of her honors year thesis, and subsequently stayed an additional year in Dr Chan's laboratory as a research assistant. In 2008, Pui-Mun enrolled in the graduate program in Biochemistry, Cellular and Molecular Biology at the Weill Cornell Graduate School of Medical Sciences. A year later, she joined the laboratory of Dr. Xuejun Jiang at Memorial Sloan Kettering Cancer Centre, where she performed her pre-doctorial work investigating the regulation of the ULK1 complex in autophagy.

I dedicate this dissertation to my husband, my family and friends for their unwavering support over the years.

ACKNOWLEDGMENTS

I would like thank my thesis advisor, Dr. Xuejun Jiang for his guidance and mentorship over the years. I would also like to thank all members of the Jiang lab both past and present, especially Dr. Ian Ganley, Dr. Noor Gammoh, Dr. Taya Feldman, Dr. Yuji Shi, Dr. Du Lam, Dr. Junru Wang, Dr. Yan Feng, Dr. Minghui Gao, Dr. Rui Zhang and my fellow graduate students Cindy Puente, Prashant Monian and Helen Kang. I am grateful to have been in the company of these amazing individuals who have greatly enriched my graduate school experience both on a personal and professional level.

I would like to thank Dr. Ronald Hendrikson and Dr. Hediye Bromage from the Proteomics and microchemistry core facility at Memorial Sloan Kettering Cancer Center (MSKCC) for their help with the mass spec analysis in this project. I would also like to thank our other collaborators over the years, who have expanded the breadth and depth of my postgraduate education by selflessly sharing their time, knowledge and skills. Nina Lampen from the Electron Microscopy facility at MSKCC, Dr. Nancy Du and members of her laboratory at Weill Cornell, Dr. Fraser Glickman and Jeanne Chiaravalli-Giganti from the High Throughput and Spectroscopy Resource Center at Rockefeller University.

I would like to express my gratitude to the members of my thesis committee: Dr. Michael Overholtzer and Dr Filippo Giancotti for their encouragement and insightful comments throughout the progression of my project. I also extend my thanks to Dr. John Blenis for taking time off his busy schedule to Chair my defense.

Lastly, I would like to express my heartfelt thanks to my family for their love and encouragement, and especially to my loving, patient and supportive husband Jiamin, who has been with me every step of the way.

TABLE OF CONTENTS

LIST OF FIGURES

Chapter 1.

Chapter 2.

Chapter 3.

Chapter 4.

Chapter 5.

CHAPTER 1. INTRODUCTION

1.1 Autophagy: A lysosomal degradative pathway

Autophagy is a conserved catabolic process that utilizes lysosomal activity to turnover cellular proteins and organelles. Mammalian cells can undergo three types of autophagy: macroautophagy, microautophagy and chaperone-mediated autophagy. These modes of autophagy differ in the type of cargo to be degraded and the methods of delivering them to lysosomes. Chaperone-mediated autophagy makes use of a protein translocation pathway that selectively feeds individual substrate proteins directly into the lysosome. Microautophagy occurs through direct sequestration of cargo involving the formation of tubular invaginations at the lysosomal membrane. Macroautophagy delivers cargo to the lysosomes through the formation and transport of specific intracellular membrane vesicles termed autophagosomes (Chen and Klionsky, 2011; Mizushima and Komatsu, 2011; Todde et al., 2009).

Of the three types of autophagy, macroautophagy is thought to occur predominantly and is the most well-studied (Mizushima and Komatsu, 2011). The process of macroautophagy, herein referred to as autophagy, starts with the formation of a cup-shaped membrane structure, termed the phagophore or isolation membrane. The phagophore elongates, sequesters cytosolic components (cargo), and eventually seals to form a double-membraned vesicle called the autophagosome. Cargo loading into autophagosomes may be selective for specific proteins, organelles or pathogens through the use of adaptors such as Atg32 (Kanki et al., 2009) in yeast, and SQSTM1/p62 (Pankiv et al., 2007), NBR1 (Kirkin et al., 2009), and NCOA4 (Mancias et al., 2014) in mammalian cells, or non-specifically through bulk loading of cytoplasmic contents (Mizushima et al., 2011). Autophagosomes fuse with lysosomes,

resulting in cargo degradation and concomitant release of the metabolic byproducts such as amino acids and other molecules through permeases in the lysosomal membrane. As a membrane trafficking pathway, autophagy shares several points of convergence with endocytosis, although these converging points, such as lysosomal fusion, can be differentially regulated in autophagy and endocytosis (Ganley et al., 2011). The turnover of long-lived, aggregated or damaged proteins and organelles by autophagy is essential for maintaining cellular homeostasis. While autophagy occurs at basal levels under normal conditions, it is activated in response to cellular stresses such as nutrient starvation, hypoxia, growth factor withdrawal, ER stress and pathogen infection. Upon these stresses, the cell employs autophagy either to re-deploy its resources to tide over the period of stress or to degrade harmful components (such as damaged mitochondria or invading pathogens) via lysosomal degradation (Kroemer et al., 2010). Dysregulation of autophagy has been implicated in a range of diseases including neurodegenerative disorders most typically involving the accumulation of pathogenic proteins, inflammatory disorders such as Crohn's Disease, and cancer (Kimmelman, 2011; Wong et al., 2011).

Molecular players in the autophagy pathway

The study of autophagy has accelerated in the last decade because of the discovery of autophagy related (Atg) genes by yeast genetics (Harding et al., 1995; Thumm et al., 1994; Tsukada and Ohsumi, 1993) and subsequently, their mammalian homologues (Mizushima et al., 2011; Yang and Klionsky, 2010a). Up to 36 Atg genes have been identified through genetic screens, and the Atg genes making up the core machinery of autophagy can be classified into several functional units: the Atg1/ULK1 complex, commonly considered as an initiator in the autophagic cascade, the VPS34 phosphatidylinositol 3-kinase (PI3K) complex, two ubiquitin-like conjugation systems

(Atg5-12, Atg8/LC3-PE), PI3P effector Atg2-Atg18 complex and the transmembrane protein Atg9. Our laboratory focuses on the Atg1/ULK1 initiator complex, because of its important role as a bridge between nutrient sensing and induction of an autophagic response both in yeast and mammalian cells.

1.2 ULK1: an autophagy essential gene

In yeast, Atg1 was originally identified from genetic screens. Through these studies, multiple complementation groups affecting both autophagosome accumulation (Thumm et al., 1994; Tsukada and Ohsumi, 1993) and cytoplasm-to-vacuole targeting (Cvt) (Harding et al., 1995) were found. Atg1 mutants failed to accumulate autophagic bodies in the presence of the protease inhibitor PMSF and died at a faster rate during nutrient starvation, linking autophagy and Atg1 with cellular metabolism (Tsukada and Ohsumi, 1993). Atg1 is a serine-threonine Kinase and the only protein kinase among the 36 Atg genes described so far.

Atg1 shares strong homology with *C. elegans* uncoordinated-51 (UNC-51) (Matsuura et al., 1997), which has two mammalian homologs known as Unc-51 like kinase-1 (ULK1) and ULK2 (Figure 1.1) (Kuroyanagi et al., 1998; Yan et al., 1999). ULK1 was independently identified as an essential component for starvation-induced autophagy in an RNAi-based screen by Tooze and colleagues to identify protein kinases involved in mammalian autophagy (Chan et al., 2007). Subsequent mechanistic analysis confirmed that ULK1 is indeed the functional equivalent of yeast Atg1 (Young et al., 2006), and functions in a complex containing ATG13, FIP200 and ATG101 to mediate signaling from mTORC1 (Ganley et al., 2009; Hara et al., 2008; Hosokawa et al., 2009; Jung et al., 2009).

ULK1 and ULK2 are very similar in sequence (55% overall sequence identity), and have redundant roles in autophagy (Lee and Tournier, 2011; Yan et al., 1999). This is best supported by genetic studies in mice. Right after birth, neonate mice face a brief period of severe starvation during which autophagy is essential for survival. While *Ulk1* and *Ulk2* double knockout mice display the same perinatal-lethal phenotype as mice lacking core autophagy genes such as *Atg5* or *Atg7* (Cheong et al., 2011; Komatsu et al., 2005; Kuma et al., 2004), *Ulk1*$^{-/-}$ mice have a relatively mild phenotype of delayed reticulocyte maturation (Kundu et al., 2008), indicating that *Ulk2* can at least partially compensate for the loss of *Ulk1*. Mechanistically, both ULK1 and ULK2 have been shown to be recruited to isolation membranes upon autophagy induction, both are able to bind to the regulatory proteins ATG13 and FIP200 (Figure 1.2), and both their kinase-dead mutants have dominant negative properties (blocks autophagy) when overexpressed in cells (Chan et al., 2009; Hara et al., 2008; Jung et al., 2009).

In addition to the N-terminal kinase domains, ULK1 and ULK2 share significant homology in their C terminal regions (Figure 1.1), suggesting that it may have a role in autophagy. Domain studies of ULK1 have shown that its C terminal domain (CTD) is required both for interaction with ATG13 and FIP200 and for translocation of ULK1 to isolation membranes (Chan et al., 2007; Chan et al., 2009; Hara et al., 2008). Mammals have three additional protein kinases that are homologous to the kinase domains of ULK1 and ULK2. They are ULK3, ULK4 and STK36 (also known as "fused") (Figure 1.1). These additional ULKs do not have the conserved C terminal sequence and are not thought to be involved in starvation-induced autophagy. It is however, possible that they may play a role in other forms of autophagy. In support of this, ULK3 was linked to autophagy induction during senescence (Young et al., 2009).

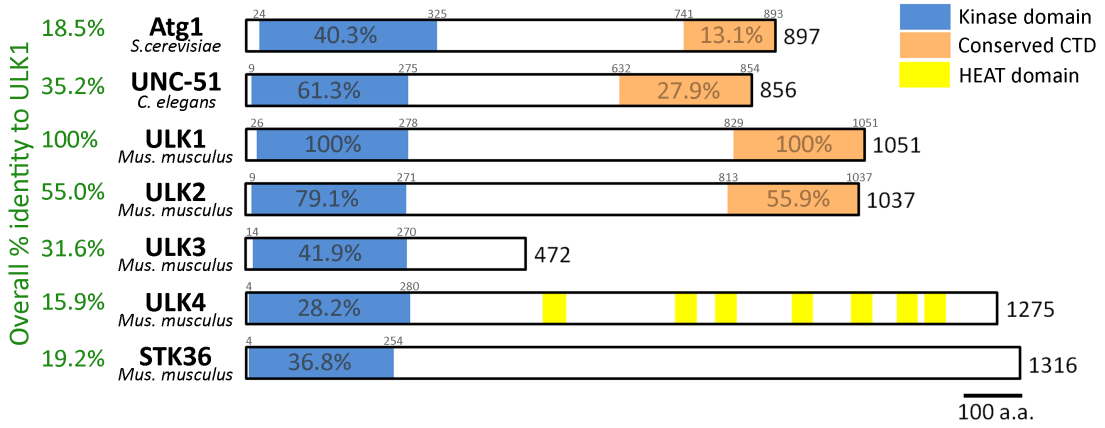

Figure 1.1 Schematic representations of Atg1 and its homologous proteins in different organisms. A representation of Atg1 (yeast), UNC-51 (*C. elegans*) and the ULK family (mice) is shown. High sequence similarity is observed mainly in the kinase domains. Significant similarity is also seen in the C-terminal of Atg1, UNC-51, ULK1 and ULK2, defining a C-terminal domain (CTD) of 150-250 amino acids. The overall sequence identity to mouse ULK1 as calculated by ClustalW is shown on the left.

1.3 The ULK1 complex: integrating signals from nutrient sensors

Previous work in both yeast and mammalian systems suggest that the ULK1 complex senses upstream signals, particularly the nutrient and energy signals, mainly via changes in its phosphorylation status. Both ULK1 and ATG13 are hyper-phosphorylated in nutrient-rich conditions and undergo global dephosphorylation upon starvation. At least 30 phosphorylation sites have been detected by mass spectometry on ULK1, although the majority of the responsible kinases and the functions of these phosphorylation events remain to be identified (Mack et al., 2012).

As a major nutrient/energy sensor, mTOR has been reported to directly phosphorylate ULK1 and ATG13. The mTOR complex 1 (mTORC1), consisting of mTOR, Raptor and mLST8, is responsive to growth factors and amino acid levels and has been shown

to phosphorylate both ULK1 and ATG13 (Ganley et al., 2009; Hosokawa et al., 2009; Jung et al., 2009). The mTORC1 complex binds to ULK1 directly through Raptor under nutrient-rich conditions and dissociates from the ULK1 complex upon starvation (Hosokawa et al., 2009; Lee et al., 2010). mTORC1-driven ULK1 phosphorylation correlates with autophagy inhibition and weaker ULK1 kinase activity (Ganley et al., 2009; Hosokawa et al., 2009; Jung et al., 2009). It is unclear if mTORC1 exerts its inhibitory effects simply by affecting the kinase activity of ULK1. Alternatively, mTORC1 phosphorylation events may influence the localization of the ULK1 complex and exert its inhibitory effects by sequestering or physically separating the ULK1 complex from its enzymatic substrates.

It has been known for some time that another important cellular energy sensor, AMPK, can play a role in autophagy induction by phosphorylating TSC2 and Raptor to inactivate mTORC1, hence indirectly activating the ULK1 complex. Recently, AMPK has also been shown to directly interact with and phosphorylate ULK1 in a nutrient-dependent manner (Egan et al., 2011; Kim et al., 2011; Lee et al., 2010; Shang et al., 2011) (Figure 1.2). Phosphorylation sites on ULK1 have been mapped by several groups and in some cases attributed to either mTORC1 or AMPK, but with very few overlapping sites between the groups (Dorsey et al., 2009; Egan et al., 2011; Kim et al., 2011; Shang et al., 2011). Among the phosphorylation sites reported, Ser555, Ser637 and Ser757 were reported by three or more independent groups (Figure 1.2). AMPK phosphorylation site Ser555 is thought to recruit phospho-binding protein 14-3-3 to the ULK1 complex (Egan et al., 2011; Lee et al., 2010; Mack et al., 2012). mTORC1 site Ser757 is required for AMPK binding as its mutation disrupts ULK1-AMPK interaction (Kim et al., 2011; Shang et al., 2011). The effect of AMPK phosphorylation on the ULK1 complex and autophagy are not well established, with

conflicting reports on whether it leads to stimulation or inhibition of autophagy. The study by Guan and colleagues (Kim et al., 2011) suggests that phosphorylation of AMPK sites on ULK1 are stimulated by glucose starvation, and contribute to ULK1 activation. In this case, ULK1 kinase activity (measured by ULK1 autophosphorylation) increased upon glucose starvation and was correlated with AMPK activation. However, the study by Shang et al. (Shang et al., 2011) identified AMPK sites that were dephosphorylated upon amino acid starvation; phospho-mutants defective in AMPK binding exhibited faster protein degradation upon autophagy stimulation, leading them to the conclude that AMPK phospho-sites are inhibitory to autophagy induction. The differences in their observations might reflect the distinct autophagy role of AMPK when sensing different triggers (i.e., glucose starvation versus amino acid starvation); they could also be due to the monitoring of different phosphorylation sites in these two studies. In yet another study by Shaw and colleagues, AMPK regulation of ULK1 was linked to mitophagy (Egan et al., 2011). This study identified four ULK1 sites that were phosphorylated upon treatment with the AMPK activators metformin and phenformin. AMPKα-null (*Ampkα1*$^{-/-}$ *Ampkα2*$^{-/-}$) primary mouse hepatocytes accumulated aberrant mitochondria, suggesting a mitophagy defect. ULK1 with compound phospho-deficient mutations at these AMPK sites could not reconstitute starvation-induced p62 degradation in *Ulk1*$^{-/-}$ mouse embryonic fibroblasts (MEFs), suggesting that the AMPK phosphorylation on ULK1 was required for ULK1 function in autophagy. However, the fact that AMPKα-null MEFs can still undergo autophagy, rules out an essential autophagic role for this kinase, at least in response to amino acid starvation (Kim et al., 2011; Mack et al., 2012). It is possible that AMPK fine-tunes ULK1 activity and the subsequent autophagy outcome in response to various energy requirements.

A

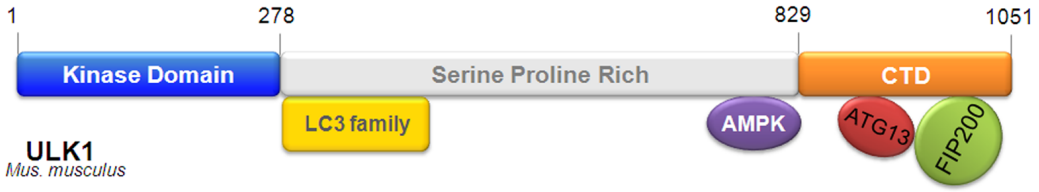

B

Residue	Modification	Reference
K162	Ac	Lin *et al.* (2012)
S317	P	Kim *et al.* (2011)
S467	P	Egan *et al.* (2011)
S555	P	Mack *et al.* (2012), Shang *et al.* (2011), Egan *et al.* (2011)
T574	P	Egan *et al.* (2011)
K606	Ac	Lin *et al.* (2012)
S637	P	Mack *et al.* (2012), Shang *et al.* (2011), Egan *et al.* (2011)
T659	P	Mack *et al.* (2012)
S757	P	Kim *et al.* (2011), Shang *et al.* (2011), Egan *et al.* (2011)
S777	P	Kim *et al.* (2011), Egan *et al.* (2011)

Figure 1.2 Domain structure and posttranslational modifications on ULK1. (**A**) ULK1 contains a kinase domain, a serine/proline rich region and a C-terminal domain (CTD). Many posttranslational modification events occur within the Serine/Proline rich region. The CTD ends with a three residue PDZ binding motif that may be involved in membrane targeting. The mapped interaction sites with ATG13, FIP200, AMPK and members of the LC3 family are indicated. The site of interaction with mTORC1 complex member RPTOR is unresolved as its interaction with the kinase domain and the Serine/Proline rich domain has been reported. (**B**) Posttranslationally modified residues on ULK1. For brevity, only experimentally verified events are listed in the table. References that have reported these modifications are listed as well.

In addition to phosphorylation, other post-translational modifications have been reported to regulate ULK1 and autophagy (Deribe et al., 2010; McEwan and Dikic, 2011). Acetylation involves the transfer of acetyl groups from acetyl-CoA to the lysine residue of the target protein. Acetyl transferase TIP60 (HIV-1 TAT-interactive protein) was found to interact with ULK1 in a serum-dependent manner and could acetylate ULK1 directly in an *in vitro* reaction. Knockdown of TIP60 impaired starvation induced autophagy and acetylation mutants of ULK1 could not rescue LC3 conversion in *Ulk1*$^{-/-}$ MEFs (Lin et al., 2012). The activity of TIP60 is regulated by GSK3B (glycogen synthase kinase 3 β), which responds to serum starvation through

the PI3K-AKT-mTOR pathway. Hence GSK3-TIP60 stimulates autophagy in response to growth factor deprivation at least in part by mediating the acetylation of ULK1. A genetic study on the histone acetyl transferase complexes in yeast also identified Esa1, the yeast homolog of TIP60, to be required for autophagy (Yi et al., 2012). By process of elimination, Atg3 was deemed to be the substrate of Esa1, opening up the possibility that aside from ULK1, other autophagy essential proteins may be acetylated in the mammalian system as well.

Protein ubiquitination is one of the most prevalent post-translational modifications involved in protein regulation and signal transduction. Although its best known function is to target proteins for degradation through the proteasome pathway through the formation of Lys48-linked poly ubiquitination chains, other ubiquitination marks have non-degradative roles such as influencing protein-protein interaction and protein function (Komander, 2009; Strieter and Korasick, 2012). Indications of both degradative and non-dgradative ubiquitination events have been found on ULK1. The stability of ULK1 and ATG13 are regulated by the HSP90-CDC37 chaperone complex. Treatment with the HSP90 antagonist 17AAG led to a decrease in ULK1 protein levels that was rescued by co-treatment with proteasomal inhibitor MG132 (Joo et al., 2011). This is corroborated by Johansen and colleagues who reported that starvation induced degradation of ULK1 can be impaired by MG132 treatment (Alemu et al., 2012). In a separate study, Cecconi and colleagues observed that starvation induced an increase in Lys63-linked poly ubiquitination (Lys63-Ub) on ULK1 (Nazio et al., 2013). As it was previously reported that E3 ligase TRAF6 could ubiquitinate ULK1 *in vitro* (Zhou et al., 2007), they proposed that TRAF6 is responsible for the Lys63-Ub observed upon starvation. In support of this, they found that TRAF6 could interact with ULK1. Overexpression of TRAF6 enhanced ULK1 protein level and

kinase activity, and conversely, depletion of TRAF6 resulted in a dramatic reduction in ULK1 protein levels, indicating that the Lys63-Ub modification functions to promote ULK1 stability and activity (Nazio et al., 2013). Taken together, the post-translational modifications on ULK1 mediated by various energy/ nutrient sensing pathways provide additional versatility for cells to control the intensity and timing of ULK1-mediated autophagy (Figure 1.3).

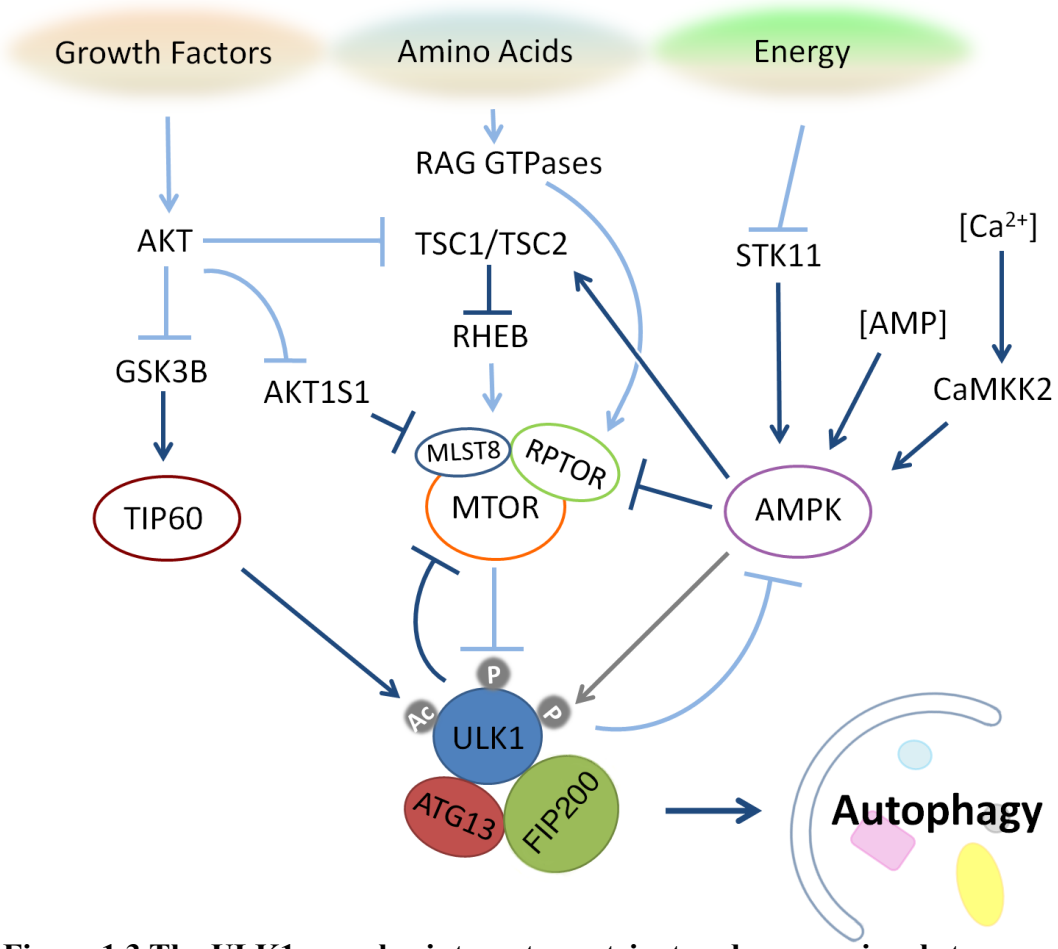

Figure 1.3 The ULK1 complex integrates nutrient and energy signals to co-ordinate autophagy induction. Nutrient sensing pathways converge on ULK1 through posttranslational modifications which regulate the activity to the ULK1 complex. Light blue arrows represent events that suppress autophagy induction while dark blue events indicate events that stimulate autophagy induction. The gray arrow between AMPK and ULK1 represents the possibility that AMPK may have multiple regulatory effects on ULK1.

Early events in autophagy

It is well established that the ULK1 complex is essential for mediating starvation-induced autophagy. However, the functional relationship between the ULK1 complex and other autophagy essential proteins is still not well defined. Recruitment of the ULK1 complex, the VPS34 complex and the ATG5 complex to isolation membranes are early events in autophagy. While the ULK1 complex is not part of the core machinery required to bring about LC3 lipidation, a hallmark for autophagy, both the VPS34 complex and ATG5 complex are necessary upstream events for LC3 lipidation. In particular, forced localization of ATG16 (member of the ATG5 complex) to the plasma membrane was sufficient to direct ectopic LC3 lipidation to that membrane, indicating that the ATG5 complex specifies the site of LC3 lipidation (Fujita et al., 2008). VPS34 activity is also required for ATG5 complex translocation, placing it upstream of ATG5 (Jaber et al., 2012; Matsunaga et al., 2010; Matsunaga et al., 2009). As mTORC1 regulates ULK1 directly, it is logical to place the ULK1 complex upstream of both VPS34 and ATG5 (Figure 1.4). In support of this, starvation induced ATG5 puncta formation is blocked in *Fip200*$^{-/-}$ cells (Hara et al., 2008). However, the relationship between these three complexes may not be a simple linear one, as starvation-induced ULK1 puncta formation cannot be observed in *Atg5*$^{-/-}$ cells (Itakura and Mizushima, 2010), suggesting that the ATG5 complex may also influence the function of the ULK1 complex, perhaps by stabilizing its association to membranes.

The VPS34 complex involved in autophagy consists of VPS34, Beclin, VPS15 and ATG14 (Itakura et al., 2008; Itakura and Mizushima, 2009). VPS34 is a lipid kinase that converts phosphatidylinositol (PI) to phosphatidylinositol-3-phosphate (PI3P) and can be incorporated into other complexes involved in membrane trafficking pathways

aside from autophagy (Brown et al., 1995; Johnson et al., 2006). The localized accumulation of PI3P in a subdomain of the endoplasmic reticulum (ER) recruits FYVE domain-containing autophagy components (WIPI, DFCP1) that result in the subsequent recruitment of autophagy proteins required for LC3 lipidation (ATG5 complex and LC3) and autophagosome formation (Axe et al., 2008; Polson et al., 2010; Proikas-Cezanne et al., 2007). Like the ULK1 complex, the VPS34 complex is another signaling hub and major point of regulation for autophagy induction. The ULK1 complex can directly regulate the VPS34 complex (Di Bartolomeo et al., 2010; Russell et al., 2013). Aside from ULK1, several other kinases have been reported to regulate members of the VPS34 complex. Some of these kinases such as EGFR (Wei et al., 2013), AKT (Wang et al., 2012), and AMPK (Kim et al., 2013) play a role in growth factor and energy-sensing pathways as well, indicating that the VPS34 complex may be activated in co-ordination with ULK1 or in a ULK1-independnet manner to stimulate autophagy (Figure 1.4).

1.4 The ULK1 complex: relaying nutrient signals

Several studies have shed light on how the ULK1 complex may influence early events to promote autophagy. Guan and colleagues reported that ULK1 phosphorylates Beclin1, a member of the VPS34 complex, at Serine 14 (S14), resulting in activation of the autophagy-specific VPS34 complex (Russell et al., 2013). When tested *in vitro*, VPS34 complexes containing phospho-mutants of Beclin1 (S14A) were less efficient at generating PI3P, suggesting that the phosphorylation event promotes the lipid kinase activity of VPS34 (Russell et al., 2013). In an earlier study, ULK1 was shown to influence localization of the VPS34 complex by phosphorylating AMBRA1, a Beclin1 interacting protein, resulting in its release from dynein for autophagy activation (Di Bartolomeo et al., 2010).

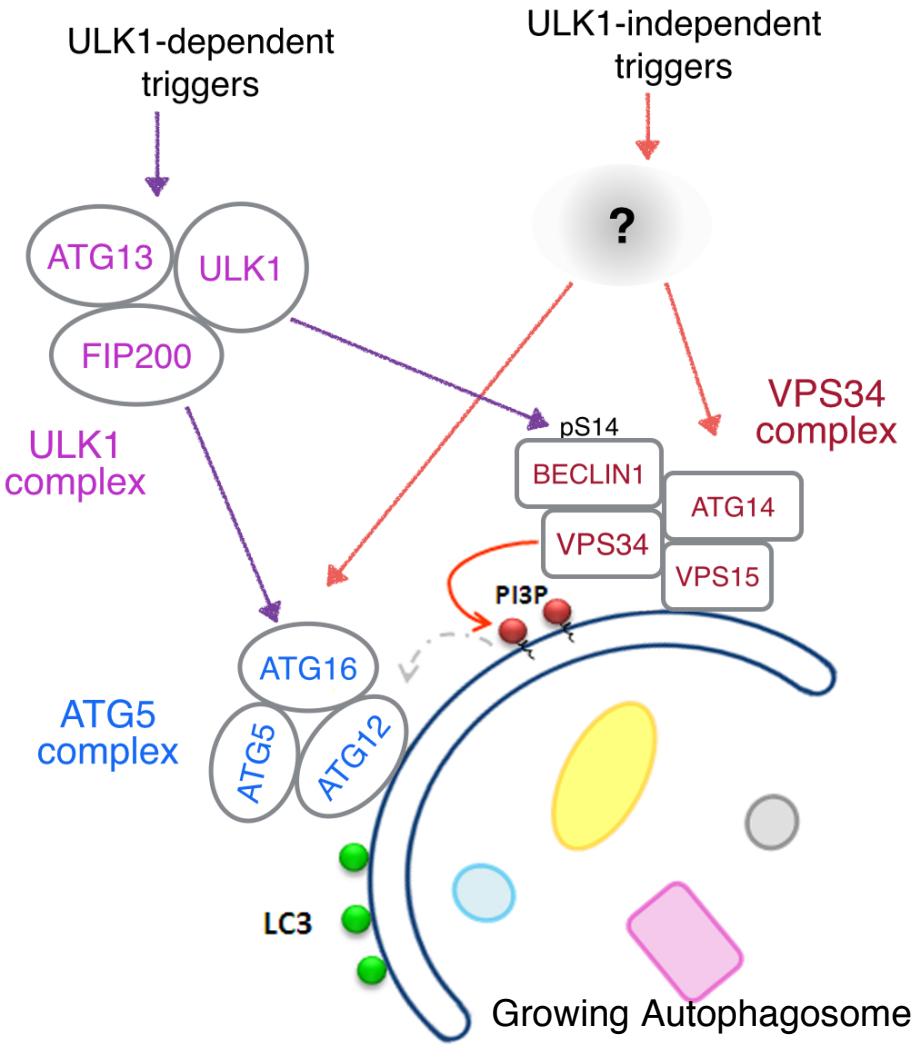

Figure 1.4 Functional relationship between the ULK1 complex, the VPS34 complex and the ATG5 complex in autophagy. The ULK1 complex has been shown to directly communicate with the ATG5 complex and the VPS34 complex. While the role of ULK1 in amino acid starvation induced autophagy is well established, other triggers for autophagy may not function through the ULK1 complex. Though currently not well understood, these triggers may stimulate the VPS34 complex and ATG5 complex through ULK1-independent means.

The ULK1 complex was also linked to ATG5 complex recruitment through direct interaction between FIP200 (member of the ULK1 complex) and ATG16 (member of the ATG5 complex) (Gammoh et al., 2013; Nishimura et al., 2013). ATG16 deficient MEFs are autophagy defective and unable to lipidate LC3 to PE (Ishibashi et al., 2011; Saitoh et al., 2008). Deletion of a FIP200 interacting domain on ATG16 resulted in a mutant that could not reconstitute amino-acid starvation induced autophagy (which requires the ULK1 complex) but could still reconstitute autophagy induced by glucose starvation (Gammoh et al., 2013), which is reported to occur in a ULK1-independent manner (Cheong et al., 2011). This indicates that the ULK1 complex promotes autophagy during amino acid starvation at least in part through direct recruitment of the ATG5 complex.

In addition, ULK1 may regulate ATG9, the only transmembrane protein among the autophagy essential proteins (Mack et al., 2012; Young et al., 2006). In yeast, Atg9 translocates to pre-autophagosomal structures (PAS) in an Atg1 and Atg17 dependent manner. Atg9 containing vesicles are thought to contribute membrane for organization and growth of the PAS (Mari et al., 2010; Reggiori et al., 2004; Sekito et al., 2009). Subsequently, Atg1 was found to directly phosphorylate Atg9 to promote autophagy (Papinski et al., 2014). ATG9 trafficking has been proposed to play a similar role in mammalian autophagy (Young et al., 2006), but this remains somewhat controversial as although ATG9 containing vesicles were seen to associate with autophagosomes, no direct fusion events were observed when live-cell imaging was used (Orsi et al., 2012). Even though the exact function of ATG9 is still unclear and *Atg9*$^{-/-}$ MEFs are only partially defective in amino acid starvation induced autophagy, *Atg9*$^{-/-}$ mice share the same neonatal starvation phenotype as mice lacking *Atg5* or *Atg7* (Saitoh et al.,

2009), indicating that ATG9 is required for starvation induced autophagy in the mammalian system.

Thus far, the ULK1 complex is commonly described as an initiator of the autophagy pathway, interacting with early complexes to stimulate autophagy in response to nutrient status in the cell. However, recent reports indicate that ULK1 may have functions in later stages of autophagy as well. LC3, the mammalian homologue of Atg8, is conjugated to phosphatidyl-ethanolamine (PE) on nascent autophagosomes and is thought to promote autophagosome expansion (Ichimura et al., 2000; Mizushima et al., 1998). It can also facilitate autophagosome cargo selection by recruiting adaptor proteins such as p62 (Pankiv et al., 2007) and NBR1 (Kirkin et al., 2009). These adaptors bind to LC3 via a conserved hydrophobic motif known as the LC3 interacting region (LIR). Both Atg1 (yeast) and ULK1 (mammalian) contain an LIR and can interact with Atg8 and LC3 respectively (Alemu et al., 2012; Nakatogawa et al., 2012; Okazaki et al., 2000). Mutation of the LIR abolished binding to Atg8/LC3 and reduced starvation-induced translocation of Atg1/ULK1 to autophagosome-like membrane structures, indicating that the interaction with Atg8/LC3 may stabilize membrane association of Atg1/ULK1 and is required for autophagy (Alemu et al., 2012; Nakatogawa et al., 2012). The exact function of this interaction is not well understood, but indicates that ULK1 has functions beyond its interactions with other early complexes (ATG5 and VPS34) and may influence later events in autophagy. Two other studies indicate that ULK1 may play a role in cargo loading and selection. Feng and colleagues found that ULK1 interacts with a mitochondria outer membrane protein, FUNDC1 (Wu et al., 2014). FUNDC1 was previously shown to contain an LIR motif and can act as an adaptor protein for mitochondrial targeting to autophagosomes during hypoxia-induced mitophagy (Liu et al., 2012). Feng and

colleagues showed that FUNDC1 is phosphorylated at Ser17 under conditions of hypoxia or FCCP treatment, and correlates with ULK1 status, namely Ser17 phosphorylation increased in cells overexpressing ULK1 and was absent in *Ulk1*$^{-/-}$ MEFs, suggesting that ULK1 is responsible for the phosphorylation event. Phospho-mimetic mutants (Ser17D) interacted more strongly with LC3 while Phospho-dead mutants (Ser17A) interacted weakly, indicating that ULK1 may promote cargo incorporation of mitochondria by phosphorylating FUNDC1 (Wu et al., 2014). In a separate study, Yue and colleagues found that ULK1 can phosphorylate p62 at its ubiquitin association domain (UBA) to affect the binding affinity between p62 and ubiquitin (Lim et al., 2015). This phosphorylation was not induced by starvation but increased with the accumulation of ubiquitinated proteins induced by MG132 treatment (proteasome inhibitor). Phopho-dead mutants of p62 (S409A) resulted in the accumulation of protein aggregates, suggesting that the phosphorylation event promotes recruitment and autophagic degradation of ubiquitinated proteins (Lim et al., 2015). Prior to this study, other groups have also reported the regulation of p62 by protein phosphorylation to promote autophagic degradation, albeit on different sites and by different protein kinases (Ichimura et al., 2013; Matsumoto et al., 2011).

In summary, the ULK1 complex can regulate early complexes in autophagy to stimulate autophagy in response to nutrient signals but may interact with subsequent autophagy essential genes traditionally thought of as “late events” in autophagy as well. With the emergence of more data, it is becoming clear that the autophagic pathway is not a simple linear one but may involve multiple crosstalk and regulation between the autophagy complexes to achieve a highly tunable and regulated pathway.

1.5 Thesis objectives

The work described in this dissertation covers both early and late events in autophagy in order to advance our understanding of this pathway. Chapter 2 investigates ER stress-induced autophagy with the unexpected finding that the lysosomal fusion step in two membrane trafficking pathways, endocytosis and autophagy, though highly interconnected, can be independently regulated.

The next part of this dissertation looks at the regulation of autophagy by the coordinated actions of mTORC1 and protein phosphatase 2A on ULK1, an autophagy-initiating protein and direct substrate of mTORC1. My interest in this project was triggered by the observation that amino acid starvation induced more rapid dephosphorylation of ULK1 and autophagy induction compared to pharmacological inhibition of mTORC1 alone, indicating that phosphatase activity is stimulated by amino acid starvation. In Chapter 3, I describe identification of the Protein Phosphatase 2A (PP2A) complex that regulates ULK1 during amino acid starvation. In Chapter 4, I attempt to elucidate the mechanism behind PP2A stimulation during starvation and find that the interaction between PP2A and an inhibitory protein, Alpha4 is sensitive to amino acid starvation, and is not regulated by mTORC1. Deregulation of PP2A is correlated with high levels of ULK1-dependent autophagy in the absence of mTORC1 inactivation, indicating that "autophagy-addicted" pancreatic cancer cells can take advantage of PP2A mediated regulation of ULK1 to reap the dual benefits of autophagy and mTOR signaling at the same time. Finally, Chapter 5 summarizes the unanswered questions raised by the work described in this dissertation and includes some speculation for further experimental research in our ongoing quest to understand the inner workings of a cell.

CHAPTER 2. LYSOSOMAL FUSION WITH AUTOPHAGOSOMES AND ENDOSOMES ARE REGULATED BY DISTINCT MECHANISMS

2.1 Introduction

A defining characteristic of Eukaryotic organisms is the presence of membrane bound organelles. Eukaryotic cells make use of membrane compartmentalization to create sub-cellular spaces of specialized functions. Vesicle and membrane trafficking pathways are used to move cargo in between compartments within the cell or to move cargo into and out of the cell. Autophagy and endocytosis are two pathways that rely on the trafficking of vesicles to transport goods. Both terms were coined by Christian de Duve in 1963 from his observations of electron micrographs of the cell (Klionsky, 2007). Autophagy is a degradation process that starts with an isolation membrane that elongates to encapsulate cytosolic contents such as damaged organelles and aggregated proteins. The fully formed autophagosome is a double membrane vesicle that eventually fuses with lysosomes resulting in degradation of its contents (Yang and Klionsky, 2010b). Endocytosis is the process of taking up cargo in the form of macromolecules or particles at the cell surface or from the extracellular environment. During endocytosis, a portion of the plasma membrane invaginates and pinches off inside the cell to form a vesicle carrying the ingested cargo. These vesicles fuse with early/sorting endosomes where in a series of homotypic fusion and fission events, the cargo is sorted and marked for transport, degradation or recycling back to the plasma membrane. Cargo marked for degradation are transferred to late endosomes/multi-vesicular bodies which eventually fuse with lysosomes (Evans and Owen, 2002).

The progression from early to late endosome involves a process of "Rab-conversion" (Cabrera and Ungermann, 2010; Hyttinen et al., 2013). Early endosomes are

characterized by the presence of small GTPase Rab5 and its effector proteins such as the class III phosphatylinositol 3-kinase Vps34 and EEA1. When early endosomes undergo maturation into late endosomes, they gradual lose Rab5 and gain late endosome marker Rab7 (Rink et al., 2005). This conversion is facilitated by SAND-1/Mon1 which displaces a Rab5 GEF (Rabex5) and recruits a member of the HOPs complex, which is required for Rab7 recruitment (Kinchen and Ravichandran, 2010; Poteryaev et al., 2010; Wang et al., 2002).

Some parallels and overlaps exist between the autophagy and the endocytic pathway. Aside from sharing a common endpoint in the form of lysosomal fusion, they share several molecular components as well. VPS34, which produces phosphatidylinositol (3)-phosphate (PI3P) is involved in both pathways, resulting in an enrichment of PI3P in endosome, lysosome and autophagosomal membranes (Evans and Owen, 2002). Late endosome marker Rab7 is also required for autophagosome maturation as without it, autophagosomes form but are unable to fuse with lysosomes (Gutierrez et al., 2004; Jäger et al., 2004). In addition, early morphological studies using cell tracers in combination with electron microscopy suggests that autophagosomes can not only fuse directly with lysosomes (Gordon et al., 1992; Lawrence and Brown, 1992) but can also interact with the endocytic pathway by fusing with endosomes to form intermediate vesicles known as amphisomes (Eskelinen, 2005; Liou et al., 1997). In an electron micrograph, amphisomes are characterized by the presence of endocytic tracer (usually in the form of endocytosed nano-gold particles) in a double-membraned vesicle containing other cytoplasmic material and membranous structures (Eskelinen, 2005).

At a molecular level, autophagosome maturation is not well understood. Live imaging data suggests that autophagosome maturation may involve multiple homotypic and heterotypic fusion events (Jahreiss et al., 2008). The canonical RAB-SNARE fusion machinery involved in endocytosis is also required for autophagy (Nair et al., 2011). Several specific SNAREs such as VAMP7 (Fader et al., 2009), Vti1b (Furuta et al., 2010), and Stx17 (Itakura et al., 2012) have been identified to be involved in autophagy maturation, but may have a role in endocytosis as well. It is unclear how these fusion factors are recruited to autophagosomes. Given the overlaps between the autophagic and endocytic pathways, it is sometimes taken for granted that they would share the same regulatory mechanisms for lysosomal fusion as well.

In this study, we provide evidence that autophagosome maturation and endosome maturation, while sharing commonalities such as a Rab7 requirement, are governed by distinct molecular players. Treating cells with ER-stess inducer Thapsigargin, we are able to selectively block autophagosome maturation by preventing Rab7 recruitment to autophagosomes without affecting the endocytic pathway. In addition, we find that HOPS complex member VPS16 which is required for endocytosis, is not required for autophagosome clearance. Therefore although both pathways may share the same endpoint in the form of lysosomes, the route of vesicle maturation in autophagy may be governed by distinct molecular mechanisms from that in endocytosis.

2.2 Results

Thapsigargin blocks autophagy

This project was carried out in my early years as a graduate student, in close collaboration with a previous postdoctoral fellow in the lab, Dr. Ian Ganley, who is currently running his own lab at the MRC Protein Phosphorylation Unit in the University of Dundee. The work has been published in full in the journal *Molecular Cell* (Ganley et al., 2011) and is included here in part. Several groups have reported that ER stress can induce autophagy, although the molecular mechanism behind this is not well understood (Grotemeier et al., 2010; Ogata et al., 2006; Sakaki et al., 2008). Thapsigargin and tunicamycin are two small molecule inhibitors commonly used as experimental tools to induce ER stress. The former inhibits a calcium pump (SERCA) in the ER while the latter inhibits N-linked glycosylation in the ER (Szegezdi et al., 2006). Ian laid the foundation of this project with his observation that autophagosomes formed during thapsigargin treatment were qualitatively different from autophagosomes formed during treatment with tunicamycin or starvation. Using mouse embryonic fibroblasts (MEFs) stably expressing autophagy marker GFP-LC3, he observed that while cells treated with tunicamycin or starvation formed numerous small GFP-LC3 puncta, thapsigargin treated cells formed larger but fewer punctate structures (Figure 2.1 A).

Autophagy is a dynamic process in which autophagosome formation is continuously offset by its turnover upon fusion with lysosomes. This autophagic flux is demonstrated by the accumulation of autophagosomes when lysosomal function is disrupted, such as through the use of Bafilomycin A1, an inhibitor that binds to vacuolar H+ ATPase to block lysosomal acidification. Addition of bafilomycin resulted in a further accumulation of GFP-LC3 puncta in starvation and tunicamycin

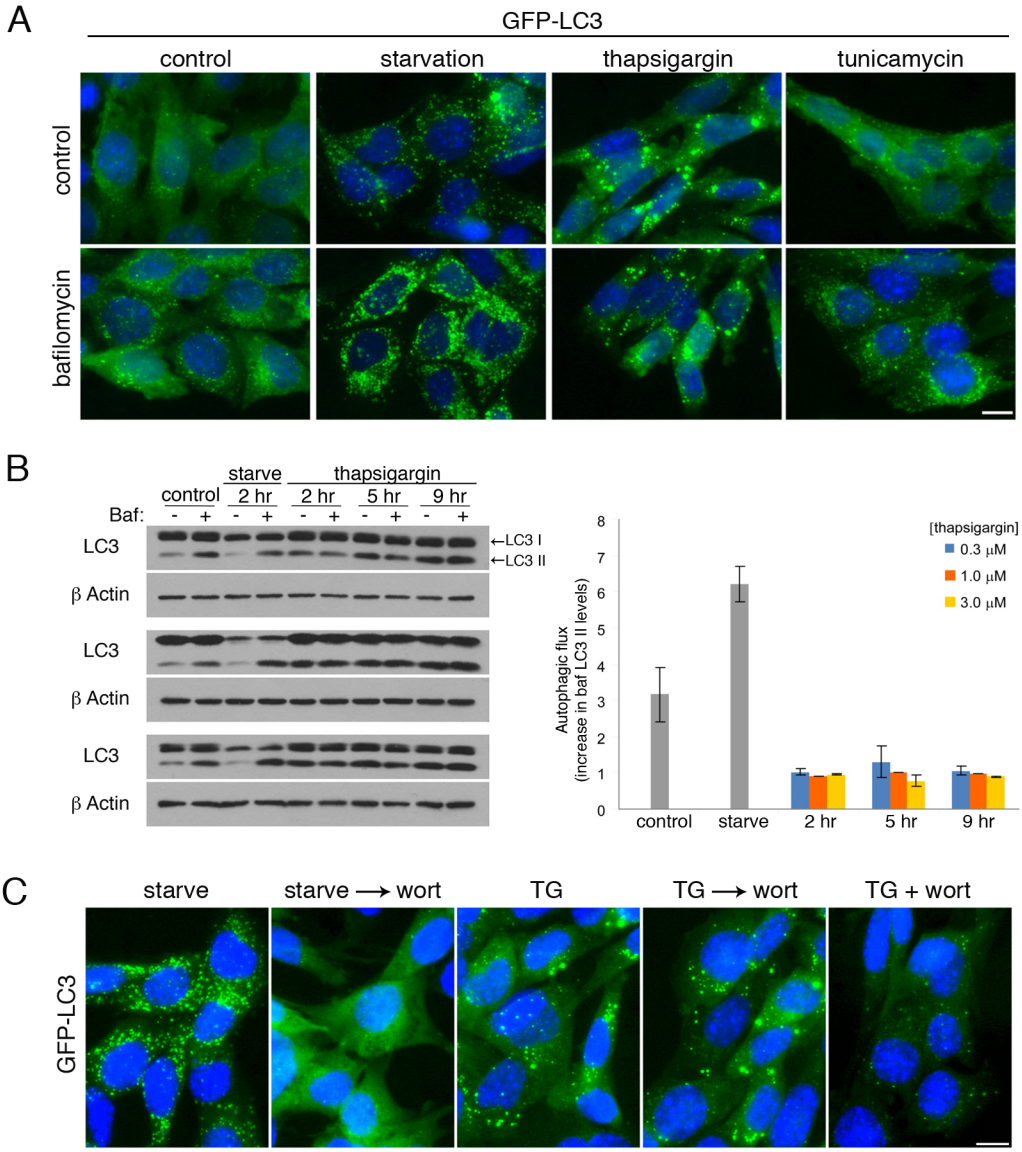

Figure 2.1 Thapsigargin blocks autophagic flux. (**A**) MEFs stably expressing GFP-LC3 were incubated in amino acid starvation for 2 hr, complete media with 3 μM thapsigargin for 5 hr or complete media with 20 μg/ml tunicamycin for 5 hr, in the presence or absence of 10 nM bafilomycin for the last 2 hr. (**B**) Time and dose response of MEFs treated with thapsigargin. Endogenous LC3 levels were monitored by immunoblotting. Quantitation of bafilomycin induced accumulation in LC3-II levels is shown on the right. (**C**) GFP-LC3 expressing MEFs were incubated in amino acid-free media for 1 h (starve), amino acid-free media for 1 h followed by addition of 50 nM wortmannin for 1 h (starve → wort), complete media with 3 μM thapsigargin for 4 h (TG), complete media with 3 μM thapsigargin for 4 h followed by addition of 50 nM wortmannin for 1 h (TG → wort), or complete media with 3 μM thapsigargin and 50 nM wortmannin together for 4 h (TG + wort). Cells were then fixed and visualized by fluorescence microscopy. Bar, 10 μm. Panel A and C were carried out by Dr. Ian Ganley.

treated cells as expected (Figure 2.1 A). However, no further accumulation of GFP-LC3 was observed in thapsigargin treated cells, indicating a block in autophagic flux.

We verified these results by monitoring endogenous LC3 conversion by western blotting. LC3 is commonly used as a readout for autophagy. The cytosolic form of LC3 runs as a 17 kDa band on a gel and is known as form I. Upon autophagy induction, LC3 is conjugated to phosphatidylethanolamine on autophagic membranes and runs as a faster migrating band known as form II. In control and starvation treated cells, treatment with bafilomycin resulted in further accumulation of LC3-II levels. However although thapsigargin treatment alone resulted in an increase in LC3-II levels, bafilomycin treatment did not bring about a further accumulation of LC3-II, mirroring our earlier observations monitoring GFP-LC3. This was true for all concentrations and timepoints of thapsigargin treatment tested (Figure 2.1 B). This block in autophagic flux is not part of the ER stress response as we do not see it in tunicamycin treated cells (Figure 2.1 A) and IRE-1$^{-/-}$ MEFs deficient in the ER stress response (Wiseman et al., 2010) still display thapsigargin-induced block in autophagy flux (Figure 2.2).

Thapsigargin blocks autophagosome fusion with lysosomes

To look at this phenomenon more closely, Ian designed an elegant assay to monitor autophagic flux. The lipid kinase VPS34 is required for autophagy induction. Inhibiting its activity with wortmannin will block autophagosome formation. When Ian starved GFP-LC3 MEFs, he could observe numerous punctate structures, indicative of autophagosome formation. Addition of wortmannin to the starved cells resulted in gradual disappearance of the punctate structures as autophagosomes fused with lysosomes and were turned over. However, when the wortmannin chase assay

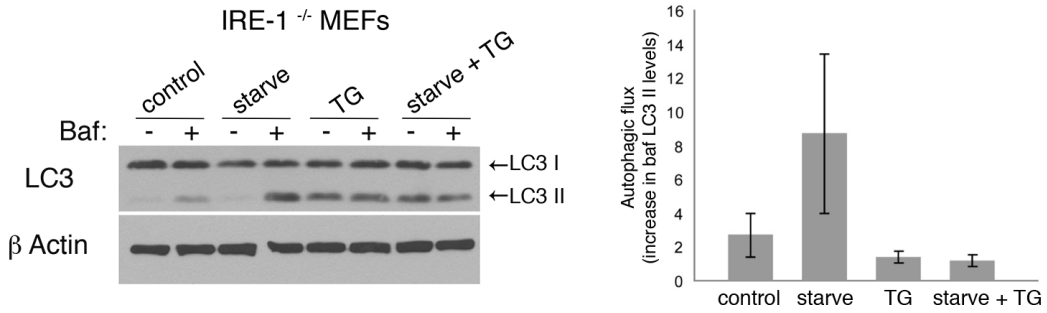

Figure 2.2 Thapsigargin blocks autophagy in IRE1$^{-/-}$ MEFs deficient in ER stress response. IRE1$^{-/-}$ MEFs were incubated in amino acid free media for 1 hr (starve), complete media with 3 μM thapsigargin for 5 hr (TG) or complete media with 3 μM thapsigargin for 4 hr followed by amino acid free media in the presence of 3 μM thapsigargin for 1 hr (starve + TG). Where indicated, 10nM bafilomycin was added for the final 1 hr of treatment. Quantitation of bafilomycin induced accumulation in LC3-II levels is shown on the right.

was carried out on thapsigargin treated cells, the GFP-LC3 puncta persisted and could not be cleared away, indicating a block in autophagosome maturation (Figure 2.1 C). As a control, wortmannin can block thapsigargin induced GFP-LC3 puncta formation when added at the start of thapsigargin treatment, indicating that the structures formed by thapsigargin treatment require VPS34 activity as well.

As further indication that the LC3 positive structures accumulated by thapsigargin treatment are autophagosomes, we carried out immunofluorescence to monitor the translocation of p62, an adaptor protein involved in incorporating poly-ubuquitinated protein aggregates into autophagosomes for degradation (Bjørkøy et al., 2005; Pankiv et al., 2007). In starvation as well as thapsigargin treatment, we could observe good co-localisation between LC3 and p62, indicating successful cargo loading in both cases (Figure 2.3 A). Monitoring p62 levels by western blotting, we could see a bafilomycin-sensitive decrease in p62 levels during starvation, indicating cargo degradation as expected. However, thapsigargin treatment did not induce a

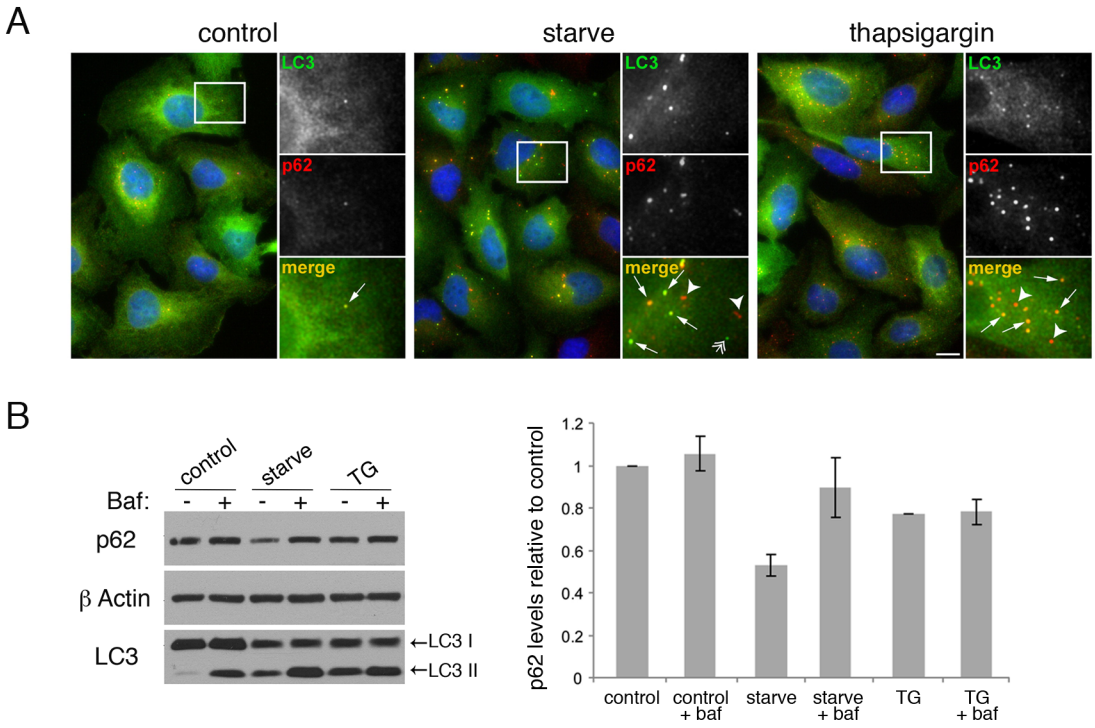

Figure 2.3 Cargo loading is not blocked in thapsigargin treated cells. (**A**) U2OS cells stably expressing GFP-LC3 were incubated in amino acid free media for 2 hr or complete media with 3 μM thapsigargin for 5 hr. Cells were then fixed and stained with antibodies against p62 (red) or GFP (green). Bar, 10 μm. Arrows indicate co-localization between p62 and LC3 and arrowheads indicate p62-only or LC3-only puncta. (**B**) U2OS cells were treated as in (A), lysed and analysed by immunoblotting against endogenous p62 and LC3. Quantitation of p62 levels relative to control are shown on the right. Panel A was carried out by Dr. Ian Ganley.

bafilomycin-sensitive decrease in p62 levels despite the co-localisation with LC3 observed by immunofluorescence, once again indicating a block in autophagosome turnover (Figure 2.3 B).

We performed electron microscopy coupled with immune-gold labeling of GFP-LC3 to take a closer look at the structures being formed during thapsigargin treatment. Using four different treatment conditions, we observed a variety of membranous structures in the cell upon which gold label was concentrated. In order to analyze these structures, we classified them into four categories: “non-circular” structures

ranging 200-500 nM in length which were often linear or slightly curved, consistent with the morphology of isolation membranes. “Circular” structures 200-600 nM, which sometimes contained cellular material, consistent with the morphology of autophagosomes. “Internal only” structures that contained gold label on the interior of a limiting membrane, consistent with the morphology of autolysosomes (autophagosomes that have fused with lysosomes) and “circular clusters” which we defined as a collection of two or more circular structures in close proximity (Figure 2.4). Cells kept in normal culture conditions (control) contained very few gold labeled structures, consistent with low basal levels of autophagy. Starved cells contained high levels of isolation membrane, autophagosome and autolysosome-like structures, reflecting high autophagy flux. Thapsigargin treated cells also had high levels of autophagosome-like structures but relatively low levels of isolation membrane-like structures and almost no autolysosome-like structures, indicating successful autophagosome formation but no turnover. In addition, thapsigargin treatment had no effect on starvation-induced increase in isolation membrane-like structures, but almost completely blocked the starvation-induced increase in autolysosome-like structures, supporting the notion that thapsigargin has no effect on autophagy initiation or autophagosome formation but blocks autophagosome fusion with lysosomes (Figure 2.4). Another striking observation was the over representation of “autophagosome clusters” in thapsigargin treated samples, and suggests that some of the larger GFP-LC3 puncta detected during fluorescence microscopy (Figure 2.1 A) could be due to the clustering of multiple autophagosomes.

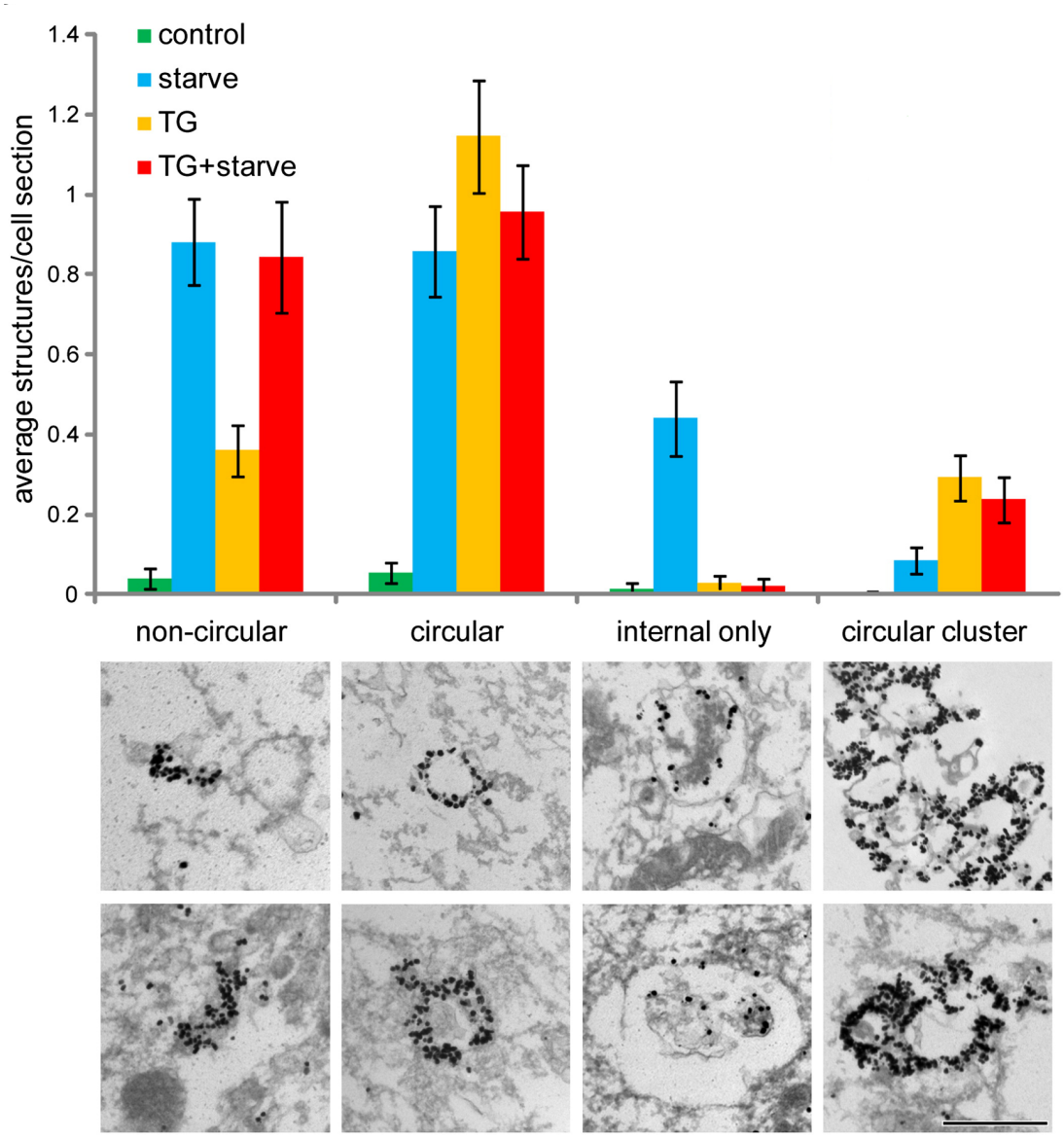

Figure 2.4 Autophagosomes accumulate and cluster in thapsigargin-treated cells. MEFs stably expressing GFP-LC3 were treated as indicated, stained for GFP-LC3 and imaged by electron microscopy. Stained GFP-LC3 structures were categorised into 4 groups: non-circular, circular, internal only and circular clusters. Bars represent mean number of structures per cell section ± SEM for control treated cells (n = 73 cell sections), 1 h 30 min amino acid-free media treated cells (starve; n = 84 cell sections), 4 h 30 min thapsigargin (3 μM) treated cells (TG; n = 103 cell sections), and 4 h 30 min thapsigargin (3 μM) plus amino acid starvation for the final 1 h 30 min (TG + starve; n = 89 cell sections). Panels below the chart represent examples of the indicated structures. Bar, 500 nm.

Block is specific to autophagy but does not affect endocytosis

To check if other membrane trafficking pathways are affected by thapsigargin, Ian monitored the turnover of epidermal growth factor receptor (EGFR), which occurs through receptor-mediated endocytosis. Upon the binding of EGF, EGFR is internalized by endocytosis and in a process involving multiple fusion events, is eventually degraded in lysosomes. This turnover can be blocked by bafilomycin treatment, which inhibits lysosomal function and therefore all degradative pathways terminating in lysosomes (including autophagy). However, using a concentration that blocks autophagosome clearance, thapsigargin treatment had no effect on EGFR degradation (Figure 2.5), suggesting that thapsigargin does not block lysosome function per se but is specifically affecting fusion events required for autophagosome maturation. In addition, the ability to block autophagy without blocking endocytosis indicates that late events in the two pathways are not completely convergent and may involved distinct molecular components.

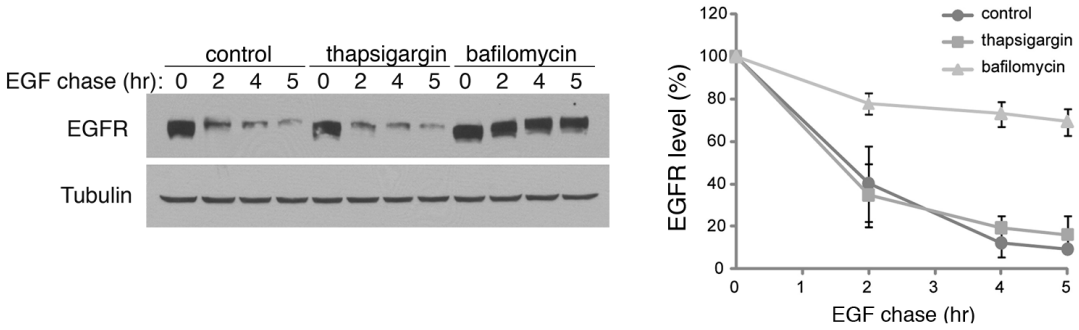

Figure 2.5 Thapsigargin does not block receptor mediated endocytosis and degradation of EGFR. MEFs were stimulated with 40 ng/ml EGF in the presence of 20 μg/ml cycloheximide and in the presence or absence of 3 μM thapsigargin or 10 nM bafilomycin. Cells were harvested at the indicated time and immunoblotted for EGFR levels. EGFR levels from three independent experiments are quantitated on the right as percentage relative to time 0. Figure 2.5 was carried out by Dr. Ian Ganley.

The molecular mechanisms governing autophagosome maturation are not well understood, however Rab7 is reported to be required (Gutierrez et al., 2004; Hyttinen et al., 2013). Monitoring Rab7 by immunofluorescence, Ian found that starvation induced partial Rab7 co-localisation with LC3, reflecting the involvement of Rab7 in multiple pathways as well as indicating successful recruitment of Rab7 to autophagosomes (Figure 2.6). In contrast, although thapsigargin treatment induced numerous LC3 positive punctate structures, there was a large reduction in co-localisation with Rab7 containing structures, indicating that thapsigargin somehow interferes with the recruitment of Rab7 to autophagosomes (Figure 2.6). In an effort to further investigate the effect of thapsigargin, we knocked down Rab7 and VPS16, a member of the HOPs complex which is reported to mediate fusion events in endosome maturation (Balderhaar and Ungermann, 2013; Luzio et al., 2009). In line with their reported functions, knockdown of Rab7 or VPS16 resulted in impairment of EGFR turnover (Figure 2.7 A). Surprisingly, knockdown of Rab7 but not VPS16 blocked

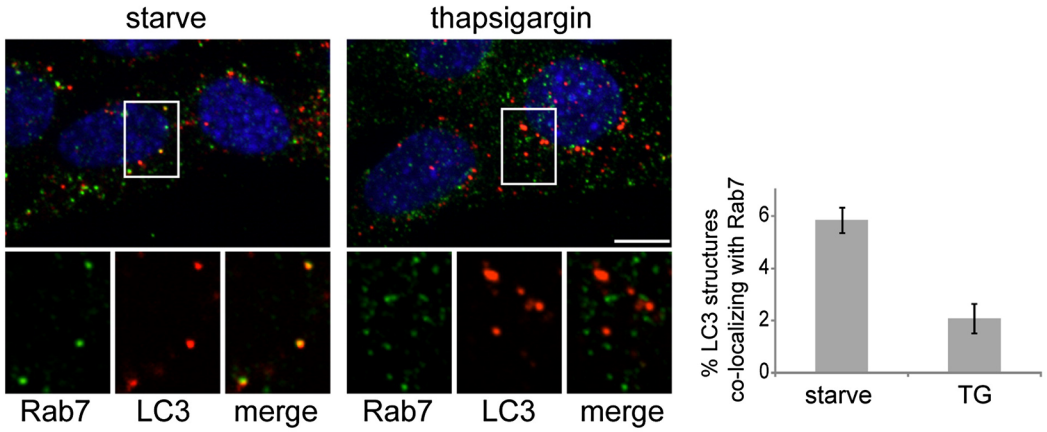

Figure 2.6 Thapsigargin inhibits Rab7 recruitment to autophagosomes. MEFs were incubated in amino acid free media or complete media with 3 μM thapsigargin. Cells were stained with antibodies against Rab7 (green) or LC3 (red) and imaged by confocal microscopy. Bar, 10 μm. Percentage of LC3 structures co-localizing with Rab7 is quantitated on the right. Figure 2.6 was carried out by Dr. Ian Ganley.

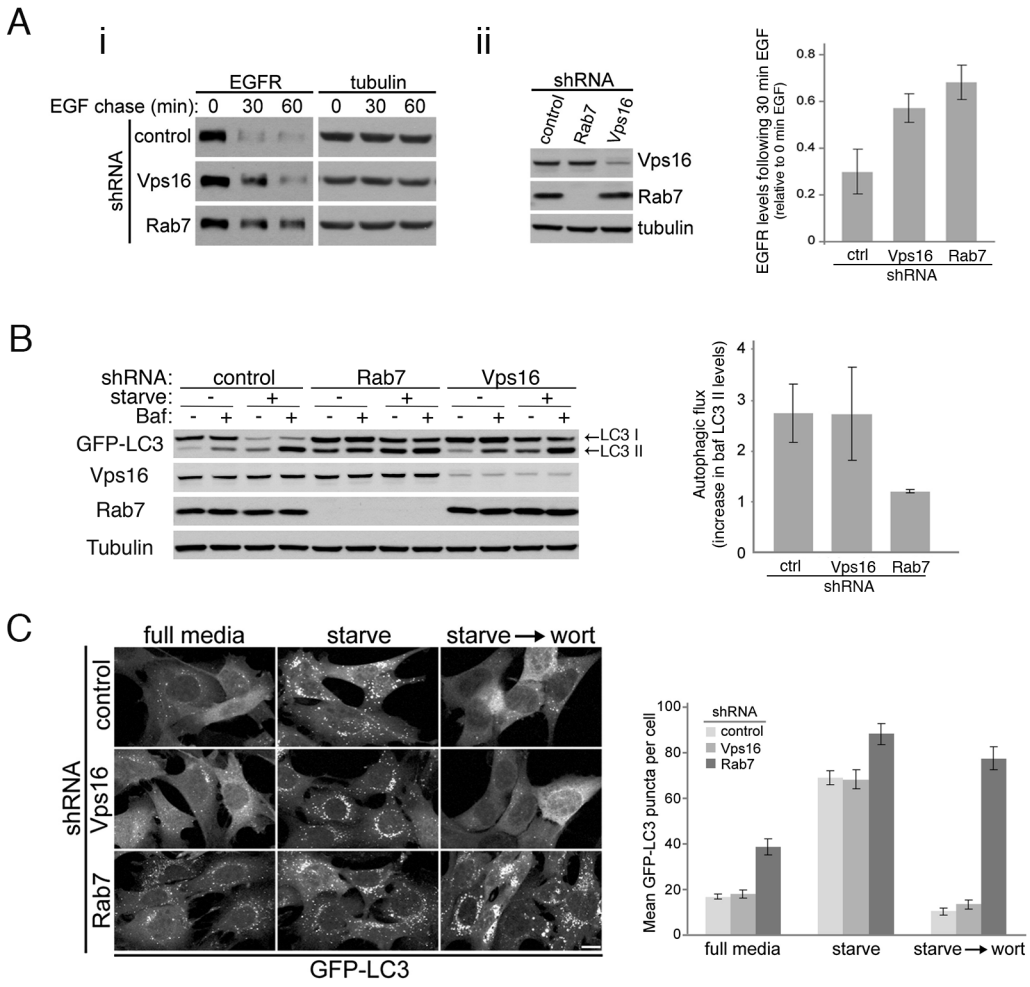

Figure 2.7 Rab7 but not Vps16 is required for autophagosome fusion with lysosomes. (**A**) (i) EGFR degradation assay to assess receptor mediated endocytosis was carried out in MEFs stably expressing Vps16 shRNA and Rab7 shRNA. Knockdown levels are shown in (ii). Quantitation of EGFR levels at 30min relative to time 0 is shown on the far right. (**B**) MEFs stably expressing GFP-LC3 and control shRNA, Vps16 shRNA or Rab7 shRNA were incubated in amino acid free media for 1 hr in the presence or absence of 10 nM bafilomycin. Cells were lysed and assed by immunoblotting for the indicated antibodies. Quantitation of bafilomycin induced accumulation in LC3-II levels is shown on the right. (**C**) MEFs used in (B) were incubated in amino acid free media for 1 hr (starve) or amino acid free media for 1 hr followed by addition of 50nM wortmannin in amino acid free media for an additional 1 hr (starve → wort). Cells were fixed and imaged by fluorescence microscopy. Bar, 10 μm. Quantitation of the mean number of GFP-LC3 puncta per cell is shown on the right.

autophagic flux. Starvation induced LC3 conversion and turnover in control knockdown and VPS16 knockdown cells (as evidenced by an increase in LC3-II and decrease in LC3-I levels) but not in Rab7 knockdown cells (Figure 2.7 B). In addition, bafilomycin treatment resulted in a further accumulation of LC3-II in control and VPS16 knockdown cells but not in Rab7 knockdown cells, indicating that autophagic flux is blocked in Rab7 knockdown cells (Figure 2.7 B). The slower rate of LC3 turnover in VPS16 cells compared to control (assessed by decrease in LC3-I levels) could be due to the impaired endocytic pathway, which may contribute to efficient LC3 turnover through amphisome formation. In addition, using the wortmannin chase assay, starvation induced GFP-LC3 puncta were cleared after the addition of wortmannin in control and VPS16 knockdown cells but not in Rab7 knockdown cells (Figure 2.7 C), phenocopying what we had observed earlier in thapsigargin treated cells. Taken together, these experiments suggest that although overlaps exist between the autophagic and endocytic pathways, late events in the two pathways such as Rab7 recruitment may be regulated by distinct molecular factors.

2.3 Discussion

In this study, using several assays to monitor autophagic flux, we conclusively show that thapsigargin blocks autophagy, preventing autophagosome maturation and degradation of its contents. We started the study with an interest in the role of ER stress in autophagy and although thapsigargin is an ER stress inducer, its inhibitory effect on autophagy is unrelated to the ER stress response as tunicamycin (another ER stress inducer) does stimulate autophagy and $IRE1^{-/-}$ cells deficient in the ER stress response still displays thapsigargin-induced block in autophagy.

The thapsigargin-induced block occurs in the late stages of the autophagy pathway, after autophagosome formation. By immunocytochemistry, we could detect the presence of cargo adaptor protein p62 in the LC3 positive structures formed as a result of thapsigargin treatment. Numerous closed vesicles morphologically consistent with autophagosomes could also be detected via electron microscopy. Strikingly, we observed a high incidence of vesicle clustering in thapsigargin treated cells. This may be a passive consequence of autophagosome accumulation, or may contribute to the block in fusion either by creating stearic hindrance, (limiting access to endosomes/lysosomes) or interfering with the recruitment of fusion factors.

Perhaps the most interesting aspect of the thapsigargin-induced block in autophagy is that it is specific to autophagy and does not affect the endocytic pathway, which we demonstrated here by monitoring receptor mediated endocytosis and degradation of EGFR. Autophagy and endocytosis are highly interconnected, with both pathways sharing common factors and terminating at lysosomes. Thus far, late events in the two pathways have been difficult to tease apart at a molecular level. Several groups have shown that depleting factors required for the endocytic pathway such as the ESCRT

machinery (Filimonenko et al., 2007; Lee et al., 2007; Rusten et al., 2007) and coatomer protein COP-I (Razi et al., 2009), also disrupts autophagosome turnover, resulting in the accumulation of autophagosome-like structures. As both pathways are affected, the results could be interpreted as either 1) these factors are somehow also directly involved in autophagosome maturation or 2) autophagosome fusion with late endosomes (amphisome formation) contributes significantly to the rate of autophagosome turnover. It is unclear how the ESCRT machinery may influence membrane fusion events as its known function is in mediating membrane scission in the biogenesis of multivesicular bodies (late endosomes) (Wollert et al., 2009). Some factors mediating autophagosome fusion with the endocytic system are known, such as Rab7 (Gutierrez et al., 2004; Jäger et al., 2004; Pankiv et al., 2010), and SNAREs (Fader et al., 2009; Furuta et al., 2010; Moreau et al., 2013). However, as with the ESCRT complex, these components function in the endocytic pathway as well.

Our results with thapsigargin show that late events in the endocytic and lysosomal pathways can be distinguished at a molecular level, suggesting that there are fundamental differences governing autophagosome and endosome maturation. As thapsigargin has no effect on the endocytic pathway, it is likely that thapsigargin generally renders autophagosomes to be "fusion-incompetent" (unable to fuse with either endosomes or lysosomes). In support of this, we observe a failure to recruit fusion factor Rab7 in thapsigargin treated cells. Identification of the thapsigargin-sensitive factors would shed light on the unique molecular handles differentiating autophagosome and endosome fusion with lysosomes.

2.4 Experimental Procedures

Reagents and Antibodies

Rabbit anti-LC3b (L7543) and mouse anti-β actin Clone AC-15 (A1978) were from Sigma. Rabbit anti-Rab7 (#2094S) was from Cell Signaling. Rabbit anti-EGFR (sc-03) were from Santa Cruz Biotech. Rabbit anti-GFP (A11122) was from Invitrogen. Mouse anti-α tubulin (clone DM1A) was from CalBiochem. Mouse anti-P62 (#610832) was from BD Biosciences. Rabbit anti-Vps16 (#17776-1-AP) was from Proteintech Group. Thapsigargin was purchased from Sigma or Enzo Life Sciences with each showing identical effects on autophagy. MISSION shRNA constructs (pLKO-puro) targeting mouse VPS16 (TRCN0000234412) and Rab7 (TRCN0000100883) as well as a non-target control shRNA (SHC002) were purchased from Sigma-Aldrich. All other chemicals were purchased from Sigma.

Cell culture

Cell lines were cultured in Dulbecco's Modified Eagles Media (DMEM), supplemented with 10% fetal bovine serum, 2 mM L-Glutamine and 1X penicillin-streptomycin at 37°C, 5% CO_2. IRE-1 (α/β) null MEFs (Wiseman et al., 2010) were a kind gift from Dr. David Ron, University of Cambridge. Stable expression of transgenes such as GFP-LC3, or shRNA cassettes were carried out by retroviral or lentiviral transduction. Lentiviral or retroviral constructs were co-transfected with packaging vectors into 293Ts for virus production. Virus preparations were passed through a 0.45 μM PES filter and supplemented with polybrene before being used to transduce cells.

Treatment conditions and cell lysis

For starvation treatment, cells were washed twice and incubated in DMEM lacking amino acids and serum for 1 hr unless otherwise indicated. For thapsigargin treatment, cells were incubated with complete media or amino acid free media containing 3 μM thapsigargin for the indicated amount of time. For thapsigargin treatment in combination with bafilomycin or starvation, cells were pre-treated with 3 μM thapsigargin for 2 hr unless otherwise stated. All samples prepared for western analysis were washed twice in cold PBS(-) and lysed in RIPA buffer (50 mM Tris pH 7.5, 150 mM NaCl, 1% Triton X-100, 0.5% sodium deoxycholate, 0.1% sodium dodecyl sulfate) supplemented with protease inhibitors and phosphatase inhibitors (P0044 and P5726 from Sigma). Protein concentration was determined using Bio-Rad Protein Assay Dye reagent (#500-0006).

EGF receptor degradation assay

MEFs were washed twice and incubated in serum-free DMEM for 3 hr. 3 μM thapsigargin or DMSO (for control) was added to indicated plates for an additional 2 hr. Media was then replaced with serum-free DMEM containing 40 ng/ml EGF and 20 μg/ml cycloheximide in the presence or absence of 3 μM thapsigargin or 10 nM bafilomycin. Samples were harvested at the indicated times and lysed in preparation for western analysis.

Wortmannin chase assay

MEFs stably expressing GFP-LC3 were plated onto glass coverslips 24 hrs prior to the experiment. Cells were starved in amino acid free media for 1 hr or incubated in complete media containing 3 μM thapsigargin for 4 hr for the formation of GFP-LC3 puncta followed by the addition of 50 nM wortmannin in starvation media or complete

media containing 3 μM thapsigargin respectively for 1 h. Cells were then fixed in 3.7% formaldehyde, mounted onto microscope slides and visualized by fluorescence microscopy.

Electron microscopy coupled with immunogold labeling

MEFs stably expressing GFP-LC3 were grown on Thermanox coverslips (Nunc). Treatment conditions were carried out as described above. Cells were permeabilized by snap freezing in liquid nitrogen followed by fixation in 3.7% formaldehyde. Immuno-labeling was carried out by incubating with rabbit anti-GFP antibody for 30 min, followed by 3 washes and incubation with anti-rabbit Nanogold Fab fragments for 30 min (Nanoprobes). To enhance the signal, GoldEnhance (Nanoprobes) was used according to manufacturers instructions, with 2 min incubation. Samples were fixed in 2.5 % Glutaraldehyde/ 2 % formaldehyde in 0.075 M Sodium Cacodylate buffer pH 7.5 for 1 hr. Samples were rinsed in Cacodylate buffer and post fixed in 2 % Osmium Tetroxide for 1 hr then rinsed in double distilled water and dehydrated in a graded series of alcohol (50%, 75%, 95% and absolute alcohol), followed by Propylene Oxide and overnight in 1:1 Propylene oxide/ Poly Bed 812 resin. Ultra thin sections were obtained with a Reichert Ultracut S microtome. Sections were stained with Uranyl Acetate and Lead Citrate and imaged using a Jeol 1200 EX 11 transmission electon microscope.

CHAPTER 3. ULK1 IS REGULATED BY PROTEIN PHOSPHATASE 2A

3.1 Introduction

The ULK1 complex is essential for autophagy induced by amino acid starvation (referred to simply as starvation herein) and is directly regulated by energy and nutrient sensing kinases mTORC1 and AMPK (Ganley et al., 2009; Kim et al., 2011; Shang et al., 2011). Physiologically, mTOR kinase is active under nutrient rich conditions and directly phosphorylates ULK1 on multiple serine/threonine (Ser/Thr) sites, resulting in inhibition of ULK1 activity. During starvation, mTORC1 is inactive and inhibitory phosphorylations on the ULK1 complex are lifted, correlating with robust autophagy induction (Ganley et al., 2009; Jung et al., 2009). Thus, the reversible Ser/Thr phosphorylation of ULK1 appears to be a powerful signaling mechanism through which starvation induced autophagy is regulated. Interestingly, I observe that ULK1 is dephosphorylated more rapidly during amino acid starvation compared to pharmacological inhibition of mTORC1. Since mTORC1 inactivation alone is insufficient to account for ULK1 dephosphorylation during starvation, I hypothesize that phosphatase activity toward ULK1 is stimulated by starvation, and may represent another signaling node from which autophagy can be regulated. While the kinases regulating ULK1 phosphorylation are well documented, relatively little is known about the phosphatases involved in this process.

Historically, the study of kinases and phosphatases has been closely intertwined, and understandably so since one catalyses the reverse reaction of the other. The first protein Ser/The phosphatase, “PR enzyme”, was initially discovered by Carl and Gerty Cori in 1945 for its ability to inactivate glycogen phosphorylase, converting it from an active form which they termed “phosphorylase *a*” to an inactive form “phosphorylase

b" (Cori and Cori, 1945). However, it was unclear how PR enzyme was doing this and its biochemical activity as a phosphatase was not recognized until the late 1950s when Fischer and Kerbs identified Phosphorylase Kinase, which converted phosphorylase *b* to phosphorylase *a* by catalyzing the transfer of the γ-phosphate group on ATP to a serine residue on phosphorylase *b* (Fischer et al., 1959; Krebs and Fischer, 1956; Krebs et al., 1958). They then deduced that the "PR enzyme", identified almost a decade earlier, catalysed the reverse reaction resulting in release of inorganic phosphate (Krebs and Fischer, 1956). Thus the concept of reversible protein phosphorylation as a regulatory mechanism was born. This and the subsequent historical development of protein phosphorylation and signal transduction as a field is masterfully chronicled elsewhere by Phillip Cohen (Cohen, 2002) and David Brautigan (Brautigan, 2013).

Sequencing technology has brought us a long way from the days that kinases and phosphatases were identified individually by biochemical purification. Due to the conserved nature of the kinase catalytic domain, potential kinases can be identified based on sequence information. The human genome contains 518 putative kinases, of which 428 are Ser/Thr kinases (Johnson and Hunter, 2005; Manning et al., 2002). Due to differences in catalytic mechanisms, phosphatase prediction is less straightforward as there is little sequence homology between the catalytic domain of different phosphatase families (McConnell and Wadzinski, 2009). This implies that a phosphatase must be known to find other potential members of the same family by this method. Based on the sequence of currently known phosphatases, the human genome is thought to encode approximately 30 putative Ser/Thr phosphatases (Cohen, 2004; Shi, 2009). At a glance, this mismatch in numbers would indicate that each Ser/Thr

phosphatase targets multiple kinase substrates. How then can phosphatase substrate specificity, if any, be achieved?

The protein Ser/Thr phosphatases are broadly characterized into 3 families: the phosphoprotein phosphatase family (PPP), the metal dependent phosphatase family (PPM), and the aspartate-based phosphatase family (FCP), characterized by its founding member, FCP1 (Brautigan, 2013; Shi, 2009). While the PPM and FCP phosphatases are generally thought to function as monomers, relying on additional domains and sequence motifs for substrate recognition, some members of the PPP family form multimeric holoenzyme complexes with a variety of regulatory proteins that determine the subcellular localization, activity and substrate affinity of the catalytic subunit (McConnell and Wadzinski, 2009; Shi, 2009; Virshup and Shenolikar, 2009). This combinatorial approach generates phosphatase holoenzyme diversity that far exceeds what is suggested by the number of genes encoding catalytic subunits alone. In addition, post-translational modifications on catalytic and regulatory subunits add an additional handle for regulating the spatial and temporal assembly of phosphatase complexes (Janssens et al., 2008).

Aside from these 30 classically described Ser/Thr phosphatases, the human genome contains an estimated 60 genes that encode Dual Specificity Phosphatases (DUSPs). The DUSPs are traditionally classified as tyrosine phosphatases (based on their catalytic structure) but can also dephosphorylate Ser/Thr residues (Alonso et al., 2004).

While phosphatases were once erroneously believed to be constitutively active and promiscuous enzymes, this view is slowly being overturned with the continual

discovery of interacting proteins that bind to phosphatase catalytic subunits to regulate their activity. In this Chapter, I monitor two mTORC1 sites on ULK1 and find that more than one phosphatase acts in opposition to mTORC1 to dephosphorylate ULK1 during starvation. I conclusively identify one of the phosphatases regulating ULK1 to be the PP2A-B55α complex, and will discuss regulation of the phosphatase in the following chapter.

3.2 Results

ULK1 is rapidly dephosphorylated during starvation

ULK1 is phosphorylated on multiple sites by mTORC1 and rapidly dephosphorylated during starvation (Ganley et al., 2009). Phosphorylation sites on ULK1 have been mapped by several groups, among which S637 and S757 were identified by three or more independent groups (Egan et al., 2011; Kim et al., 2011; Mack et al., 2012; Shang et al., 2011). Phospho-specific antibodies recognizing ULK1 S637 and S757 phosphorylation (Shang et al., 2011) were used to monitor ULK1 in this study. In collaboration with an attachment student in the lab (Rong Shi), we verified the specificity of the antibodies using *Ulk1*$^{-/-}$*Ulk2*$^{-/-}$ double knockout (ULK1/2 DKO) MEFs reconstituted with Flag-S-doubly tagged ULK1. The antibodies picked up a signal only in cells ectopically expressing ULK1, and decreased upon starvation as previously reported. Interestingly, a kinase dead version of ULK1 (K46I) underwent dephosphorylation at a slower rate compared to wild type ULK1 (Figure 3.1 A).

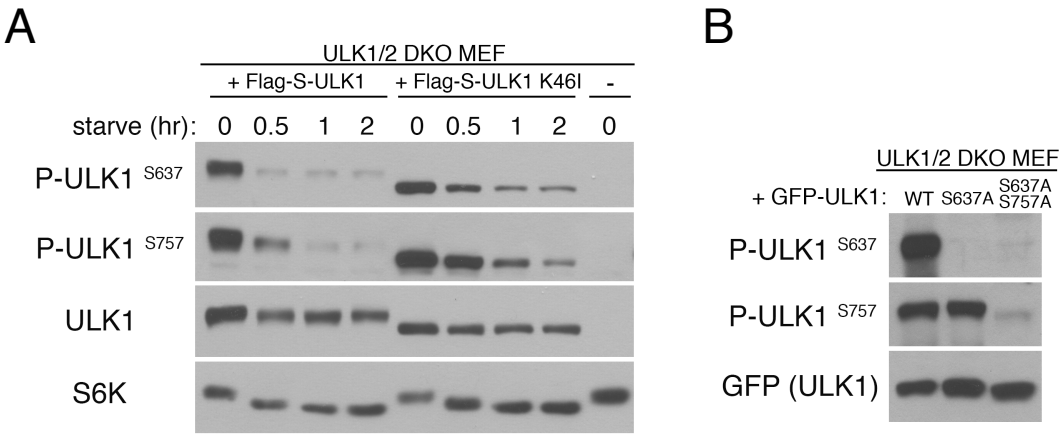

Figure 3.1 ULK1 S637 and S757 phospho antibody validation. (**A**) No signal is detected in ULK1/2 DKO MEFs. The antibodies recognized ectopic ULK1 (WT and K46I mutant) expressed in ULK1/2 DKO MEFs, and the signal was reduced upon starvation, correspondent with dephosphorylation of ULK1. (**B**) The antibodies cannot recognize ULK1 when the respective sites of ULK1 (S637, S757) are mutated to alanine. Panel B was carried out by Rong Shi.

Mutating the respective serine residues to alanine resulted in a loss of signal, indicating that the anitbodies specifically recognize the phosphorylated form of ULK1 (Figure 3.1 B).

Phosphatase activity is required for autophagy induction

To identify the phosphatase for ULK1, I first tested the effect of Okadaic acid (OA), a pharmacological inhibitor of the phosphoprotein phosphatase (PPP) family (Swingle et al., 2007). OA treatment inhibited starvation-induced dephosphorylation of ULK1 at S637 in a dose dependent manner, but had no effect on the dephosphorylation of S6K T389 and other well established mTORC1 substrates 4EBP1 and DAP1 (Figure 3.2 and Figure 3.3 B). Remarkably, OA treatment also did not inhibit dephosphorylation of ULK1 at S757, suggesting that more than one phosphatase is involved in the regulation of ULK1 (Figure 3.2). As a positive control, OA could inhibit

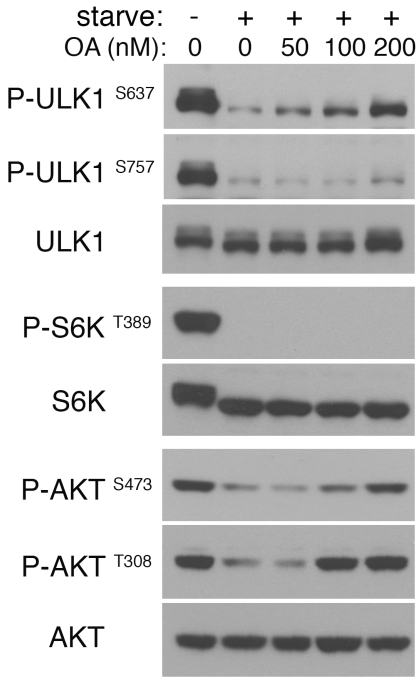

Figure 3.2 Okadaic Acid (OA) inhibits ULK1 S637 dephosphorylation in a dose dependent manner. MEF cells were incubated in starvation media with increasing amounts of OA for 1 hr. Phosphorylation on ULK1 and S6K were monitored using site specific phospho-antibodies. AKT, previously reported as OA sensitive, was included as a positive control for OA treatment.

dephosphorylation of AKT, which has been reported to be sensitive to OA (Gao et al., 2005). This observation was consistent in all tested cell lines, ruling out the possibility of a cell line specific artifact (Figure 3.3 A)

The inhibition in ULK1 dephosphorylation translated to a decrease in autophagy response to starvation as evidenced by reduced lipidation of endogenous LC3 and decreased puncta formation of GFP-LC3 in the presence of OA (Figure 3.3 B and C). Autophagy is a multistep process that ultimately leads to autophagosome fusion with lysosomes hence it is conceivable that OA treatment may affect dephosphorylation of proteins other than ULK1 to bring about the block in autophagy. However, as the ULK1 complex has been shown to be indispensible for efficient induction of autophagy in response to starvation, I favor the hypothesis that ULK1 dephosphorylation is one of the key events being blocked. In support of this, two early events in autophagosome formation: the translocation of ULK1 itself and recruitment of ATG16 complex to punctate structures is greatly reduced in OA treated cells (Figure 3.3 C).

PP2A dephosphorylates ULK1 at S637

OA is a potent inhibitor of several PPP family members, with a reported IC50 in the nano molar range when used *in vitro* (Swingle et al., 2007). Of the PPP family members inhibited by OA, PP1 and PP2A are the most abundant and ubiquitously expressed in cells, hence were the clearest candidates to start off with. Knockdown of the PP2A catalytic subunit (PP2AC) or scaffolding subunit (PRL65) clearly blocked starvation induced dephosphorylation of Ulk1 at S637 (Figure 3.4 A and B) whereas knockdown of PP1 catalytic subunit (PP1C) had no effect despite a near complete depletion of PP1C (Figure 3.4 C). Remarkably, knockdown of either

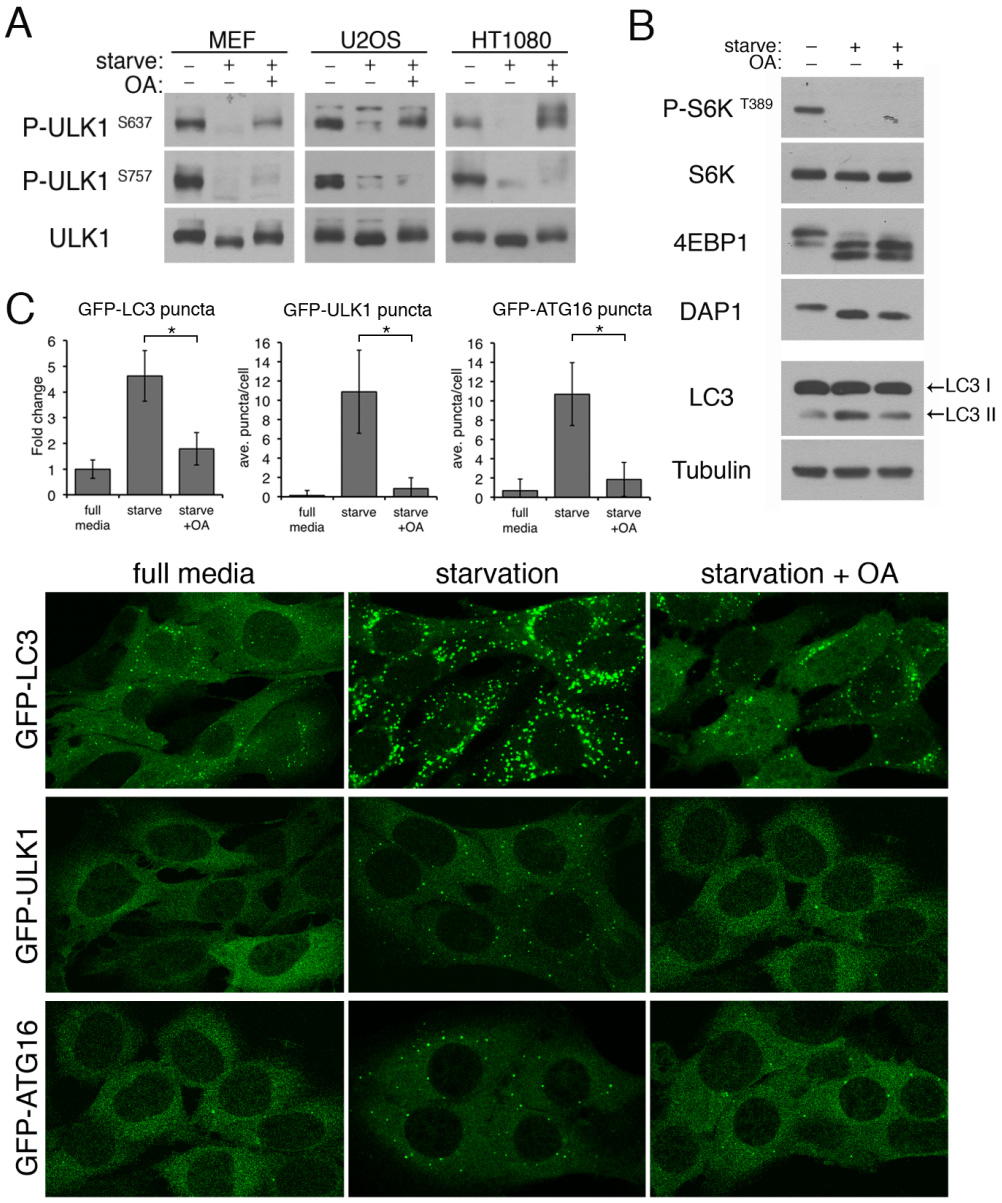

Figure 3.3 Okadaic acid (OA) treatment inhibits autophagy. (**A**) OA inhibits the dephosphorylation of ULK1 at S637 but not S757. MEF, U2OS or HT1080 cells were incubated in starvation media or starvation media with 200 nM OA for 1 hr. (**B**) MEFs were treated as in (A) and lysates were probed for three reported mTOR substrates (S6K, 4EBP1 and DAP1) and endogenous LC3. (**C**) MEFs stably expressing GFP-LC3, GFP-ULK1 or GFP-ATG16 were incubated in starvation media or starvation media containing 200 nM OA for 1 hour. Cells were fixed and imaged for GFP-LC3, GFP-ULK1 or GFP-ATG16 translocation. Average number of puncta per cell were quantitated and expressed as such or as fold change relative to full media (fold change or mean ± s.d., n=20. two-tail student's t-Test, * $p<0.05$).

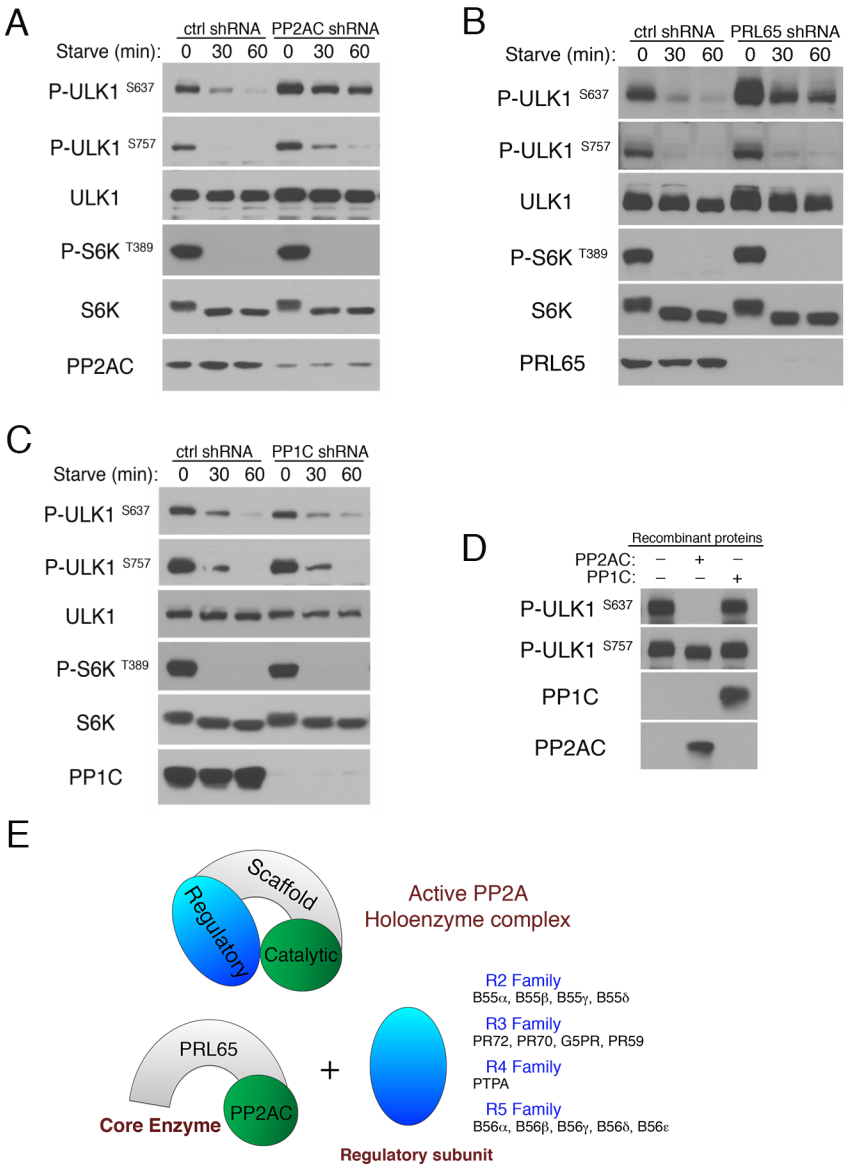

Figure 3.4 PP2A but not PP1 dephosphorylates ULK1 at S637. (**A, B**) PP2A is required for dephosphorylation of ULK1 at S637. MEFs were transduced with lentivirus containing control shRNA, shRNA targeting the catalytic subunit of PP2A (PP2AC) or scaffolding subunit of PP2A (PRL65). 48-72 hrs post transduction, cells were incubated in starvation media and lysed for immuno-blotting. (**C**) PP1C is not required for ULK1 dephosphorylation. MEF cells were treated as in (A) with shRNA targeting the catalytic subunit of PP1 (PP1C). (**D**) PP2AC directly dephosphorylates ULK1 S637 in vitro. Catalytic subunit of PP1 (PP1C) was included as a control. Flag-S-ULK1 substrate was incubated with 50 nM of recombinant PP2AC or PP1C at 30^{o}C for 20 min. (**E**) Diagram representing the PP2A Ser/Thr phosphatase complex. Regulatory subunits confer substrate specificity to the core enzyme.

phosphatase had no significant effect on S757 dephosphorylation, supporting my earlier observation that S757 is regulated by a different phosphatase. In order to verify that ULK1 is a direct substrate of PP2A, I carried out an *in vitro* phosphatase reaction using recombinant proteins of PP1 and PP2A catalytic subunits. Indeed, the substrate specificity displayed in cells could also be recapitulated *in vitro* as PP2AC but not PP1C could dephosphorylate ULK1 at S637 and neither phosphatase could dephosphorylate ULK1 at S757 (Figure 3.4 D).

Identification of PP2A regulatory subunit involved in autophagy

In cells, PP2A functions as a heterotrimer consisting of a catalytic subunit, a scaffolding subunit and a variable regulatory subunit (Figure 3.4 E). It is generally thought that the regulatory subunit confers substrate specificity and thus dictates the biological function of the phosphatase complex (Janssens et al., 2008; Mumby, 2007). I sought to identify the regulatory subunit targeting ULK1 by biochemical fractionation, hence developed an in vitro assay to measure phosphatase activity against ULK1 (Figure 3.5). With great help from my thesis advisor, Dr. Xuejun Jiang, we were able to purify the regulatory subunit from whole cell lysate after a series of

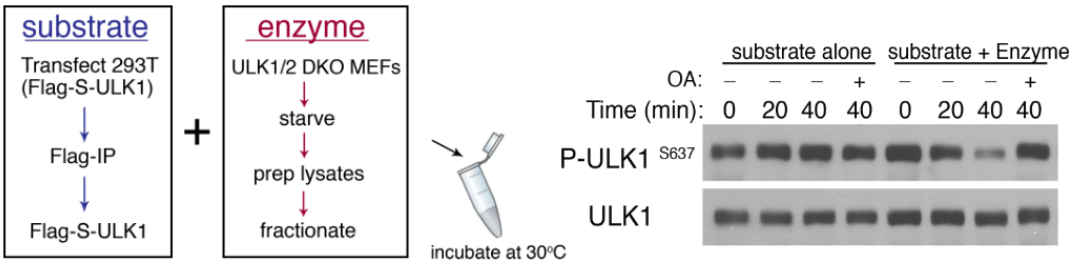

Figure 3.5 Set up of *in vitro* phosphatase assay used to purify regulatory subunit. Left panel shows a shematic of the phosphatase assay. The substrate (Flag-S-ULK1) was expressed in 293Ts to ensure proper phosphorylation and isolated by Flag immune-precipitation. Right panel shows the reaction. The substrate is stable in the reaction over time and dephosphorylated only in the presence of an enzyme source (total or fractionated cell extract).

seven chromatographic steps (Figure 3.6 A). Large scale cultures of ULK1/2 DKO MEFs were used for the fractionation as they lacked endogenous ULK1 that could interfere with the assay results. After each run of a chromatographic column, fractions were analyzed for phosphatase activity against ULK1 S637. A representative example is shown in Figure 3.6 B. Active fractions were combined and loaded onto the next column. From relatively early on in the purification, it was clear that only a sub population of PP2A in the cell could dephosphorylate ULK1 S637 (Figure 3.6 B and C). Fractions from the final column were analyzed by SDS-PAGE followed by silver staining (Figure 3.6 D). Three distinct bands at 36 kDa, 65 kDa and 55 kDa could be detected in fractions that correlated with phosphatase activity against ULK1 S637. As expected, mass spectrometry analysis identified the 36 kDa and 65 kDa bands to be the PP2A catalytic and scaffolding subunits respectively. The 55 kDa band was PP2A regulatory subunit B55α (Figure 3.7). As an initial validation step the purification was repeated with minor changes to the original scheme and fractions were analyzed for B55α distribution (Figure 3.6 E). B55α correlated perfectly with PP2AC-containing fractions that were active against ULK1 (Figure 3.6 E, fractions 11 and 12). In line with being a regulatory subunit with no catalytic activity on its own, fractions containing B55α but no PP2AC had no activity against ULK1 (Figure 3.6 E, fractions 7 and 8).

Regulatory subunit B55α directs PP2A phosphatase activity against ULK1

To verify that B55α was truly the regulatory subunit directing PP2A activity towards ULK1 in cells, I carried out shRNA knockdown of B55α using a lentiviral based tet-inducible system. Two independent shRNAs targeting B55α were designed, one targeting the 3'UTR region of B55α (shRNA1) and another targeting the coding region of B55α (shRNA2). Both shRNA sequences efficiently inhibited ULK1

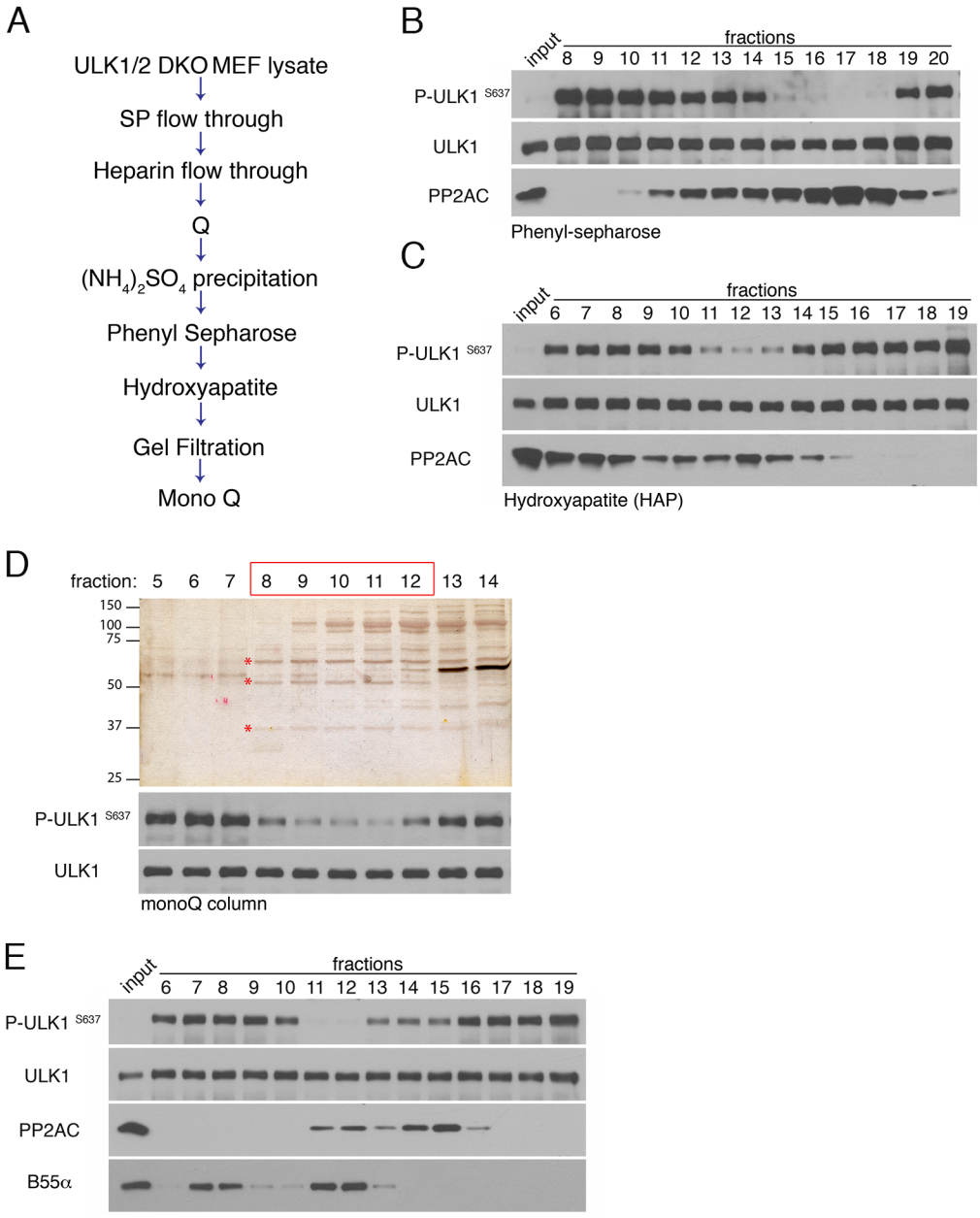

Figure 3.6 Identification of PP2A regulatory subunit by biochemical purification. (**A**) Purification scheme used to identify the PP2A regulatory subunit from starved ULK1/2 DKO cell lysate. (**B**,**C**) Examples of phosphatase assay reaction during PP2A regulatory subunit purification. Fractions from Phenyl Sepharose column and Hydroxyapatite column were assessed for activity against ULK1. (**D**) Silver staining (top) and phosphatase activity assay (bottom) of fractions from the final purification step. Active fractions are boxed in red. Indicated bands were excised for mass spectrometric analysis. (**E**) Western blot showing distribution of PP2AC, B55α, and ULK1 S637 phosphatase activity after a Q column.

A

Serine/threonine-protein phosphatase 2A catalytic subunit beta isoform (PPP2CB)

```
  1 MDDKAFTKEL DQWVEQLNEC KQLNENQVRT LCEKAKEILT KESNVQEVRC
 51 PVTVCGDVHG QFHDLMELFR IGGKSPDTNY LFMGDYVDRG YYSVETVTLL
101 VALKVRYPER ITILRGNHES RQITQVYGFY DECLRKYGNA NVWKYFTDLF
151 DYLPLTALVD GQIFCLHGGL SPSIDTLDHI RALDRLQEVP HEGPMCDLLW
201 SDPDDRGGWG ISPRGAGYTF GQDISETFNH ANGLTLVSRA HQLVMEGYNW
251 CHDRNVVTIF SAPNYCYRCG NQAAIMELDD TLKYSFLQFD PAPRRGEPHV
301 TRRTPDYFL
```

sequence coverage: 38.5%

B

Serine/threonine-protein phosphatase 2A 65 kDa regulatory subunit A alpha isoform (PPP2R1A)

```
  1 MAAADGDDSL YPIAVLIDEL RNEDVQLRLN SIKKLSTIAL ALGVERTRSE
 51 LLPFLTDTIY DEDEVLLALA EQLGTFTTLV GGPEYVHCLL PPLESLATVE
101 ETVVRDKAVE SLRAISHEHS PSDLEAHFVP LVKRLAGGDW FTSRTSACGL
151 FSVCYPRVSS AVKAELRQYF RNLCSDDTPM VRRAAASKLG EFAKVLELDN
201 VKSEIIPMFS NLASDEQDSV RLLAVEACVN IAQLLPQEDL EALVMPTLRQ
251 AAEDKSWRVR YMVADKFTEL QKAVGPEITK TDLVPAFQNL MKDCEAEVRA
301 AASHKVKEFC ENLSADCREN VIMTQILPCI KELVSDANQH VKSALASVIM
351 GLSPILGKDN TIEHLLPLFL AQLKDECPEV RLNIISNLDC VNEVIGIRQL
401 SQSLLPAIVE LAEDAKWRVR LAIIEYMPLL AGQLGVEFFD EKLNSLCMAW
451 LVDHVYAIRE AATSNLKKLV EKFGKEWAHA TIIPKVLAMS GDPNYLHRMT
501 TLFCINVLSE VCGQDITTKH MLPTVLRMAG DPVANVRFNV AKSLQKIGPI
551 LDNSTLQSEV KPILEKLTQD QDVDVKYFAQ EALTVLSLA
```

sequence coverage: 37.2%

C

Serine/threonine-protein phosphatase 2A 55 kDa regulatory subunit B alpha isoform (PPP2R2A)

```
  1 MAGAGGGNDI QWCFSQVKGA VDDDVAEADI ISTVEFNHSG ELLATGDKGG
 51 RVVIFQQEQE NKIQSHSRGE YNVYSTFQSH EPEFDYLKSL EIEEKINKIR
101 WLPQKNAAQF LLSTNDKTIK LWKISERDKR PEGYNLKEED GRYRDPTTVT
151 TLRVPVFRPM DLMVEASPRR IFANAHTYHI NSISINSDYE TYLSADDLRI
201 NLWHLEITDR SFNIVDIKPA NMEELTEVIT AAEFHPNSCN TFVYSSSKGT
251 IRLCDMRASA LCDRHSKLFE EPEDPSNRSF FSEIISSISD VKFSHSGRYM
301 MTRDYLSVKI WDLNMENRPV ETYQVHEYLR SKLCSLYEND CIFDKFECCW
351 NGSDSVVMTG SYNNFFRMFD RNTKRDITLE ASRENNKPRT VLKPRKVCAS
401 GKRKKDEISV DSLDFNKKIL HTAWHPKENI IAVATTNNLY IFQDKVN
```

sequence coverage: 43.2%

Figure 3.7 Mass spectrometry analysis of p36, p65 and p50 bands from ULK1 phosphatase purification. The peptides detected during mass spectrometry analysis are shown in red. (**A**) The p36 band produced peptide fragments that matched to the catalytic subunit of PP2A with a sequence coverage of 38.5%. (**B**) Peptide fragments from the p65 band matched to the scaffolding subunit of PP2A with a sequence coverage of 37.2%. (**C**) Peptide fragments from the p50 band matched to the B55α regulatory subunit of PP2A with a sequence coverage of 43.2%. Identified proteins: At $p<0.01$, average false discovery rate, FDR: 0%.

dephosphorylation at S637 (Figure 3.8 A) and resulted in a reduction in starvation-induced autophagy, as assessed by turnover of endogenous LC3 as well GFP-LC3 puncta formation (Figure 3.8 A and C). Expression of shRNA resistant Flag-S-B55α was sufficient to reverse the effects of B55α knockdown on ULK1 S637 dephosphorylation, indicating that the inhibition in dephosphorylation is specifically due to reduction in B55α levels (Figure 3.8 B).

Crystal structure data of the PP2A hetero-trimer suggests that the regulatory subunit greatly facilitates substrate recognition and recruitment (Xu et al., 2008). I therefore checked if B55α could interact with ULK1 in cells. Upon co-overexpression of ULK1 together with either B55α or an unrelated regulatory subunit from another family (PR72), I found that ULK1 could interact more strongly with B55α compared to PR72, suggesting that B55α indeed plays a significant role in directing the PP2A complex to ULK1 in cells.

To demonstrate that B55α makes PP2A a more efficient phosphatase towards ULK1, I reconstituted the phosphatase reaction *in vitro* using recombinant proteins of PP2AC, PRL65 and B55α. Recombinant PP2AC and PRL65 were co-expressed in insect cells using baculovirus vectors while B55α was expressed and purified to homogeneity separately. As I had shown previously that PP2AC alone is sufficient to dephosphorylate ULK1 *in vitro* when used at sufficiently high concentrations (Figure 3.4 D), I titrated down the amount of PP2AC in the reaction from the 50 nM used earlier to 5 nM. When used at 5 nM on its own, the catalytic subunit could barely dephosphorylate ULK1 after 20 min of incubation at 30 ^{o}C. However, with the addition of B55α to the reaction, the same amount of PP2AC could dephosphorylate ULK1 much more efficiently. The stimulatory effect of B55α on PP2A activity

occurred in a dose dependent manner and B55α alone when used at its highest dose had no phosphatase activity against ULK1, indicating that the increase in phosphatase activity was due to a synergistic effect between B55α and PP2AC rather than an experimental artifact due to contaminating phosphatases in the protein preparation (Figure 3.8 E).

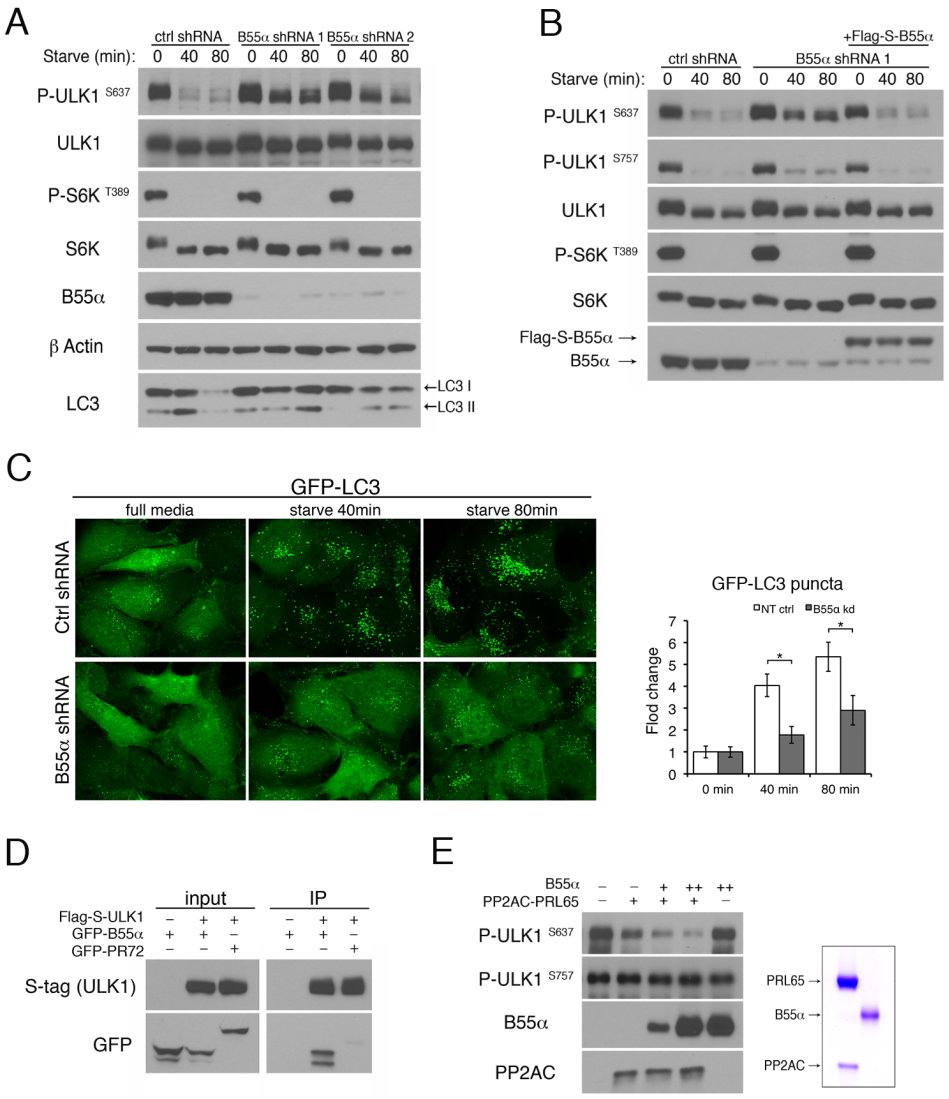

Figure 3.8 Regulatory subunit B55α directs PP2A phosphatase activity against ULK1. (**A**) B55α is required for ULK1 S637 dephosphorylation. HT1080 cells expressing tet-inducible shRNAs were cultured in 100 ng/ml Doxycycline and incubated in starvation media. (**B**) Over- expression of Flag-S- B55α can rescue the effect of B55α shRNA1 in HT1080. (**C**) Knockdown of B55α in HT1080 blocks starvation-induced autophagy as monitored by florescence imaging of GFP-LC3. Average number of puncta per cell was quantitated and expressed as fold change relative to 0 min (fold change ± s.d., n=20. two-tail student's t-Test, * $p<0.05$) (**D**) ULK1 interacts preferentially with B55α. 293Ts were co-transfected with Flag-S-ULK1 and GFP-B55α or GFP-PR72 (regulatory subunit from a different family). Cells were lysed and incubated with S-beads. (**E**) B55α stimulates PP2A activity towards ULK1. In vitro phosphatase assay was carried out using 5 nM of recombinant PP2AC co-purified with PRL65 and increasing amounts of B55α (10 nM or 40 nM). Coomassie brilliant blue staining of recombinant protein preparations is shown on the right.

3.3 Discussion

For awhile okadaic acid has been known to inhibit autophagy in hepatocytes (Blankson et al., 1995; Holen et al., 1993) and some neurodegenerative models (Magnaudeix et al., 2013) but it was never clear how this occurred mechanistically. Here we show that OA exerts its inhibitory effects at an early stage of autophagy and identify an OA sensitive phosphorylation site on key autophagy protein; ULK1. It should be noted that as many as 30 phosphorylation sites on ULK1 has been detected by mass spectrometry (Dorsey et al., 2009; Wong et al., 2013). Hence data on the two sites monitored in this study (S637 and S757) each most likely represent the behavior of a subset of phosphorylation sites on ULK1. Although it is not addressed in this study, OA may block dephosphorylation of other early autophagy genes as well, such as Beclin 1, a reported substrate of AKT (Wang et al., 2012), and ATG13, which is also a member of the ULK1 complex and a reported substrate of mTORC1 (Jung et al., 2009).

Through a combination of pharmacological inhibition, shRNA knockdown and biochemical fractionation, I identified the phosphatase regulating ULK1 S637 to be the PP2A-B55α complex. Prior to this study, two PP2A complexes had been implicated in the regulation of autophagy in drosophila, although the substrates of PP2A were not identified (Bánréti et al., 2012). Interestingly, while the effects on ULK1 S637 were clear, in my hands OA treatment and subsequently knockdown of PP2AC did not affect dephosphorylation of other mTOR substrates S6K and 4EBP1, suggesting that different substrates of the same kinase may be regulated by distinct phosphatases. The substrate specificity of PP2A is also demonstrated at an intra-molecular level as the second site monitored in this study (ULK1 S757) was not dephosphorylated by PP2A in both our cellular experiments and in all subsequent *in*

vitro phosphatase assays. As there are numerous examples of multiple kinases targeting different sites on the same protein, it perhaps should not come as a surprise that the same phenomenon may be true for phosphatases. A search of literature revealed that AKT is also regulated by more than one phosphatase, with AKT T308 being a substrate of PP2A while dephosphorylation of AKT S473 is mediated by PHLPP (PH domain leucine-rich repeat protein phosphatase); a member of the PPM phosphatase family (Gao et al., 2005).

The PP2A holoenzyme is a hetero trimer consisting of a scaffolding (A), a regulatory subunit (B) and a catalytic (C) subunit (Eichhorn et al., 2009). As we and others have shown, the core enzyme consisting of the A-C dimer has activity *in vitro* when used at sufficiently high concentrations (Xu et al., 2008). This may have contributed to early views of PP2A as a promiscuous enzyme. It is not clear if A-C dimmers without regulatory subunits exist in the cell. In this study, I identified the regulatory subunit targeting PP2A to ULK1 to be B55α and demonstrated that B55α can synergistically increase PP2A activity towards ULK1 *in vitro*, supporting its proposed function in substrate recruitment (Xu et al., 2008). During the purification of B55α, it was clear that only a sub population of PP2A in the cell could dephosphorylate ULK1 S637. Depletion of B55α also greatly impaired starvation induced ULK1 S637 dephosphorylation and autophagy induction, indicating that the PP2A-B55α complex mediates autophagy induction.

PP2A regulatory subunits are classified into four distinct families, termed R2/PR55/B, R3/PR72/B'', R4 and R5/PR61/B' with little sequence homology between families (Janssens et al., 2008; Mumby, 2004). The B55α subunit is reported to be one of the most widely expressed regulatory subunits in cells (Mumby, 2004) and has been

reported to target PP2A other substrates including AKT (Kuo et al., 2008), FOXO1 (Yan et al., 2012), retinoblastoma protein (Rb) family member p107 (Kolupaeva et al., 2013), and microtubule subunit Tau (Xu et al., 2008), though the conditions under which these substrates are dephosphorylated are not always well documented. It is thus possible that in addition to ULK1, other substrates are being dephosphorylated by PP2A-B55α during starvation as well. On the other hand, given the complexities of signaling networks in the cell, additional targeting mechanisms could be in place to limit the number of substrates being dephosphorylated by PP2A-B55α during starvation, such as localized activation of PP2A-B55α, and maintaining or increasing the activity of kinases regulating other PP2A-B55α substrates during starvation to compensate for PP2A-B55α activity.

3.4 Experimental Procedures

Reagents and Antibodies

Rabbit anti-LC3b (L7543), mouse anti-β actin Clone AC-15 (A1978), mouse anti-B55α Clone 2G9 (SAB4200241) were from Sigma. Mouse anti-α tubulin (clone DM1A) was from CalBiochem. Rabbit anti-phos S6K (Thr389) (9205), Rabbit anti-S6K (2708), Rabbit anti-4EBP1 (9452), rabbit anti-PRL65 Clone 81G5 (2041), rabbit anti-DAP1 (2282), rabbit anti-His Tag (2365), rabbit anti-B subunit (2290) were from Cell Signaling. Rabbit anti-phos-ULK1 (S637) and rabbit anti-phos-ULK1 (S757) were a generous gift from Dr. Xiaodong Wang, National Institute of Biological Science, Beijing, China. N.B. corresponding sites in human ULK1 are S638 and S758 respectively. Rabbit anti-total ULK1 (A7481) used to detect mouse ULK1 was purchased from Sigma. Rabbit anti-total ULK1 (sc33182) used to detect human ULK1, rabbit anti-PP2AC (sc130237) and mouse anti-PP1C (sc7482) were from Santa Cruz. Mouse anti-S-tag antibody (71549-3) was from Novagen. Mouse anti-PP2AC clone 1D6 (05-421) was from Millipore. Okadaic acid was purchased from Sigma (O9381) or Enzo Life sciences (ALX-350-003) with each showing identical effects on ULK1 dephosphorylation.

Cell culture

MEFs and U2OS cell lines were cultured in Dulbecco's Modified Eagles Media (DMEM), supplemented with 10% fetal bovine serum, 2 mM L-Glutamine and 1X penicillin-streptomycin at 37°C, 5% CO_2. ULK1/2 DKO MEF cells were courtesy of Dr. Craig Thompson, Memorial Sloan Kettering Cancer Center, New York, USA. Stable expression of transgenes such as GFP-LC3, Flag-S-B55α, or shRNA cassettes were carried out by retroviral or lentiviral transduction. Lentiviral or retroviral constructs were co-transfected with packaging vectors into 293Ts for virus production.

Retro/Lentivirus preparations were passed through a 0.45 μM PES filter and supplemented with polybrene before being used to transduce cells.

Treatment conditions and cell lysis

For amino acid starvation experiments, cells were washed twice and incubated in DMEM lacking amino acids and serum for the indicated amount of time. For Okadaic acid (OA) treatments to inhibit PPP family phosphatases, as OA is a hydrophobic inhibitor, cells were pretreated with 200 nM OA in full media before switching to starvation media with 200 nM OA to allow time for cellular uptake of OA.

All samples prepared for western analysis were washed twice in cold PBS(-) and lysed in RIPA buffer (50 mM Tris pH 7.5, 150 mM NaCl, 1% Triton X-100, 0.5% sodium deoxycholate, 0.1% sodium dodecyl sulfate) supplemented with protease inhibitors and phosphatase inhibitors (P0044 and P5726 from Sigma). Protein concentration was determined using Bio-Rad Protein Assay Dye reagent (#500-0006).

Fluorescence microscopy

Cells stably expressing the GFP tagged protein for visualization were plated onto glass coverslips 24 hours prior to the experiment. Following treatment, cells were fixed in 3.7% formaldehyde for 20 min. Cover slips were washed and mounted onto microscope slides using ProLong Gold antifade reagent with DAPI (Molecular probes). Slides were visualized on a Nikon Eclipse TE2000-U microscope or a Nikon Eclipse Ti-U confocal Microscope. Acquired images were processed using Adobe Photoshop.

In vitro dephosphorylation assay

Generation of substrate (Flag-S-ULK1) used in phosphatase assays

ULK1 substrate was generated in a mammalian system to ensure proper phosphorylation. pBabe-Flag-S-ULK1 construct generated previously (Ganley et al., 2009) was transfected into 293T cells using Lipofectamine2000 (Invitrogen) according to the manufacturer's recommendations. Cells were split 24 hours post transfection to prevent overgrowth and harvested 48 hours post transfection. Cells were lysed in phosphatase assay buffer (50 mM Hepes, pH 7.5, 100 mM NaCl, 2 mM $MgCl_2$, 1 mM DTT, 0.5% NP-40) supplemented with protease inhibitors and phosphatase inhibitors (P0044 and P5726 from Sigma) to preserve phosphorylation. Lysate was incubated with Anti-Flag M2 affinity gel (A2220 from Sigma) at 4^{o}C with rotation overnight. Following 4-5 washes, Flag-S-ULK1 substrate was eluted in phosphatase assay buffer containing 400 μg/ml 3X FLAG peptide (Sigma).

The Flag-S-ULK1 substrate was stable in reactions containing cell lysate but not in buffer alone when incubated at 30^{o}C. To stabilize the substrate in reactions that use recombinant phosphatases, we used ULK1/2 DKO MEF cell lysate devoid of phosphatase activity. To generate this protective lysate, we incubated ULK1/2 DKO MEF cell lysate (in 20 mM Hepes pH 7.5, 50 mM KCl, 5 mM Pi, 1 mM DTT + 0.5% NP-40 buffer) with hydroxyapatite beads at 4^{o}C overnight with rotation. Approximately 50 μl bead volume was used per mg of total cell lysate. Protective lysate was tested for ability to stabilize Flag-S-ULK1 substrate and lack of remnant phosphatase activity before use in assays (Figure 4A). Incubation with hydroxyapatite beads was repeated if phosphatase activity was not completely depleted. Protective lysate was concentrated in a Amicon Ultra-4 centrifugal filter unit (UFC801024 from EMD Millipore) if total protein concentration was too low.

For phosphatase assays with cell lysate: Flag-S-ULK1 substrate was incubated with 10 μg of total cell lysate at 30°C for the indicated amount of time. For phosphatase assays with recombinant proteins or for biochemical purification of B55α subunit: Flag-S-ULK1 substrate plus 7-10 μg of phosphatase-depleted protective lysate was incubated with recombinant proteins or column eluted fractions at 30°C for 20 min.

Biochemical purification of B55α subunit

A 20 ml cell pellet of starved ULK1/2 DKO MEF cells was lysed by douncing in 90 ml of Buffer A (20 mM Hepes pH 7.5, 10 mM NaCl, 1 mM DTT). Cell lysate was centrifuged at 10'000 rpm for 10 min at 4°C. Supernatant was further clarified by centrifugation at 45'000 rpm for 1 hour at 4°C. Clarified cell lysate was loaded into SP column. Flow-through from SP column was collected and loaded into Heparin column. Flow-through from Heparin column was collected and loaded into Q column (Buffer A: 20 mM Hepes pH 7.5, 10 mM NaCl, 1 mM DTT; Buffer B: 20 mM Hepes pH 7.5, 1000 mM NaCl, 1 mM DTT). Q column was washed with 15%B and eluted with 35% Buffer B. Ammonium sulfate was added to a final concentration of 20% and incubated at 4°C for 30 min. Precipitated proteins were removed by centrifugation at 20,000 rpm for 10 min. Supernatant was collected and diluted to 10% Ammonium sulfate before loading into a Phenyl Sepharose column (Buffer A: 5 mM Hepes pH 7.5, 1 mM DTT; Buffer B: 20% Ammonium sulfate, 20 mM Hepes pH 7.5, 400 mM NaCl, 1 mM DTT). Phenyl Sepharose column was eluted with a gradient of 50% to 0% Buffer B across 20 fractions. Fractions were dialysed and assayed for activity. Active fractions were combined and loaded into Hydroxyapatite column (Buffer A: 20 mM Hepes pH 7.5, 10 mM NaCl, 1mM DTT; Buffer B: 1M Pi, 1mM DTT pH 7.5). Column was washed with 3% Buffer B and eluted with a gradient of 3% to 18%

Buffer B across 20 fractions. Fractions were dialysed and assayed for activity. Active fractions were combined and concentrated with a Q-column. Gel filtration column was run and active fractions were combined and loaded into a mono Q column (same buffer conditions as Q column). Mono-Q column was washed with 18% Buffer B (180 mM NaCl) and eluted in 20 x 1 ml fractions across a 19% Buffer B (190 mM NaCl) to 34% Buffer B (340 mM NaCl) gradient. 8 µl of each fraction was assayed for activity.

Purification of recombinant proteins

The full length of human PP2A catalytic subunit (PP2AC, α isoform NM_002715) or regulatory subunit B55α (human, NM_002717) was cloned into baculovirus transfer vector pFastBac as N-terminal 9x His-tagged proteins. Full length human PP2A scaffolding subunit (PRL65, α isoform NM_014225) was cloned into pFastBac as N-terminal 9x His and Flag tandem-tagged proteins. Recombinant baculovirus was produced using Bac-to-Bac expression system from Invitrogen. PP2AC and PRL65 were co-expressed in a suspension culture of Sf9 cells for co-purification. Briefly, cell pellets were lysed by douncing and purified by Ni-NTA resin, followed by gel filtration to isolate fractions containing both PP2AC and PRL65. B55α was expressed in Sf9 cells and purified by Ni-NTA resin followed by ion exchange chromatography through a Q column.

Knockdown by shRNA

The following shRNA constructs were purchased from Sigma: pLKO non-target control (CAACAAGATGAAGAGCACCAA), pLKO mPP2AC shRNA (GCGACATTGTTGGTCAAG AAT), pLKO mPRL65 shRNA (GCCACCAGCAACCTTAAGAAA), pLKO mPP1C shRNA (CCAGATCGTTTGTACAGAAAT). The following shRNAs were cloned into

pLKOtet-ON inducible shRNA plasmid system purchased from Addgene: hB55α sh 1 (TCCTGCTTAGTTGAGATAGTT), hB55α sh 2 (GTAGATGATGATGTAGCAGAA). Lenti- viruses were made by co-transfecting shRNA constructs and packaging vectors into 293Ts. Lentiviral preparations were passed through a 0.45 μM PES filter and supplemented with polybrene before being used to transduce cells. Stable cell lines were typically assayed for knockdown 48-72 hours post transduction. For inducible knockdown, cell lines were grown in complete media containing 100 ng/ml Doxycycline 48-72 hours before assaying for knockdown.

Expression constructs

Autophagy marker LC3 was subcloned into pBabe/blast vector containing N-terminal GFP tag. pMIC vector was made by modifying pMIG vector (Addgene) to replace GFP in the backbone with mCherry. The coding sequence (cds) of human B55α or human PP2AC were cloned into pMIC vector along with an N-terminal Flag-S tandem tag. pMSCV GFP-B55α and pMSCV GFP-PR72 used in immunoprecipitation experiments were a generous gift from Dr. Emily Foley, Memorial Sloan Kettering Cancer Center, New York, USA.

Immunoprecipitations

Constructs expressing Flag-S-ULK1 and GFP-B55α or GFP-PR72 were co-transfected into 293Ts using Lipofectamine 2000 (Invitrogen) according to the manufecturer's recommendations. 24-48 hours post transfection, cells were washed twice in cold PBS(-) and lysed in IP buffer (20 mM Tris pH 7.5, 150 mM NaCl, 1 mM DTT, 0.5% Triton X-100) supplemented with protease inhibitors. Cell lysate was centrifuged at 20,000 x g for 10 min at 4^{o}C and incubated with 10 μl of S-protein agarose beads (69704 from EMD Millipore) in a total volume of 1 ml overnight at 4^{o}C with rotation.

CHAPTER 4. PHOSPHATASE ACTIVITY IS STIMULATED BY AMINO ACID STARVATION

4.1 Introduction

Amino acid starvation is a well characterised trigger for autophagy in both yeast and mammalian cells. At the center of signaling events leading to starvation-induced autophagy is inactivation of the mTOR kinase and concurrent activation of the ULK1 complex (Chan, 2009; Ganley et al., 2009). ULK1 is a direct substrate of mTORC1 at several sites including S637 and S757 and undergoes global dephosphorylation upon starvation (Shang et al., 2011). In the previous chapter, I identified the phosphatase complex regulating ULK1 S637 to be PP2A-B55α.

PP2AC is one of the most abundant and ubiquitously expressed Ser/Thr phosphatases in the PPP family. In some cell types, it may account for up to 1% of total cellular proteins (Slupe et al., 2011). PP2A has been implicated in the regulation of many cellular processes including cell survival, cell cycle control, proliferation and death, cytoskeletal dynamics and migration (Shi, 2009; Virshup and Shenolikar, 2009). Given its abundance and involvement in multiple cellular processes, regulation of PP2A is understandably complex. PP2A functions as a heterotrimeric complex composed of a catalytic (PP2AC), a scaffolding (PRL65) and a variable regulatory subunit that is thought to play a role in substrate recognition and recruitment. In addition to the canonical regulatory subunit family which consists of ~15 genes, a host of other proteins have been reported to interact with PP2A, modulating its activity (Goudreault et al., 2009; Herzog et al., 2012). The PP2A complex is tightly regulated at every stage, from transcription and translation of its individual complex components

to post translational modifications that may regulate phosphatase complex stability and assembly (Janssens et al., 2008).

In this study, I look into the regulation of PP2A activity on ULK1 during starvation-induced autophagy. Under fed conditions the PP2A catalytic subunit is sequestered by inhibitory protein Alpha4, keeping it in an inactive state. Starvation triggers the release of PP2A from this latent complex, while Torin1 treatment does not, correlating with faster dephosphorylation of ULK1 and autophagy induction during starvation. In addition, I found that this phosphatase activity is abnormally high in Pancreatic Ductal Adenocarcinoma cell line 8988T, which requires high basal autophagy for optimal fitness. I propose that activation of the phosphatase activity toward ULK1 represents a mechanism that allows cancer cells to activate a strong autophagy flux without turning off mTORC1 activity, thus reaping the benefits of both.

4.2 Results

Starvation activates phosphatase activity against ULK1

It is well established that suppression of mTORC1 induces ULK1 complex dependent autophagy (Ganley et al., 2009; Jung et al., 2009). Given the central role of mTORC1 in starvation-induced autophagy, it was puzzling to observe that starvation could induce a stronger autophagic response compared to pharmacological inhibition of mTORC1. Mouse embryonic fibroblasts (MEFs) stably expressing GFP-LC3 formed clear puncta under both treatment conditions, indicating autophagy induction (Figure 4.1 A). However, MEFs treated with starvation formed a larger number of GFP-LC3 puncta and in a shorter time, indicating a stronger autophagy response. Supporting this observation, depletion of LC3 I as detected by western blotting was also more rapid in starvation treated cells, indicating efficient turnover of autophagosome contents (Figure 4.1 B).

To gain better insight into this process, I compared the kinetics of ULK1 dephosphorylation during starvation compared to pharmacological inhibition of mTORC1. As reported previously, ULK1 was rapidly dephosphorylated during starvation in MEFs, with nearly complete dephosphorylation at S637 and S757 within 30 min of starvation (Figure 4.1 C). In contrast, a phospho-signal could still be detected after 30 min of treatment with rapamycin. Rapamycin functions as an indirect inhibitor of mTORC1, by binding to the 12-kD FK506-binding protein (FKBP12) and is therefore thought to be a weaker inhibitor compared to ATP competitive inhibitors of mTOR such as Torin1 (Benjamin et al., 2011; Thoreen et al., 2009). However, the same trend could be detected in cells treated with Torin1 compared to starvation (Figure 4.1 C), even though it could be observed at earlier time points that Torin1 treatment was more effective at shutting down mTORC1 activity (Figure 4.1 D).

Phosphorylation events in a cell are regulated by a balance between kinase and phosphatase activities towards a substrate. As mTORC1 inactivation is insufficient to account for the rapid dephosphorylation and thereby activation of ULK1 during starvation, I hypothesized that starvation stimulates phosphatase activity toward ULK1. Consistent with this hypothesis, using ULK1 as a substrate, higher phosphatase activity could be detected in whole cell lysate from starved MEFs compared to MEFs in full media or rapamycin (Figure 4.1 E).

Interestingly, under the conditions used to monitor ULK1 S637 dephosphorylation *in vitro*, ULK1 S757 was very inefficiently dephosphorylated (Figure 4.1 E). This could be interpreted in several ways: the phosphatase responsible for ULK1 S757 is not as abundant as PP2A, the S757 phosphatase is labile under the specific buffer conditions used in this assay, or the substrate due to the way it was prepared, lacks a co-factor or context (eg subcellular localization) required for recruiting the S757 phosphatase. Unfortunately, this precluded the possibility of purifying the S757 phosphatase through biochemical fractionation as we had done for PP2A-B55α (the S637 phosphatase).

A latent population of PP2A is activated during starvation

How does starvation stimulate the activity of PP2A toward ULK1 S637? It is notoriously difficult to overexpress PP2AC due to the already high levels of endogenous PP2AC and tight regulatory control over PP2AC levels in the cell (Baharians and Schönthal, 1998). To isolate PP2AC complexes in the cell, I knocked

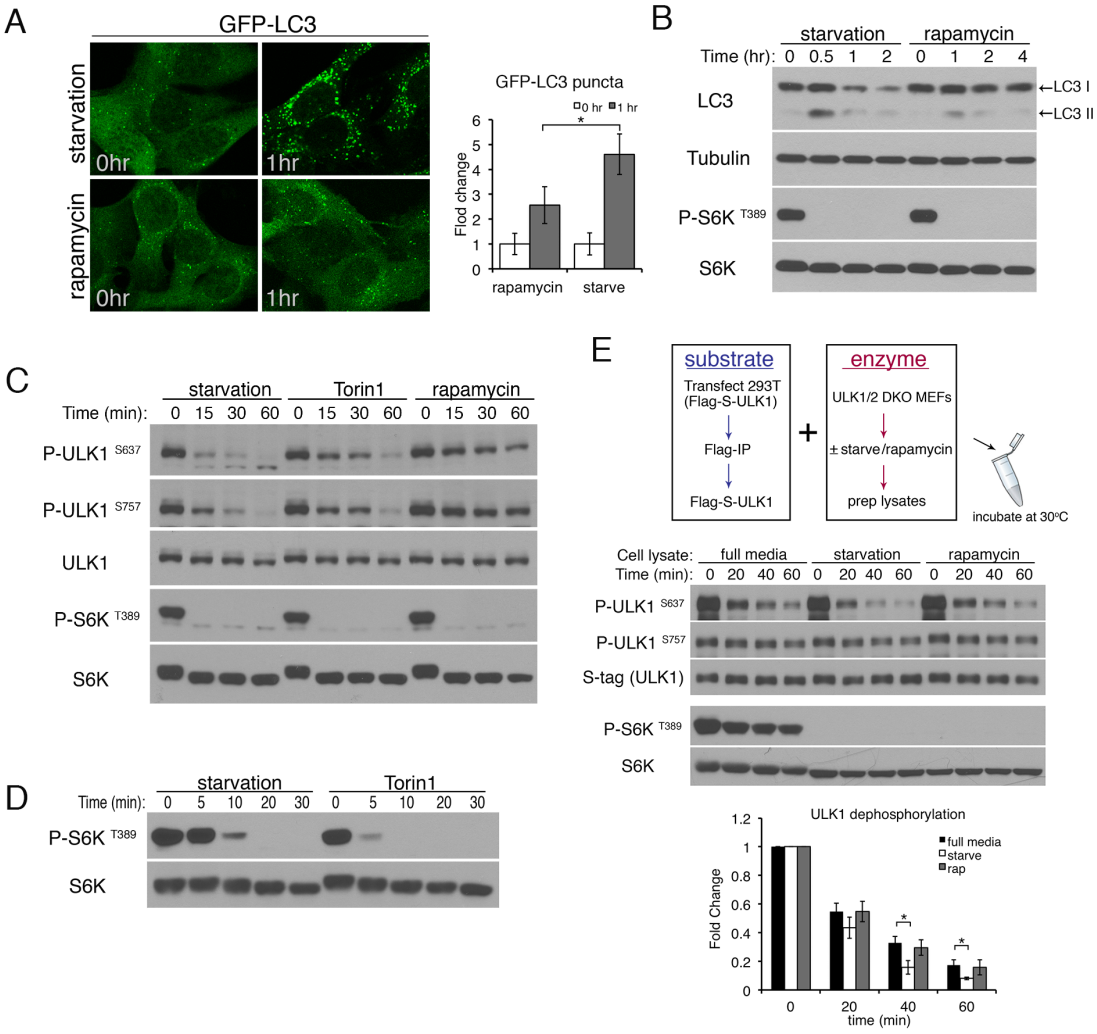

Figure 4.1 Amino acid starvation stimulates phosphatase activity for ULK1. (**A, B**) Starvation induces a stronger autophagic response than rapamycin. In (A), MEFs stably expressing GFP-LC3 were incubated in starvation media or treated with 1 μM rapamycin. Average number of puncta per cell was quantitated. (fold change ± s.d., n=30. two-tail student's t-Test, * $p<0.05$). In (B), MEFs were lysed and immunoblotted for endogenous LC3 and other proteins. (**C**) Kinetics of mTOR substrate dephosphorylation. MEFs were incubated in starvation media or media containing 1 μM of either Torin1 or rapamycin. (**D**) Torin1 shuts down mTOR activity more efficiently than starvation. MEFs were incubated in starvation media or media containing 1 μM Torin1. (**E**) Starvation increases phosphatase activity for ULK1 S637 in MEFs. Upper panel shows a Schematic representation of the in vitro phosphatase assay. Middle panel shows outcome of the phosphatase assay comparing lysates from starved, fed or rapamycin treated cells. S-tag and total S6K are loading controls for the amount of substrate and enzyme, respectively. Lower panel shows quantitation of ULK1 S637 phosphorylation relative to time 0. (fold change ± s.d., n=4. two-tail student's t-Test, * $p<0.05$).

down endogenous PP2AC in MEFs and replaced it with an shRNA resistant Flag-S doubly tagged PP2AC that was more convenient for experimental manipulation. Using this system, I was able to verify that PP2A complexes isolated from starved cells had higher activity against ULK1 (Figure 4.2).

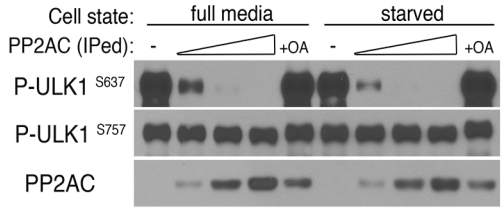

Figure 4.2 PP2A complexes from starved cells have higher phosphatase activity. MEFs stably expressing shRNA targeting the 3'UTR region of PP2AC were generated and reconstituted with Flag-S-PP2AC. Cells were incubated in full media or starvation media, lysed and incubated with Flag beads to pull down PP2A complexes. PP2A complexes were then titrated in a phosphatase assay against ULK1.

In yeast, Pph21 (PP2AC homologue) is regulated by Tap42 in a nutrient dependent manner (Di Como and Arndt, 1996). Tap42 is a highly conserved regulator of PP2AC with a mammalian homologue, Alpha4. It has been reported that Alpha4 is involved in mediating cell survival during glutamine starvation (Reid et al., 2013). While early studies suggested that Alpha4 may activate PP2A towards certain substrates (Chung et al., 1999), more recent studies indicate that PP2AC is inactive when bound to Alpha4 (Jiang et al., 2013). To clarify the role of Alpha4 in PP2AC regulation, I co-expressed Alpha4 with PP2AC in an insect cell system and purified the recombinant protein complex. In an *in vitro* phosphatase assay, the recombinant PP2AC-Alpha4 complex could not dephosphorylate ULK1 (Figure 4.3 A and B). To further confirm that the Alpha4-containing PP2A complex is inactive in cells, I used a potent small molecule phosphatase inhibitor, microcystine-LR (MCLR) conjugated to agarose beads to isolate endogenous PP2AC complexes from WT MEFs. MCLR binds to the catalytic

site of PP2AC when the enzyme is in an active conformation (Xing et al., 2006; Xu et al., 2006). Interestingly, the MCLR-beads pulled down PP2A holo-enzyme complexes containing the scaffolding (PRL65) and regulatory subunits (B55α was monitored as a representative regulatory subunit) but did not pull down PP2A complexes containing Alpha4, indicating that Alpha4-associated PP2AC is inactive in cells. This is in agreement with partial crystal structure data of PP2AC showing that the conformation of the catalytic site is greatly altered when PP2AC is bound to Alpha4 (Jiang et al., 2013). For comparison, Alpha4 interaction was easily detected when S-beads were used to pull down PP2AC in Flag-S-PP2AC reconstituted cells. (Figure 4.3 C).

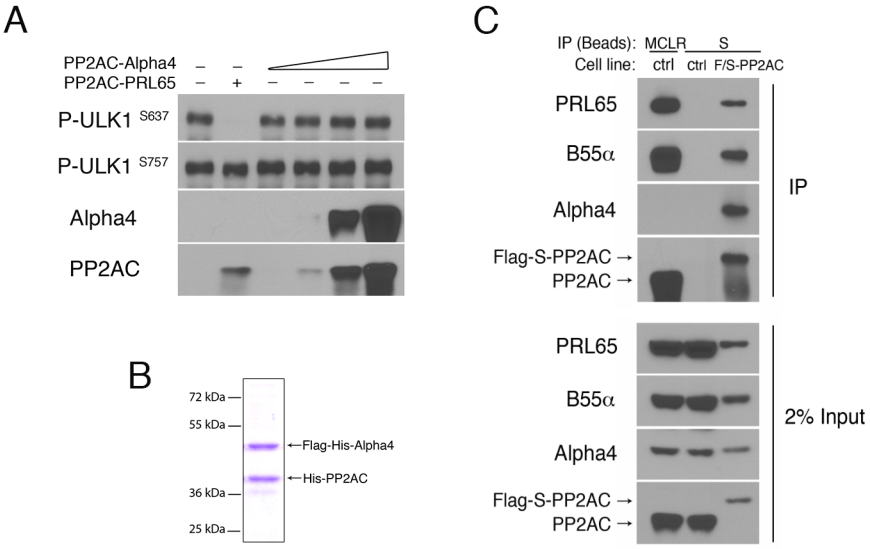

Figure 4.3 PP2A bound to Alpha4 is inactive. (**A**) Recombinant PP2AC-Alpha4 complex is inactive. Phosphatase assay was carried out *in vitro* using increasing amounts of recombinant PP2AC (3-90 nM) co-purified with Alpha4. Recombinant PP2AC-PRL65 complex (20 nM) was used as a control. (**B**) Coomassie brilliant blue staining of recombinant PP2AC-Alpha4 used in the reaction. (**C**) Endogenous PP2AC-Alpha4 complex is catalytically inactive. WT MEFs (ctrl) were lysed and incubated with microcystin-LR (MCLR) beads which bind to the catalytic pocket of PP2AC. As a comparison, MEFs expressing Flag-S-PP2AC as described in figure 4.2 were lysed and incubated with S-beads to pull down total PP2A complexes in the cell.

To assess Alpha4 distribution among PP2AC complexes in the cell, I repeated part of the biochemical fractionation protocol used to identify B55α. MEF cell lysates were passed through a Q column followed by a HAP column which distributed PP2AC complexes across 9 fractions. Alpha4 was detected in fractions that had no activity against ULK1 and were separate from fractions containing B55α (Figure 4.4 A), supporting the idea that Alpha4 containing PP2AC complexes are a distinct population in the cell. PP2AC has been reported to bind Alpha4 and PRL65 in a mutually exclusive manner (Jiang et al., 2013; Prickett and Brautigan, 2004). To confirm this, I carried out immunoprecipitation reactions with B55α and Alpha4. Immuno-precipitation of Alpha4 pulled down PP2AC but not PRL65 or B55α (Figure 4.4 B). Likewise immunoprecipitation of B55α (Figure 4.4 C) could pull down PRL65 and PP2AC but not Alpha4, indicating that they are in separate complexes (Figure 4.4 D).

In yeast, the Pph21-Tap42 (PP2AC-Alpha4 homologues) interaction is sensitive to both nutrient deprivation and rapamycin treatment (Di Como and Arndt, 1996). I performed immunoprecipitation of endogenous PP2AC to check if the same was true in mammalian cells. Surprisingly, although starvation induced a clear decrease in the interaction of PP2AC with Alpha4, Torin1 treatment had no effect (Figure 4.5 A), indicating that regulation of the PP2AC-Alpha4 complex is different from yeast and independent of mTOR. Notably, I could detect a concurrent increase in PP2AC association with PRL65 and B55α during starvation when crosslinking reagent DSP was used to stabilize the complex for immunoprecipitation (Figure 4.5B). This result indicates that starvation induces release of PP2AC from latent complexes containing Alpha4 to form active complexes containing PRL65 and regulatory subunits including B55α. As the starvation conditions used in my experiments thus far excluded both amino acids and serum, I wanted to clarify if it was amino acid or growth factor

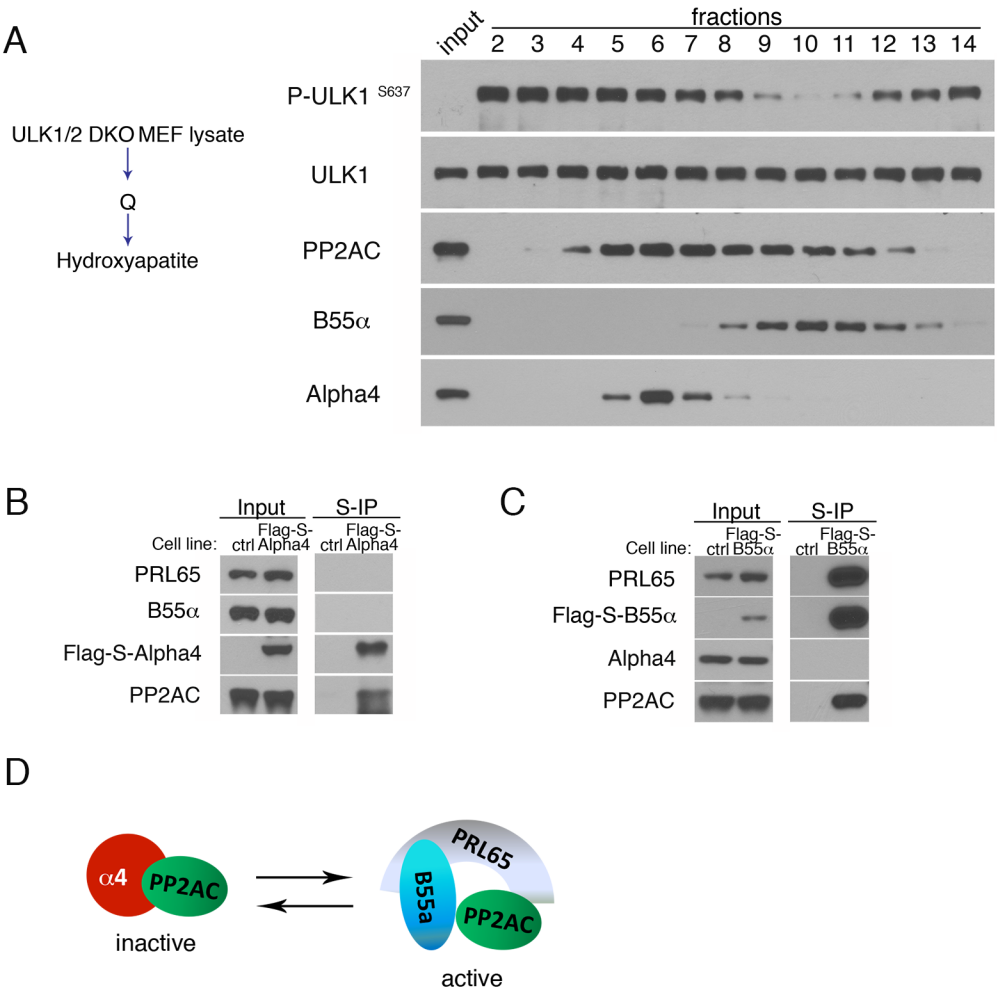

Figure 4.4 PP2AC binds Alpha4 and PRL65 in a mutually exclusive manner. (**A**) Distribution of Alpha4 and regulatory subunit B55α among endogenous PP2A complexes. Cell lysate from ULK1/2 DKO MEFs were separated on a Hydroxyapatite column and assessed for activity against ULK1. (**B**) WT MEFs (ctrl) and MEFs stably expressing Flag-S-Alpha4 were incubated with S-Beads for immunoprecipitation. Western analysis was carried out to detect the presence of the indicated proteins. (**C**) WT HT1080 cells (ctrl) and HT1080 stably expressing Flag-S-B55α were incubated with S-Beads for immunoprecipitation. Western analysis was carried out to detect the presence of the indicated proteins. (**D**) Schematic of PP2AC complexes correlating with activity.

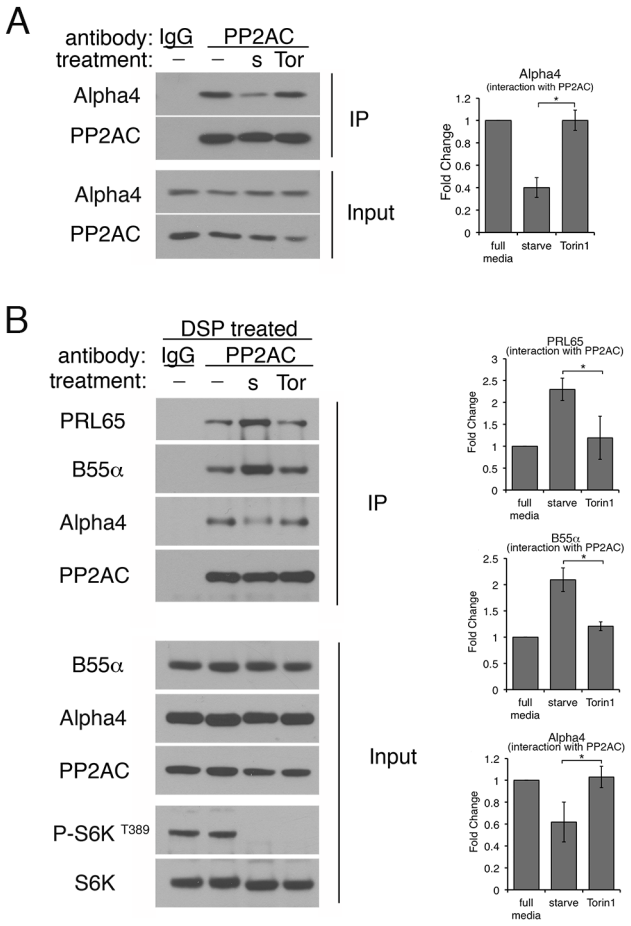

Figure 4.5 Starvation stimulates release of PP2A catalytic subunit from inhibitory protein Alpha4. (**A**) WT MEFs were incubated in starvation media or media containing 1 μM Torin1 for 1 hour, lysed and incubated with control antibody or antibody against PP2AC. The amount of Alpha4 interacting with PP2AC under each condition was monitored by Immunoblotting and quantitated on the right (fold change relative to full media ± s.d., n=5. two-tail student's t-Test, * $p<0.05$). (**B**) Starvation induces dissociation of PP2AC from Alpha4. 293T cells were starved or incubated in complete media containing 1 μM Torin1 for 2 hr. Cell lysate was prepared, cross-linked with DSP and incubated with the indicated antibodies to pull down endogenous PP2A complexes for immunoblot analysis. Quantitation of co-IPed proteins relative to full media is shown on the right. (fold change ± s.d., n=3. two-tail student's t-Test, * $p<0.05$)

signaling that triggered alpha4 dissociation from PP2AC. Starvation media supplemented with dialysed serum still induced dissociation of Alpha4 from PP2A and serum starvation alone had no effect on PP2AC-Alpha4 interaction (Figure 4.6), confirming that the interaction was sensitive to amino acid levels.

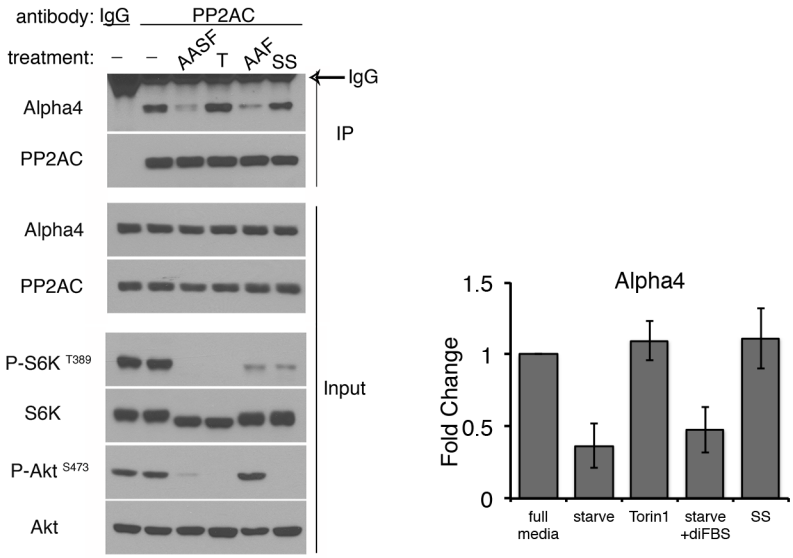

Figure 4.6 Amino acid but not serum starvation stimulates release of PP2A catalytic subunit from Alpha4. MEFs were incubated in starvation media (amino acid and serum free, AASF), complete media with 1 μM Torin1 (T), amino acid free media supplemented with 10% dialysed FBS (AAF), or serum free media (SS). Cells were lysed and incubated with control antibody or antibody against PP2AC. The amount of Alpha4 interacting with PP2AC under each condition was monitored by immunoblotting and quantitated on the right (fold change relative to full media ± s.d., n=3)

To further demonstrate that Alpha4 can affect the dynamics of active PP2A complex formation, we overexpressed Flag-S doubly tagged Alpha4 in 293T cells and assessed the effect on active PP2A complex formation by immune-precipitation of endogenous PP2AC. This experiment was carried out by Dr. Yan Feng, a postdoctoral fellow in our laboratory. Compared to control cells, less PRL65 co-immunoprecipitated with PP2AC in Alpha4 over-expressing cells (Figure 4.7 A). I also generated a stable MEF

cell line overexpressing Alpha4 in order to assess if this has any functional consequence on starvation-induced ULK1 dephosphorylation. Overexpression of Alpha4 reduced the rate of dephosphorylation at ULK1 S637, consistent with its role as a negative regulator of PP2A activity (Figure 4.7 B). In agreement with earlier observations, dephosphorylation at S757 was not affected by Alpha4 overexpression. I was unable to do the converse experiment by RNAi as knockdown of Alpha4 results in depletion of PP2AC expression and cell death, as reported previously (Kong et al., 2004).

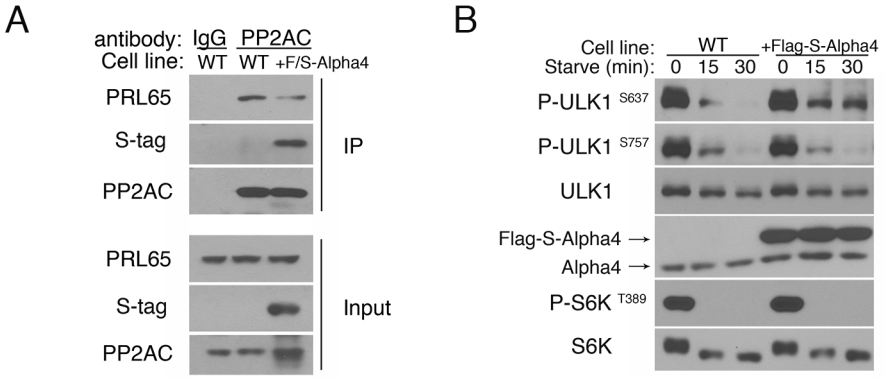

Figure 4.7 Alpha4 overexpression reduces PP2A activity. (**A**) Alpha4 overexpression reduces PRL65 binding to PP2AC. 293T cells were transfected with Flag-S-Alpha4. Cells were lysed, and incubated with antibodies to pull down endogenous PP2AC. Immunoblotting was carried out to monitor the amount of PRL65 interacting with PP2AC. (**B**) Alpha4 overexpression blocks ULK1 S637 dephosphorylation. MEF cells stably overexpressing Flag-S-Alpha4 were incubated in complete or starvation media for the indicated amount of time. Panel A was carried out by Dr. Yan Feng.

"Autophagy-addicted" cells have high basal levels of phosphatase activity

During nutrient starvation, PP2A phosphatase is activated with concurrent inactivation of the kinase phosphorylating ULK1 (mTORC1), resulting in a rapid and strong induction of autophagy. To follow up with my observation that PP2A is activated independently of mTORC1, I searched for a biological context in which the

phosphatase might influence ULK1 activation and autophagy independent of mTORC1 activity.

Recent reports indicate that some cancers, in particular pancreatic cancers carrying Ras mutations are "addicted" to autophagy, requiring high basal autophagy levels in order to maintain viability and growth (Guo et al., 2011; Guo et al., 2013; Yang et al., 2011). It is unclear as to how these "autophagy addicted" cell lines are able to maintain high levels of autophagy in the absence of mTORC1 inactivation since mTORC1 activity is generally thought to suppress autophagy by inhibiting the ULK1 complex. One possibility is that ULK1-independent mechanisms may be driving autophagy in these cells, but an alternate hypothesis is that signaling through the PP2A phosphatase pathway may be driving ULK1-dependent autophagy while maintaining mTORC1 function intact. As shown in Figure 4.8 A, cell lysates of pancreatic ductal adenocarcinoma (PDAC) cell lines BXPC3 and 8988T had significantly higher phosphatase activity toward ULK1 S637 site compared to control cancer cell lines U2OS (osteosarcoma) and H460 (non-small cell lung cancer) that are not "addicted" to autophagy. Interestingly, I detected higher expression of regulatory subunit B55α in BXPC3 cells and lower levels of Alpha4 in 8988T cells (Figure 4.8 B), correlating with the high phosphatase activity against ULK1 in these cell lines.

I confirmed high basal levels of autophagy in these cell lines using two complimentary assays. In the first assay, I treated cells with bafilomycin to block degradation of LC3 and observed more dramatic accumulation of LC3 form II in the two PDAC cell lines (Figure 4.8 C and D). In the second assay, I blocked synthesis of new LC3 using translational inhibitor cycloheximide and tracked the degradation of existing LC3 over time. A significantly faster rate of LC3 turnover was detected in both PDAC cell lines

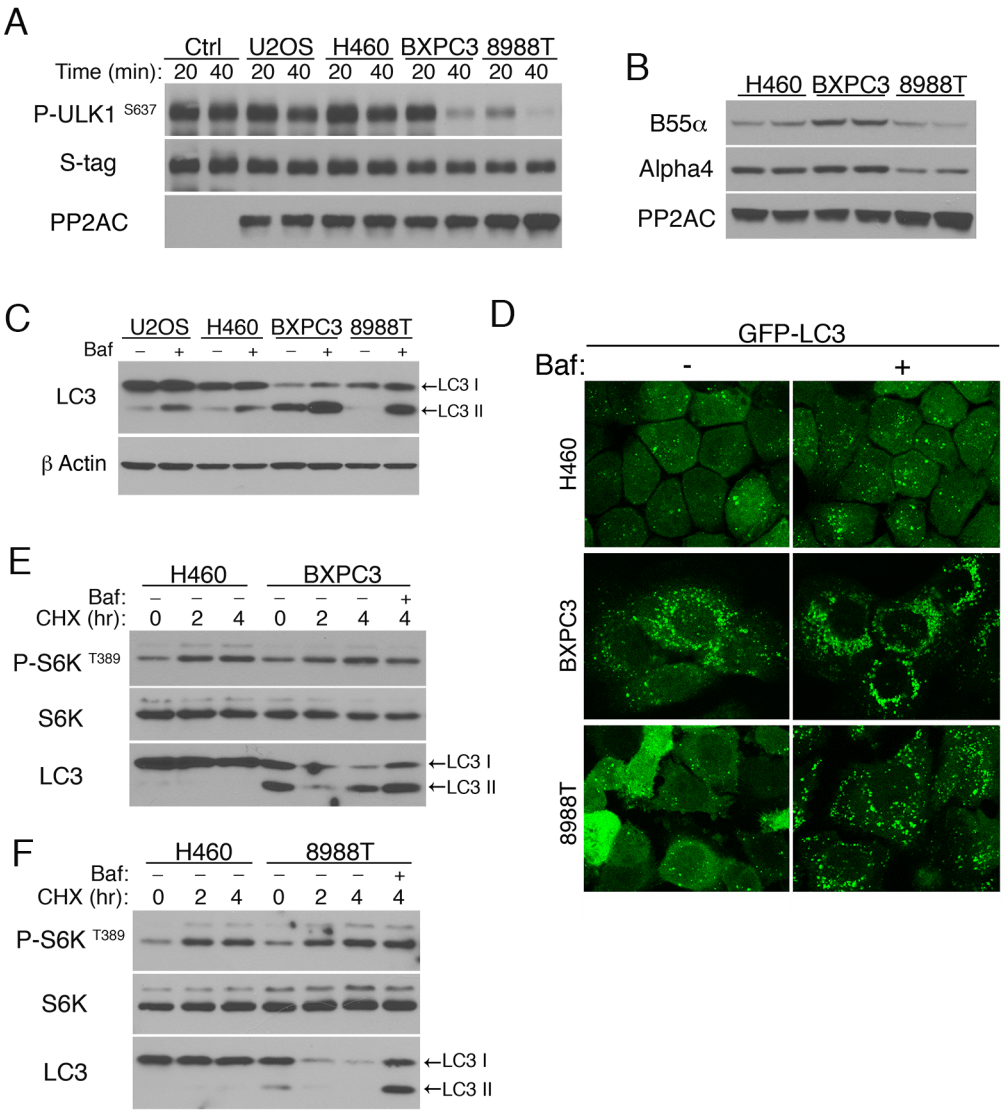

Figure 4.8 Phosphatase activity correlates with high basal levels of autophagy in pancreatic ductal adenocarcinoma cell lines. (**A**) Pancreatic ductal adenocarcinoma (PDAC) cell lines have high phosphatase activity. In vitro phosphatase assay was carried out using Flag-S-ULK1 as a substrate and 10 μg of total cell lysates from indicated cancer cell lines. (**B**) Immunoblot for endogenous levels of PP2A regulatory proteins B55α and Alpha4 in control cell line H460 and PDAC cell lines BXPC3 and 8988T. (**C-F**) PDAC cell lines have high basal autophagy. In (C), cell lines were kept in complete media in the presence or absence of 20 nM bafilomycin (Baf) for 90 min and lysed for immunoblotting of endogenous LC3. In (D), Cell lines stably expressing GFP-LC3 were kept in complete media in the presence or absence of 20 nM bafilomycin (Baf) for 90 min. In (E, F) cells were kept in complete media with 20 μg/ml cycloheximide (CHX) for the indicated amount of time. Where indicated, 10 nM bafilomycin was added at the start of CHX treatment. Cells were lysed and immunoblotted for endogenous LC3.

compared to control cell line H460 (Figures 4.8 E and F). The LC3 turnover in both cell lines could be blocked by the addition of bafilomycin, consistent with degradation occurring through the autophagosome-lysosome pathway. Importantly, mTORC1 remained active during the course of cycloheximide treatment (Figures 4.8 E, F and Figure 4.9 C and D), indicating that basal autophagy in these cell lines was occurring independent of mTOR inactivation.

Subsequently, I confirmed that both PP2A activity and the ULK1 complex are required for high basal autophagy in PDAC cell line 8988T. Treatment with OA or knockdown of PP2AC blocked basal turnover of LC3 (Figure 4.9 A and B). The same result was achieved when ULK1 complex components (either ULK1 or FIP200) were knocked down (Figure 4.9 C and D). Furthermore, knockdown of ULK1 reduced proliferation and anchorage-independent growth of 8988T cells (Figure 4.10 A and B), supporting previous reports that disrupting basal autophagy has a functional consequence on the fitness of PDAC cells such as 8988T (Yang et al., 2011). As a control, knockdown of ULK1 had no effect on "non-addicted" cancer cell line H460 (Figure 4.10 A and B). Hence, high PP2A activity can drive basal autophagy in an mTOR-independent manner through regulation of the ULK1 complex, contributing to robust growth of "autophagy-addicted" cancer cells (Figure 4.11).

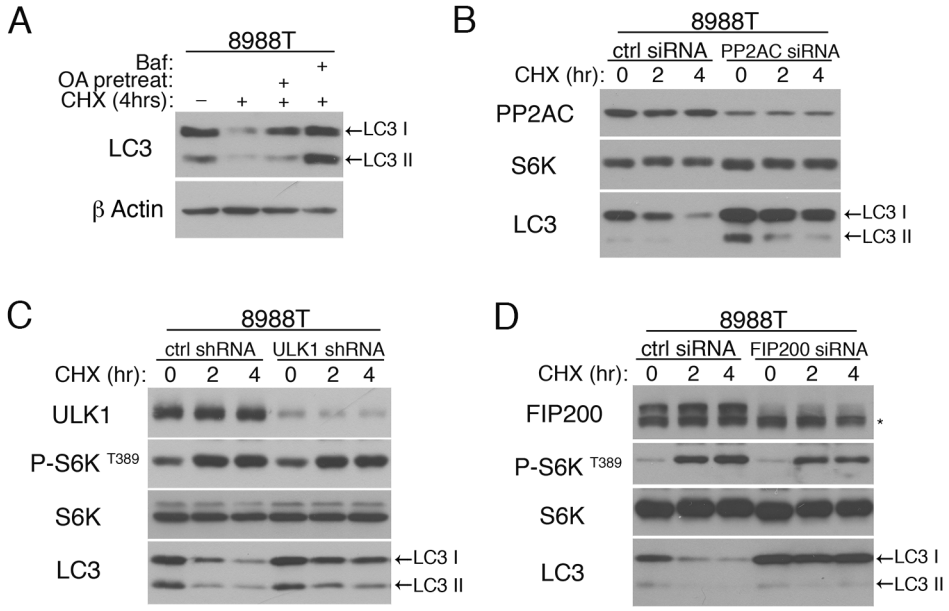

Figure 4.9 PP2AC and the ULK1 complex are required for basal turnover of LC3 in 8988T cells. (**A**) PDAC cell line 8988T was kept in complete media with 20 μg/ml cycloheximide (CHX) for 4 hrs. Where indicated, 10 nM Baf was added at the start of CHX treatment. To assess phosphatase involvement, cells were pretreated with 200 nM okadaic acid (OA) in full media for 2 hours and removed at the start of CHX treatment. (**B**) 8988T was transduced with control siRNA or siRNA targeting the catalytic subunit of PP2A. Cells were kept in complete media with 20 μg/ml cycloheximide (CHX) for the indicated amount of time and immunoblotted for endogenous LC3. (**C**) 8988T cells were transduced with control shRNA or shRNA targeting ULK1. Cells were treated as in (B). (**D**) 8988T was transduced with control siRNA or siRNA targeting FIP200. Cells were treated as in (B). * denotes non-specific band.

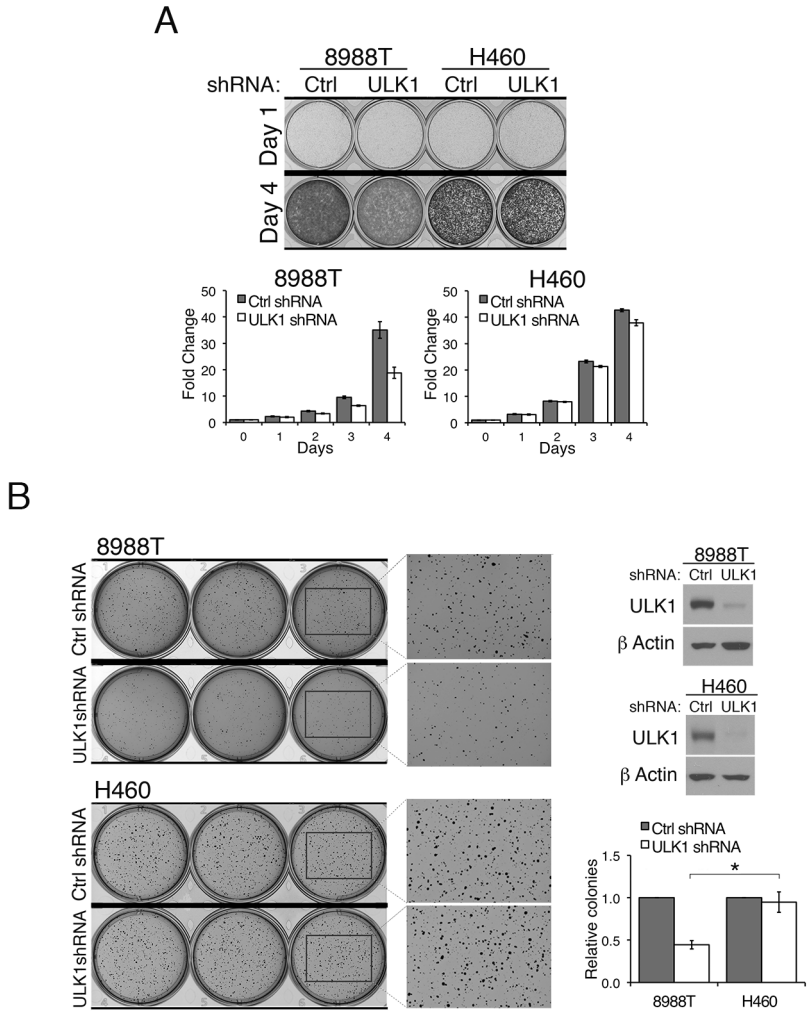

Figure 4.10 The ULK1 complex is required for robust growth of PDAC cell line 8988T. (**A**) Equal number of 8988T or H460 cells stably expressing control shRNA or shRNA targeting ULK1 were seeded on Day 0. Upper panel shows cells fixed and stained with crystal violet on Day 1 and Day 4 respectively. Histograms on the lower panel show quantitation of crystal violet stain over time, relative to Day 0. Error bars are standard deviation from triplicates. (**B**) ULK1 complex is required for sustained anchorage-independent growth of 8988T. Cell lines in (A) were used in a soft agar assay. Representative images and knockdown efficiencies are shown. Histogram shows quantitation of colonies in each cell line relative to control shRNA. (relative colony number ± s.d., n=3. two-tail student's t-Test, ** $p<0.01$)

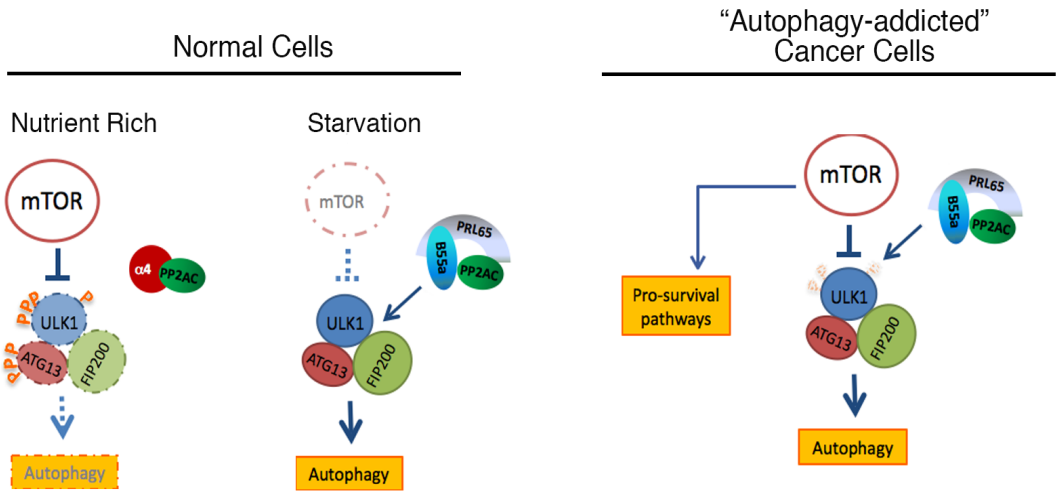

Figure 4.11 Schematic representation of PP2A signaling to the ULK1 complex. In normal cells, PP2A activity is low under nutrient rich conditions. Amino acid starvation induces release of PP2A catalytic subunit from latent complexes containing Alpha4 for incorporation into active complexes containing the scaffolding subunit PRL65 and regulatory subunits such as B55α, resulting in a stimulation of PP2A activity. This dissociation event is not regulated by mTOR. "Autophagy-addicted" cancer cells are able to maintain high phosphatase activity to drive ULK1-dependent autophagy even in the absence of mTOR inactivation, allowing them to reap the dual benefits of mTOR activation and autophagy at the same time.

4.3 Discussion

Several kinases have been reported to regulate autophagy, including mTOR (Chan, 2009), AMPK (Egan et al., 2011), PKA (Cherra et al., 2010), STK3/STK4 (Wilkinson et al., 2015) and DAPK (Zalckvar et al., 2009). In contrast, the role of phosphatases in this process has rarely been broached. It is known that mTOR directly phosphorylates ULK1 under nutrient rich conditions and it is generally thought that mTOR phosphorylation of ULK1 keeps its activity low under conditions of amino acid sufficiency (Hara et al., 2008). In this study we shed light on the phosphatases that regulate ULK1 during starvation-induced autophagy. Inhibition of mTOR by rapamycin or Torin1 treatment is sufficient to result in ULK1 dephosphorylation and autophagy induction, indicating that basal levels of phosphatase activity are always present in the cell. What was remarkable to me was that ULK1 dephosphorylation at both S637 and S757 was more rapid during starvation compared to Torin1/ rapamycin treatment, suggesting that starvation could stimulate phosphatase activity. Importantly, the increased phosphatase activity correlated with a stronger autophagy response elicited by starvation compared to rapamycin treatment, indicating that the phosphatases regulating ULK1 could be another signaling node for regulating autophagy.

Having identified PP2A to be the phosphatase regulating ULK1 at S637, I attempted to elucidate the mechanism behind PP2A activity stimulation during starvation. PP2AC is one of the most abundant phosphatase catalytic subunits in the cell and is controlled by complex regulatory mechanisms at several levels. Aside from the scaffolding and regulatory subunits, a number of other proteins such as PP2A Inhibitor-1 (I_1^{PP2A}aka PHAP-I or ANP32a) and Inhibitor-2 (I_2^{PP2A}aka SET or PHAP-II) (Li et al., 1995), Cancerous Inhibitor of PP2A (CIP2A) (Junttila et al., 2007),

methyl esterase PME-1 (Ogris et al., 1999) and Alpha4 (Kong et al., 2004) have been reported to bind PP2AC directly and affect its activity. I was interested in Alpha4 in particular due to previous reports in yeast that its interaction with PP2AC is nutrient dependent (Di Como and Arndt, 1996).

To my knowledge, the detection of free PP2A catalytic subunits in the cell has not been reported. When detected, it is either in complex with its scaffolding subunit PRL65 or another binding partner that can modulate its activity. It is likely that free PP2AC is rapidly turned over to prevent unchecked phosphatase activity in the cell (Virshup and Shenolikar, 2009). In agreement with recent reports, I found PP2AC bound to Alpha4 to be catalytically inactive *in vitro*. Fractionation of PP2A complexes from the cell also showed Alpha4 to be associated with inactive PP2A complexes and is distinct from active B55α- containing complexes. While my fractionation data suggests that only a sub-population of PP2AC is associated with Alpha4, it is an essential regulator of PP2AC. Knocking out Alpha4 in a conditional mouse model results in a concurrent depletion in type 2 phosphatase levels (PP2AC, PP4C, PP6C), rapidly resulting in cell death (Kong et al., 2009). Supporting the role of Alpha4 in maintaining PP2AC stability, overexpression of Alpha4 suppresses PP2AC polyubiquitination (McConnell et al., 2010). The drastic phenotype of knocking out Alpha4 supports the idea that it has a fundamental "chaperone-like" role in maintaining cellular pools of PP2AC (Kong et al., 2009), in contrast to other PP2AC binding partners such as PME-1, whose function is more regulatory in nature. PP2AC levels are not as drastically perturbed in PME-$1^{-/-}$ mice, which show a moderate reduction in PP2AC levels only in some tissues and have no gross defects developmentally but die within the first day of birth (Ortega-Gutiérrez et al., 2008). This has led to a model of "latent stability" where Alpha4 binds PP2AC keeping it

stable but inactive until it is required for incorporation into active complexes containing the scaffolding and regulatory subunits. How the assembly of active PP2A complexes is co-ordinated remains unclear and may involve other proteins that incorporate post-translational modifications in the highly conserved C-terminal tail of PP2AC (Janssens et al., 2008; Sents et al., 2013).

In yeast, interaction between PP2AC and Tap42 (the yeast counterpart of Alpha4) is dramatically disrupted by rapamycin treatment (Di Como and Arndt, 1996), indicating that TOR inactivation is sufficient to stimulate PP2A activity in yeast. Tap42 was also shown to be a direct substrate of TOR, leading to a model in which TOR regulated PP2AC-Tap42 interaction through phosphorylation of Tap42 (Jiang and Broach, 1999). In my hands starvation was a much stronger trigger for Alpha4 dissociation from PP2AC compared to Torin1 treatment, indicating that PP2AC regulation is different and likely more complex in mammalian cells. This difference could account for the observation that ULK1 dephosphorylation occurs more rapidly in starvation compared to Torin1 inhibition of mTOR and supports the hypothesis that the PP2A phosphatase represents a separate pathway feeding into autophagy activation.

This finding has some implications in cancer biology. mTOR plays a fundamental role in regulating cell growth through controlling translation and ribosomal biogenesis. The oncogenic PI3K/AKT pathway exerts its effects primarily through mTORC1 (Guertin and Sabatini, 2007), making it an attractive target for cancer treatment. On the other hand, it has been proposed that autophagy (which is inhibited by mTORC1) can support cancer growth by alleviating metabolic stress (Kimmelman, 2011; Leone and Amaravadi, 2013). In line with this, knockdown of autophagy related genes has also

been shown to impact tumor growth in several cancer models (Guo et al., 2011; Rao et al., 2014; Wei et al., 2011).

In this study, I observed that high phosphatase activity is correlated to high basal levels of autophagy in 2 pancreatic cancer cell lines (BxPC3 and 8988T) that were previously reported to be "autophagy-addicted". Depletion of PP2A or members of the ULK1 complex impaired the basal rate of autophagy, suggesting that high phosphatase activity drives ULK1-dependent autophagy in these cell lines. Activation of the protein phosphatase targeting ULK1 can explain the seemingly contradictory co-existence of intact mTORC1 signaling and autophagy activity in various cancers.

While I have shown that both PP2A and ULK1 are required for the high basal autophagy, the exact phosphorylation events involved are unclear. Ideally, this should be worked out through the use of phospho-mimetic mutants, however phospho-mimetic mutants of ULK1 that block autophagy have not yet been reported despite multiple groups having mapped phosphorylation sites on ULK1. Personally I have also tried S637D and S757D mutants, but they did not block autophagy induction. This may be a purely technical issue, in that phospho mimetic mutations do not always effectively recapitulate a phosphorylation event. It may also indicate that mutations on 2 residues is insufficient to affect a protein that is not only phosphorylated on multiple sites but is part of a complex containing other proteins (ATG13 and FIP200) that are also phosphorylated.

The mechanisms driving phosphatase activity in 8988T and BxPC3 are also unclear. I detect higher levels of B55α in BxPC3 and lower levels of Alpha4 expression in 8988T, correlating with higher phosphatase activity in these cell lines. What controls

the levels of these proteins and whether the same mechanism is in play in both cell lines is unknown. Based on our current understanding of Alpha4 function, the lower levels of Alpha4 may not be causative but simply reflect the higher phosphatase activity in 8988T.

In summary, the data presented here supports an interesting model in which the deregulation of PP2A activity may be an avenue through which cancer cells simultaneously reap the benefits of both mTORC1 signaling and autophagy activation. It also provides a preliminary indication that ULK1 may be a viable therapeutic target for some cancers. Further experiments in mouse models would better support this as the physiological environment in vivo is much more complex.

4.4 Experimental Procedures

Reagents & Antibodies

For antibody information, please refer to experimental procedures in Chapter 3. Rapamycin was purchased from Enzo Life sciences (A-275). Torin1 was purchased from Tocris Bioscience. Okadaic acid was purchased from Sigma (O9381) or Enzo Life sciences (ALX-350-003) with each showing identical effects on ULK1 dephosphorylation. Cycloheximide was purchased from Calbiochem (239-763) and Bafilomycin A1 (B1793) was purchased from Sigma.

Cell culture

HT1080, and 8988T cell lines were cultured in Dulbecco's Modified Eagles Media (DMEM), supplemented with 10% fetal bovine serum, 2 mM L-Glutamine and 1X penicillin-streptomycin at 37°C, 5% CO_2. H460 and BXPC3 cell lines were grown in RPMI Media, supplemented with 10% fetal bovine serum, 2 mM L-Glutamine and 1x penicillin-streptomycin. H460 and 8988T cell lines were a kind gift from Dr. Alec Kimmelman, Dana Farber Cancer Institute, Boston, USA. Stable expression of transgenes such as Flag-S-Alpha4 and Flag-S-PP2AC or shRNA cassettes were carried out by retroviral or lentiviral transduction.

Treatment conditions and cell lysis

For amino acid starvation experiments, cells were washed twice and incubated in DMEM lacking amino acids and serum for the indicated amount of time. Rapamycin and Torin1 treatments to inhibit mTOR activity were both done at a final concentration of 1 μM in complete media. To assess basal autophagy, a cycloheximide chase experiment was carried out. Cells were treated with translational inhibitor cycloheximide (used at a final concentration of 20 μg/ml in complete media)

to block synthesis of nascent LC3. Turnover of existing LC3 was tracked over time by SDS-PAGE analysis. Lysosomal inhibitor Bafilomycin A1 was used at a final concentration of 10 nM or 20 nM as indicated to assess autophagy flux.

All samples prepared solely for western analysis were lysed in RIPA buffer (50 mM Tris pH 7.5, 150 mM NaCl, 1% Triton X-100, 0.5% sodium deoxycholate, 0.1% sodium dodecyl sulfate) supplemented with protease inhibitors and phosphatase inhibitors (P0044 and P5726 from Sigma). Protein concentration was determined using Bio-Rad Protein Assay Dye reagent (#500-0006).

Fluorescence microscopy

Fluorescence microscopy was carried out as in Chapter 3.

In vitro dephosphorylation assay

For phosphatase assays with cell lysate: Flag-S-ULK1 substrate was incubated with 10 μg of total cell lysate at 30^{o}C for the indicated amount of time. For phosphatase assays with recombinant proteins: Flag-S-ULK1 substrate plus 7-10 μg of phosphatase-depleted protective lysate was incubated with recombinant proteins at 30^{o}C for 20 min.

Purification of recombinant proteins

Full length mouse Alpha4 (NM_008784) was cloned into pFastBac as N-terminal 9x His and Flag tandem-tagged proteins. Recombinant baculovirus was produced using Bac-to-Bac expression system from Invitrogen. PP2AC and Alpha4 were co-expressed in a suspension culture of Sf9 cells for co-purification. Cell pellets were lysed by douncing and purified by Ni-NTA resin, followed by incubation with Anti-Flag M2

affinity gel (A2220 from Sigma) at 4°C for 5 hrs. PP2AC bound to Alpha4 was eluted with 3x Flag peptide and assayed for activity immediately.

Knockdown by shRNA or siRNA

The following shRNA constructs were purchased from Sigma: pLKO hULK1 shRNA (GCCCTTTGCGTTATATTGT AT). The following shRNAs were cloned into pLKOtet-ON inducible shRNA plasmid system purchased from Addgene: mPP2AC shRNA (GCGACATTGTTGGTCAAGAAT). Lenti- viruses were made by co-transfecting shRNA constructs and packaging vectors into 293Ts. Lentiviral preparations were passed through a 0.45 μM PES filter and supplemented with polybrene before being used to transduce cells. Stable cell lines were typically assayed for knockdown 48-72 hours post transduction. For inducible knockdown, cell lines were grown in complete media containing 100 ng/ml Doxycycline 48-72 hours before assaying for knockdown.

For knockdown by siRNA, siGENOME Control siRNA (D-001210-05-20) and siGENOME SMARTpool FIP200 (RB1CC1) siRNA (M-021117-01) were purchased from Dharmacon. siRNAs were transfected into cells at a final concentration of 100 nM with 2 μl Lipofectamine 2000 (Invitrogen) as per manufecturer's protocol. Cells were assayed 48 hrs after transfection.

Expression constructs

The coding sequence (cds) of human PRL65 or mouse Alpha4 were cloned into pMIC vector along with an N-terminal Flag-S tandem tag. PRL65 was also cloned into pBabe-Flag-S (puro) vector.

Immunoprecipitations

For pull down of Flag-S-PP2A complexes: Following treatment, Flag-S-PP2AC expressing cells were washed twice in cold PBS(-) and lysed in IP buffer supplemented with protease inhibitors. Cell lysate was centrifuged at 20,000 x g for 10 min at 4^{o}C. Protein concentration of clarified cell lysate was determined by Bio-Rad Protein Assay Dye reagent. An equal amount of clarified cell lysate from each treatment condition was incubated with 10 µl of S-protein agarose beads (69704 from EMD Millipore) for 4 hours at 4^{o}C with rotation. For IP with MCLR beads (16-147 from EMD Millipore), cells were washed twice in cold PBS(-) and lysed in IP buffer supplemented with protease inhibitors. Cell lysate was centrifuged at 20,000 x g for 10 min at 4^{o}C. 500 µg of clarified cell lysate was incubated with 10 µl of MCLR beads for 4 hours at 4^{o}C with rotation. In all cases, beads were then washed 5 times in IP buffer before elution in SDS-loading dye and analysis by SDS-PAGE.

For pull down of endogenous PP2A complexes: Following treatment, cells were washed twice in cold PBS(-) and lysed in KCl-IP buffer (20 mM Tris pH 7.5, 100 mM KCl, 0.5 mM DTT, 0.2% NP-40, 10% glycerol) supplemented with protease inhibitors. Cell lysate was centrifuged at 20,000 x g for 10 min at 4^{o}C. Protein concentration was measured. An equal amount of clarified cell lysate from each treatment condition (500 mg-1mg) was incubated with 0.6-1 ml of Mouse anti-PP2AC antibody (clone 1D6 #05-421 from Millipore) at 4^{o}C with rotation overnight. Lysates were then incubated with Protein G agarose for 3 hrs at 4^{o}C with rotation. For 293Ts overexpressing Alpha4, PP2A IP was carried out 48 hrs post transfection.

For DSP (Lomant's reagent, Thermo Scientific #22585) crosslinking in 293T cells: Cells were grown in 10-cm dishes, treated and lysed in 1 ml DSP-IP buffer (20 mM

Hepes pH 7.5, 100 mM KCl, 1 mM Mn^{2+}, 0.1% NP-40) supplemented with protease inhibitors. Cell lysate was centrifuged at 20,000 x g for 10 min at 4^{o}C. 1 ml of clarified cell lysate was gently added to 4 ml of crosslinking reagent DSP (125 mg/ml stock in DMSO) to make a final concentration of 0.5 mg/ml DSP. This was rotated at room temperature for 4 min. Reaction was quenched by the addition of 25 ml of 1 M Tris pH 7.5. Lysates were then centrifuged at 20,000 x g for 10 min at 4^{o}C to remove any precipitated DSP. Protein concentration of clarified lysates was measured. 1 mg crosslinked cell lysate was incubated with 1 ml anti-PP2AC antibody (clone 1D6) and immunoprecipitation was carried out as described above. Crosslinking was reversed prior to gel run by boiling samples 3 x 10-min in SDS-loading dye supplemented with additional β-mercaptoethanol (25% V/V). After gel run, PAGE gel was rinsed in transfer buffer for 15-30 min prior to transfer.

Cell growth assay

Cells were plated onto a 12 well plate in triplicate at 15'000 cells per well. The day after plating was considered day 0. Cells were fixed in 10% formalin for 10 min and stained with 0.1% crystal violet for 20 min. Excess dye was removed by washing 3 times with water. Stained cells were left to air dry before dye was extracted with 10% acetic acid. Relative proliferation was determined by measuring absorbance at 570 nm.

Soft agar assay

Soft agar assay was carried out in 6 well plates in triplicate for each cell line. An underlay of 2 ml media with 0.5% agar (2-Hydroxyethylagarose, Sigma A4018) was dispensed into each well and allowed to set. Cells were resuspended in media containing 0.4% agar and seeded at 5000 cells per well in a volume of 1.5 ml. After 10 to 14 days, colonies were stained with iodonitrotetrazolium chloride (Sigma, I10406)

and visualized with GELCOUNT™ imaging system (Oxford Optronix). Total colony number for each well was enumerated based on colony size and staining intensity.

CHAPTER 5. PERSPECTIVES

mTOR signaling to the ULK1 complex

The ULK1 complex integrates signaling inputs from several sources (Figure 1.3), and is a direct substrate of mTORC1. In this dissertation, I compared the rate of ULK1 dephosphorylation and autophagy induction during starvation versus pharmacological inhibition of mTOR by rapamycin or Torin1 treatment. Interestingly, I observed differences even between the two mTOR inhibitors used. Although both rapamycin and Torin1 treatment result in S6K dephosphorylation, rapamycin treatment resulted in slower ULK1 dephosphorylation and autophagy induction. While Torin1 binds directly to the catalytic site of mTOR and thus inhibits both mTORC1 and mTORC2, rapamycin inhibits mTOR in an allosteric manner by binding to FKBP12 and is largely specific to mTORC1 though there have been reports that assembly of the mTORC2 complex may be inhibited as well in some cell types during prolonged rapamycin treatment (Sarbassov et al., 2006). The effects of rapamycin on mTOR signaling is complex, and may be cell line specific, with some groups reporting that certain functions of mTORC1 are resistant to inhibition by rapamycin (Choo et al., 2008; Feldman et al., 2009; Thoreen et al., 2009). Given the difference in rate of dephosphorylation of ULK1 between the two conditions (Torin1 versus rapamycin treatment) and since neither condition results in PP2A activation, perhaps ULK1 dephosphorylation is one of the rapamycin-resistant functions of mTORC1. Another way to account for the difference is that Torin1 inhibits mTORC2 as well, which can feed into the mTORC1 pathway through AKT (Figure 5.1).

The starvation conditions used in my studies deprives cells both of amino acids as well as growth factors, resulting in dephosphorylation of both S6K and AKT after one hour

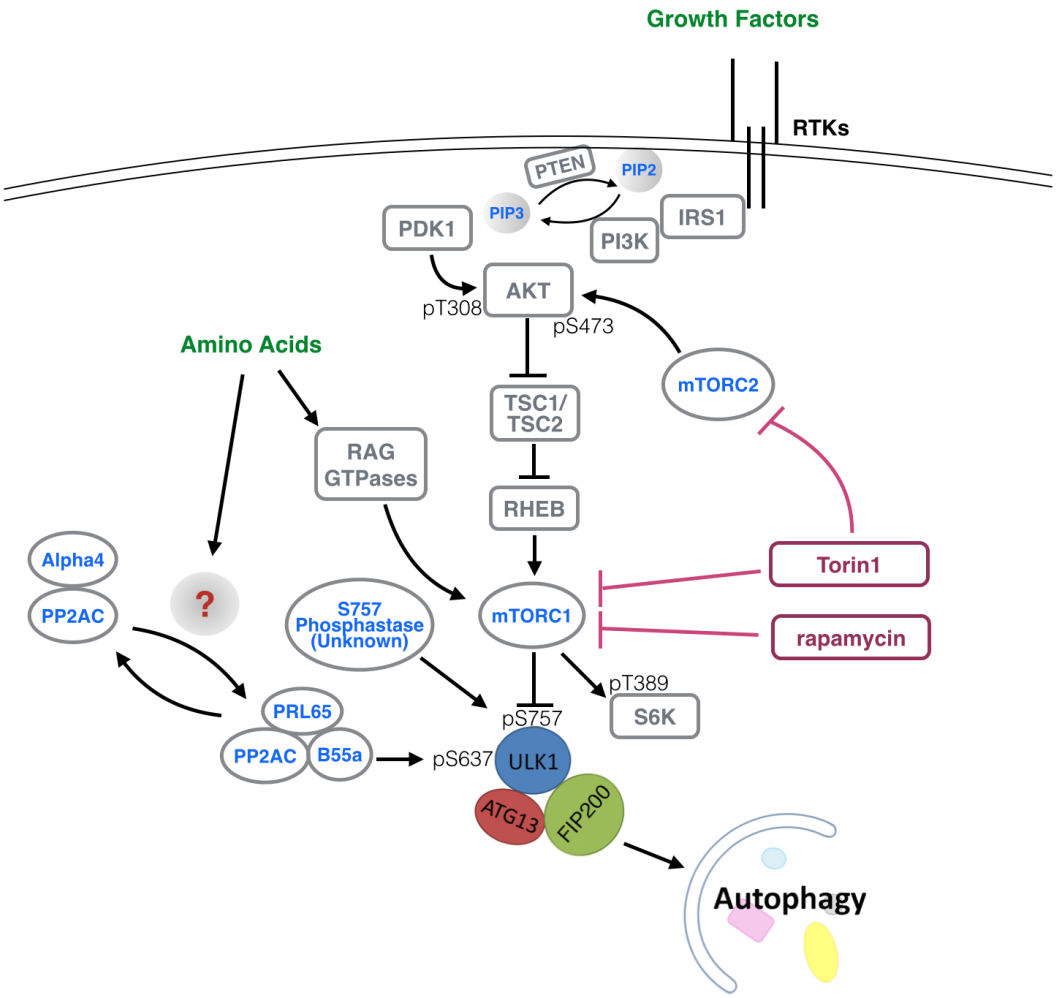

Figure 5.1 Schematic representation of mTOR and phosphatase signaling to the ULK1 complex. Growth factor and amino acids regulate ULK1 complex activity through the mTOR complexes and phosphatases. Under nutrient rich conditions, mTORC1 phosphorylates ULK1 at several sites, including S637 and S757. Growth factor and amino acid starvation inactivates the mTOR complexes and stimulates phosphatase activity toward ULK1. Assembly of the PP2A-B55a complex is stimulated by amino acid signaling and dephosphorylates ULK1 at S637. Dephosphorylation of ULK1 at S757 is mediated by an unknown phosphatase.

of starvation and indicating an inactivation of both mTORC1 and mTORC2. Despite withdrawal of both amino acids and growth factors, Torin1 treatment was more effective in shutting down mTORC1 compared to starvation (as monitored by S6K phosphorylation status), possibly indicating that it is rapidly cell permeable and binds to the catalytic subunit with high affinity. For a more complete picture of mTORC1 status, other mTORC1 substrates such as 4EBP1 and the phosphorylation status of mTOR itself should be monitored. Even though Torin1 appears to shut down mTORC1 more rapidly, starvation induced faster dephosphorylation of ULK1, supporting our initial hypothesis of phosphatase activity stimulation during starvation.

The second ULK1 phosphatase

In the third chapter of this dissertation, I describe the characterization of ULK1 dephosphorylation during starvation and identify the phosphatase targeting ULK1 S637 dephosphorylation to be Protein Phosphatase 2A (PP2A). Blocking PP2A activity in cells blocked dephosphorylation of S637 but did not block dephosphorylation of ULK1 at a second site, S757. Likewise in an in vitro assay, recombinant PP2A dephosphorylated ULK1 at S637 but had no effect on S757, indicating that a second phosphatase is involved in the regulation of ULK1.

To date, two groups have published targeted siRNA screens attempting to identify protein phosphatases involved in autophagy regulation, but with limited success (Martin et al., 2011; Puustinen et al., 2014). With the number of phosphorylation events that have been reported throughout the autophagy pathway (ULK1, ATG13, Beclin-1, VPS34, LC3, p62 etc), this would seem unusual. The lack of hits identified in the two screens could be due to many reasons, the siRNA knockdown efficiencies were not monitored hence it is unclear if the phosphatases tested were not involved in

autophagy or were not sufficiently depleted to show a phenotype. It is also possible that the relevant phosphatases are completely novel and hence not included in the siRNA library. I have also tried an siRNA approach specifically to identify the second ULK1 phosphatase, but without success. Perhaps the best way to identify the second ULK1 phosphatase is still through biochemical purification, which can be combined with sub cellular fractionation to expand the searchable space from soluble proteins to include membrane proteins as well.

Phosphatase regulation of the ULK1 complex

The significance of having an mTORC1 independent signaling input (PP2A-B55α) to the ULK1 complex and the significance of having more than one phosphatase regulate the ULK1 complex is unclear but would certainly allow for greater control over ULK1 function. Previously our understanding of the ULK1 complex was very much framed by the observation that it is a direct substrate of mTORC1, placing it as an initiator complex with a role in mediating amino acid starvation. However, there are an increasing number of reports suggesting that ULK1 can influence downstream events in autophagy (Lim et al., 2015) and can play a role in other types of autophagy (e.g. mitophagy (Wu et al., 2014) and xenophagy (Kageyama et al., 2011)) that may or may not involve mTOR inactivation. As our understanding of ULK1 complex function expands beyond its role as merely an initiator of starvation-induced autophagy, different groups of phosphorylation events on ULK1, or the balance between the kinases and phosphatases regulating these sites may provide a handle for modulating ULK1 function between these roles. To address this possibility, we would first need to identify ULK1 dependent forms of autophagy that do not involve mTORC1 inactivation and determine the requirement of phosphatase activity in those contexts.

Previously it was reported that long mTORC1 is reactivated during prolonged starvation (Yu et al., 2010). The significance of this is not known. It is speculated that the reactivation of mTORC1 may be to limit the catabolic effects of autophagy or could be to reactivate some anabolic processes governed by mTORC1 such as protein and lipid synthesis for cellular maintenance during prolonged periods of starvation. Perhaps signaling input from the phosphatase can keep ULK1 and hence some levels of autophagy active during mTORC1 reactivation, thereby continuing to provide a steady source of biological material to sustain anabolic processes. In light of this, it would be interesting to carry out a time course for phosphatase activity (or ULK1 phosphorylation status) to see if there is an inverse relationship with mTOR activity status (eg. is there a further increase in phosphatase activity when mTORC1 is re-activated?). Alternatively, the PP2AC-Alpha4 interaction could be monitored as well.

PP2AC-Alpha4 interaction

Protein phosphatases are certainly an interesting and under-studied group of proteins, and we are only now beginning to appreciate some of the complex mechanisms that regulate their function. In this dissertation, I was able to show that starvation induces dissociation of PP2AC from Alpha4 and this interaction is not regulated by mTORC1 as Torin1 treatment did not induce dissociation of the complex. The mechanism regulating PP2AC-Alpha4 interaction is an interesting question that remains unanswered in this study. I would speculate that what lies upstream of the PP2AC-Alpha4 interaction points to a novel amino acid sensing mechanism in the cell that may or may not also feed into mTORC1 signaling (Figure 5.1). Over the years, much work has been done on amino acid sensing by mTORC1, resulting in a model whereby Rheb (Garami et al., 2003; Inoki et al., 2002) and Rag GTPases (Sancak et al., 2008; Sancak and Sabatini, 2009) co-ordinately regulate mTORC1 activation in response to

growth factor and amino acid levels respectively. More players in this pathway have since been reported (Bar-Peled et al., 2012; Peterson et al., 2009; Sancak et al., 2010; Wang et al., 2015), yet our understanding of amino acid sensing in the cell remains far from complete. Studying the PP2AC-Alpha4 interaction may allow us to uncover more players involved in amino acid sensing in the cell.

mTORC1 is reported to be particularly responsive to levels of Leucine and Arginine in the cell, in that addition of these amino acids alone is sufficient to re-activate mTORC1 after starvation (Hara et al., 1998; Sancak et al., 2008). In support of this, lysosomal Arginine transporter SLC38A9 (Wang et al., 2015) and Leucyl-tRNA synthetase (Han et al., 2012) were shown to regulate mTORC1. Overnight glutamine starvation (24 hours) has been reported to induce Alpha4 dissociation from PP2AC. While short (1 – 2 hours) timepoints were used to monitor PP2AC-Alpha4 interaction in my study, glutamine starvation might be a good starting point to find upstream regulators of PP2AC-Alpha4 that differentiate it from mTORC1 signaling. Recently it was reported that cells can reactivate mTORC1 in response to Glutamine as well, but the effect was observed in cells lacking Rag GTPases (thus no longer responsive to Leucine and Arginine) (Jewell et al., 2015), arguing that Glutamine signaling may not have a major effect on mTORC1 in cells with intact Rag function.

ULK1 as a target for cancer treatment

Based on mouse models and work in cancer cell lines, several groups have proposed targeting autophagy for cancer treatment (Kimmelman, 2011; Leone and Amaravadi, 2013). Currently, small molecule inhibitors used to block autophagy include bafilomycin, chloroquine, and hydroxychloroquine, which target the lysosomes- the endpoint of autophagy; wortmannin, 3-Methyladenine and LY294002, which target

PI3Ks, including class III PI3K VPS34- whose activity is required for autophagy. Efforts have been made to develop more specific VPS34 inhibitors (Bago et al., 2014; Dowdle et al., 2014; Ronan et al., 2014) that have less activity toward class I and class II PI3Ks. However, as PI3P generation by VPS34 is required for other membrane trafficking processes, targeting other autophagy essential genes such as ULK1 may result in more specific autophagy inhibitors. To this end, several attempts to develop small molecule inhibitors against ULK1 are already underway (Lazarus et al., 2015; Petherick et al., 2015; Rosenberg et al., 2015). The crystal structure of human ULK1 kinase domain by Shokat and colleagues would certainly be a useful tool in the optimization of new compounds (Lazarus et al., 2015).

The relationship between autophagy and cancer is complex and has been reported to be both context and cancer dependent. In this study, I demonstrate that "autophagy addicted" PDAC cell line 8988T requires both PP2A activity and the ULK1 complex to maintain high basal levels of autophagy, rapid proliferation, and sustained anchorage-independent growth in the absence of mTOR inactivation. While the mechanism driving phosphatase activation is unclear, I observed a correlation of low Alpha4 levels in 8988T and high B55α levels in BxPC3. It would be interesting to see if these proteins together with ULK1 could be used as predictive markers to identify cancers that would be susceptible to ULK1 inhibition.

REFERENCES

Alemu, E.A., Lamark, T., Torgersen, K.M., Birgisdottir, A.B., Larsen, K.B., Jain, A., Olsvik, H., Øvervatn, A., Kirkin, V., and Johansen, T. (2012). ATG8 family proteins act as scaffolds for assembly of the ULK complex: sequence requirements for LC3-interacting region (LIR) motifs. J Biol Chem *287*, 39275-39290.

Alonso, A., Sasin, J., Bottini, N., Friedberg, I., Osterman, A., Godzik, A., Hunter, T., Dixon, J., and Mustelin, T. (2004). Protein tyrosine phosphatases in the human genome. Cell *117*, 699-711.

Axe, E.L., Walker, S.A., Manifava, M., Chandra, P., Roderick, H.L., Habermann, A., Griffiths, G., and Ktistakis, N.T. (2008). Autophagosome formation from membrane compartments enriched in phosphatidylinositol 3-phosphate and dynamically connected to the endoplasmic reticulum. J Cell Biol *182*, 685-701.

Bago, R., Malik, N., Munson, M.J., Prescott, A.R., Davies, P., Sommer, E., Shpiro, N., Ward, R., Cross, D., Ganley, I.G.*, et al.* (2014). Characterization of VPS34-IN1, a selective inhibitor of Vps34, reveals that the phosphatidylinositol 3-phosphate-binding SGK3 protein kinase is a downstream target of class III phosphoinositide 3-kinase. Biochem J *463*, 413-427.

Baharians, Z., and Schönthal, A.H. (1998). Autoregulation of protein phosphatase type 2A expression. J Biol Chem *273*, 19019-19024.

Balderhaar, H.J., and Ungermann, C. (2013). CORVET and HOPS tethering complexes - coordinators of endosome and lysosome fusion. J Cell Sci *126*, 1307-1316.

Bar-Peled, L., Schweitzer, L.D., Zoncu, R., and Sabatini, D.M. (2012). Ragulator is a GEF for the rag GTPases that signal amino acid levels to mTORC1. Cell *150*, 1196-1208.

Benjamin, D., Colombi, M., Moroni, C., and Hall, M.N. (2011). Rapamycin passes the torch: a new generation of mTOR inhibitors. Nat Rev Drug Discov *10*, 868-880.

Bjørkøy, G., Lamark, T., Brech, A., Outzen, H., Perander, M., Overvatn, A., Stenmark, H., and Johansen, T. (2005). p62/SQSTM1 forms protein aggregates degraded by autophagy and has a protective effect on huntingtin-induced cell death. J Cell Biol *171*, 603-614.

Blankson, H., Holen, I., and Seglen, P.O. (1995). Disruption of the cytokeratin cytoskeleton and inhibition of hepatocytic autophagy by okadaic acid. Exp Cell Res *218*, 522-530.

Brautigan, D.L. (2013). Protein Ser/Thr phosphatases--the ugly ducklings of cell signalling. FEBS J *280*, 324-345.

Brown, W.J., DeWald, D.B., Emr, S.D., Plutner, H., and Balch, W.E. (1995). Role for phosphatidylinositol 3-kinase in the sorting and transport of newly synthesized lysosomal enzymes in mammalian cells. J Cell Biol *130*, 781-796.

Bánréti, A., Lukácsovich, T., Csikós, G., Erdélyi, M., and Sass, M. (2012). PP2A regulates autophagy in two alternative ways in Drosophila. Autophagy *8*.

Cabrera, M., and Ungermann, C. (2010). Guiding endosomal maturation. Cell *141*, 404-406.

Chan, E. (2009). mTORC1 phosphorylates the ULK1-mAtg13-FIP200 autophagy regulatory complex. Sci Signal *2*, pe51.

Chan, E., Kir, S., and Tooze, S. (2007). siRNA screening of the kinome identifies ULK1 as a multidomain modulator of autophagy. J Biol Chem *282*, 25464-25474.

Chan, E., Longatti, A., McKnight, N., and Tooze, S. (2009). Kinase-inactivated ULK proteins inhibit autophagy via their conserved C-terminal domains using an Atg13-independent mechanism. Mol Cell Biol *29*, 157-171.

Chen, Y., and Klionsky, D.J. (2011). The regulation of autophagy - unanswered questions. J Cell Sci *124*, 161-170.

Cheong, H., Lindsten, T., Wu, J., Lu, C., and Thompson, C.B. (2011). Ammonia-induced autophagy is independent of ULK1/ULK2 kinases. Proc Natl Acad Sci U S A *108*, 11121-11126.

Cherra, S.J., Kulich, S.M., Uechi, G., Balasubramani, M., Mountzouris, J., Day, B.W., and Chu, C.T. (2010). Regulation of the autophagy protein LC3 by phosphorylation. J Cell Biol *190*, 533-539.

Choo, A.Y., Yoon, S.O., Kim, S.G., Roux, P.P., and Blenis, J. (2008). Rapamycin differentially inhibits S6Ks and 4E-BP1 to mediate cell-type-specific repression of mRNA translation. Proc Natl Acad Sci U S A *105*, 17414-17419.

Chung, H., Nairn, A.C., Murata, K., and Brautigan, D.L. (1999). Mutation of Tyr307 and Leu309 in the protein phosphatase 2A catalytic subunit favors association with the alpha 4 subunit which promotes dephosphorylation of elongation factor-2. Biochemistry *38*, 10371-10376.

Cohen, P. (2002). The origins of protein phosphorylation. Nature Cell Biology *4*, E127-E130.

Cohen, P.W. (2004). Overview of protein serine/threonine phosphatases. In Protein Phosphatases, J. Ariño, and D. Alexander, eds. (Springer Berlin Heidelberg), pp. 1-20.

Cori, G.T., and Cori, C.F. (1945). The enzymatic conversion of phosphorylase *a* to *b*. the Journal of Biological Chemistry *158*, 321-332.

Deribe, Y.L., Pawson, T., and Dikic, I. (2010). Post-translational modifications in signal integration. Nat Struct Mol Biol *17*, 666-672.

Di Bartolomeo, S., Corazzari, M., Nazio, F., Oliverio, S., Lisi, G., Antonioli, M., Pagliarini, V., Matteoni, S., Fuoco, C., Giunta, L.*, et al.* (2010). The dynamic interaction of AMBRA1 with the dynein motor complex regulates mammalian autophagy. J Cell Biol *191*, 155-168.

Di Como, C.J., and Arndt, K.T. (1996). Nutrients, via the Tor proteins, stimulate the association of Tap42 with type 2A phosphatases. Genes Dev *10*, 1904-1916.

Dorsey, F., Rose, K., Coenen, S., Prater, S., Cavett, V., Cleveland, J., and Caldwell-Busby, J. (2009). Mapping the phosphorylation sites of Ulk1. J Proteome Res *8*, 5253-5263.

Dowdle, W.E., Nyfeler, B., Nagel, J., Elling, R.A., Liu, S., Triantafellow, E., Menon, S., Wang, Z., Honda, A., Pardee, G.*, et al.* (2014). Selective VPS34 inhibitor blocks autophagy and uncovers a role for NCOA4 in ferritin degradation and iron homeostasis in vivo. Nat Cell Biol *16*, 1069-1079.

Egan, D.F., Shackelford, D.B., Mihaylova, M.M., Gelino, S., Kohnz, R.A., Mair, W., Vasquez, D.S., Joshi, A., Gwinn, D.M., Taylor, R.*, et al.* (2011). Phosphorylation of ULK1 (hATG1) by AMP-activated protein kinase connects energy sensing to mitophagy. Science *331*, 456-461.

Eichhorn, P.J., Creyghton, M.P., and Bernards, R. (2009). Protein phosphatase 2A regulatory subunits and cancer. Biochim Biophys Acta *1795*, 1-15.

Eskelinen, E.L. (2005). Maturation of autophagic vacuoles in Mammalian cells. Autophagy *1*, 1-10.

Evans, P.R., and Owen, D.J. (2002). Endocytosis and vesicle trafficking. Curr Opin Struct Biol *12*, 814-821.

Fader, C.M., Sánchez, D.G., Mestre, M.B., and Colombo, M.I. (2009). TI-VAMP/VAMP7 and VAMP3/cellubrevin: two v-SNARE proteins involved in specific steps of the autophagy/multivesicular body pathways. Biochim Biophys Acta *1793*, 1901-1916.

Feldman, M.E., Apsel, B., Uotila, A., Loewith, R., Knight, Z.A., Ruggero, D., and Shokat, K.M. (2009). Active-site inhibitors of mTOR target rapamycin-resistant outputs of mTORC1 and mTORC2. PLoS Biol *7*, e38.

Filimonenko, M., Stuffers, S., Raiborg, C., Yamamoto, A., Malerød, L., Fisher, E.M., Isaacs, A., Brech, A., Stenmark, H., and Simonsen, A. (2007). Functional multivesicular bodies are required for autophagic clearance of protein aggregates associated with neurodegenerative disease. J Cell Biol *179*, 485-500.

Fischer, E.H., Graves, D.J., Crittenden, E.R.S., and Krebs, E.G. (1959). Structure of the site phosphorylated in the phosphorylase b to a reaction. the Journal of Biological Chemistry *234*, 1698-1704.

Fujita, N., Itoh, T., Omori, H., Fukuda, M., Noda, T., and Yoshimori, T. (2008). The Atg16L complex specifies the site of LC3 lipidation for membrane biogenesis in autophagy. Mol Biol Cell *19*, 2092-2100.

Furuta, N., Fujita, N., Noda, T., Yoshimori, T., and Amano, A. (2010). Combinational soluble N-ethylmaleimide-sensitive factor attachment protein receptor proteins VAMP8 and Vti1b mediate fusion of antimicrobial and canonical autophagosomes with lysosomes. Mol Biol Cell *21*, 1001-1010.

Gammoh, N., Florey, O., Overholtzer, M., and Jiang, X. (2013). Interaction between FIP200 and ATG16L1 distinguishes ULK1 complex-dependent and -independent autophagy. Nat Struct Mol Biol *20*, 144-149.

Ganley, I., Lam, d.H., Wang, J., Ding, X., Chen, S., and Jiang, X. (2009). ULK1.ATG13.FIP200 complex mediates mTOR signaling and is essential for autophagy. J Biol Chem *284*, 12297-12305.

Ganley, I.G., Wong, P.M., Gammoh, N., and Jiang, X. (2011). Distinct autophagosomal-lysosomal fusion mechanism revealed by thapsigargin-induced autophagy arrest. Mol Cell *42*, 731-743.

Gao, T., Furnari, F., and Newton, A.C. (2005). PHLPP: a phosphatase that directly dephosphorylates Akt, promotes apoptosis, and suppresses tumor growth. Mol Cell *18*, 13-24.

Garami, A., Zwartkruis, F.J., Nobukuni, T., Joaquin, M., Roccio, M., Stocker, H., Kozma, S.C., Hafen, E., Bos, J.L., and Thomas, G. (2003). Insulin activation of Rheb, a mediator of mTOR/S6K/4E-BP signaling, is inhibited by TSC1 and 2. Mol Cell *11*, 1457-1466.

Gordon, P.B., Høyvik, H., and Seglen, P.O. (1992). Prelysosomal and lysosomal connections between autophagy and endocytosis. Biochem J *283 (Pt 2)*, 361-369.

Goudreault, M., D'Ambrosio, L.M., Kean, M.J., Mullin, M.J., Larsen, B.G., Sanchez, A., Chaudhry, S., Chen, G.I., Sicheri, F., Nesvizhskii, A.I*., et al.* (2009). A PP2A phosphatase high density interaction network identifies a novel striatin-interacting phosphatase and kinase complex linked to the cerebral cavernous malformation 3 (CCM3) protein. Mol Cell Proteomics *8*, 157-171.

Grotemeier, A., Alers, S., Pfisterer, S.G., Paasch, F., Daubrawa, M., Dieterle, A., Viollet, B., Wesselborg, S., Proikas-Cezanne, T., and Stork, B. (2010). AMPK-independent induction of autophagy by cytosolic Ca2+ increase. Cell Signal *22*, 914-925.

Guertin, D.A., and Sabatini, D.M. (2007). Defining the role of mTOR in cancer. Cancer Cell *12*, 9-22.

Guo, J.Y., Chen, H.Y., Mathew, R., Fan, J., Strohecker, A.M., Karsli-Uzunbas, G., Kamphorst, J.J., Chen, G., Lemons, J.M., Karantza, V*., et al.* (2011). Activated Ras requires autophagy to maintain oxidative metabolism and tumorigenesis. Genes Dev *25*, 460-470.

Guo, J.Y., Xia, B., and White, E. (2013). Autophagy-mediated tumor promotion. Cell *155*, 1216-1219.

Gutierrez, M.G., Munafó, D.B., Berón, W., and Colombo, M.I. (2004). Rab7 is required for the normal progression of the autophagic pathway in mammalian cells. J Cell Sci *117*, 2687-2697.

Han, J.M., Jeong, S.J., Park, M.C., Kim, G., Kwon, N.H., Kim, H.K., Ha, S.H., Ryu, S.H., and Kim, S. (2012). Leucyl-tRNA synthetase is an intracellular leucine sensor for the mTORC1-signaling pathway. Cell *149*, 410-424.

Hara, K., Yonezawa, K., Weng, Q.P., Kozlowski, M.T., Belham, C., and Avruch, J. (1998). Amino acid sufficiency and mTOR regulate p70 S6 kinase and eIF-4E BP1 through a common effector mechanism. J Biol Chem *273*, 14484-14494.

Hara, T., Takamura, A., Kishi, C., Iemura, S., Natsume, T., Guan, J., and Mizushima, N. (2008). FIP200, a ULK-interacting protein, is required for autophagosome formation in mammalian cells. J Cell Biol *181*, 497-510.

Harding, T.M., Morano, K.A., Scott, S.V., and Klionsky, D.J. (1995). Isolation and characterization of yeast mutants in the cytoplasm to vacuole protein targeting pathway. J Cell Biol *131*, 591-602.

Herzog, F., Kahraman, A., Boehringer, D., Mak, R., Bracher, A., Walzthoeni, T., Leitner, A., Beck, M., Hartl, F.U., Ban, N.*, et al.* (2012). Structural probing of a protein phosphatase 2A network by chemical cross-linking and mass spectrometry. Science *337*, 1348-1352.

Holen, I., Gordon, P.B., and Seglen, P.O. (1993). Inhibition of hepatocytic autophagy by okadaic acid and other protein phosphatase inhibitors. Eur J Biochem *215*, 113-122.

Hosokawa, N., Hara, T., Kaizuka, T., Kishi, C., Takamura, A., Miura, Y., Iemura, S., Natsume, T., Takehana, K., Yamada, N.*, et al.* (2009). Nutrient-dependent mTORC1 association with the ULK1-Atg13-FIP200 complex required for autophagy. Mol Biol Cell *20*, 1981-1991.

Hyttinen, J.M., Niittykoski, M., Salminen, A., and Kaarniranta, K. (2013). Maturation of autophagosomes and endosomes: a key role for Rab7. Biochim Biophys Acta *1833*, 503-510.

Ichimura, Y., Kirisako, T., Takao, T., Satomi, Y., Shimonishi, Y., Ishihara, N., Mizushima, N., Tanida, I., Kominami, E., Ohsumi, M.*, et al.* (2000). A ubiquitin-like system mediates protein lipidation. Nature *408*, 488-492.

Ichimura, Y., Waguri, S., Sou, Y.S., Kageyama, S., Hasegawa, J., Ishimura, R., Saito, T., Yang, Y., Kouno, T., Fukutomi, T.*, et al.* (2013). Phosphorylation of p62 activates the Keap1-Nrf2 pathway during selective autophagy. Mol Cell *51*, 618-631.

Inoki, K., Li, Y., Zhu, T., Wu, J., and Guan, K.L. (2002). TSC2 is phosphorylated and inhibited by Akt and suppresses mTOR signalling. Nat Cell Biol *4*, 648-657.

Ishibashi, K., Fujita, N., Kanno, E., Omori, H., Yoshimori, T., Itoh, T., and Fukuda, M. (2011). Atg16L2, a novel isoform of mammalian Atg16L that is not essential for canonical autophagy despite forming an Atg12–5-16L2 complex. Autophagy *7*, 1500-1513.

Itakura, E., Kishi, C., Inoue, K., and Mizushima, N. (2008). Beclin 1 forms two distinct phosphatidylinositol 3-kinase complexes with mammalian Atg14 and UVRAG. Mol Biol Cell *19*, 5360-5372.

Itakura, E., Kishi-Itakura, C., and Mizushima, N. (2012). The hairpin-type tail-anchored SNARE syntaxin 17 targets to autophagosomes for fusion with endosomes/lysosomes. Cell *151*, 1256-1269.

Itakura, E., and Mizushima, N. (2009). Atg14 and UVRAG: mutually exclusive subunits of mammalian Beclin 1-PI3K complexes. Autophagy *5*, 534-536.

Itakura, E., and Mizushima, N. (2010). Characterization of autophagosome formation site by a hierarchical analysis of mammalian Atg proteins. Autophagy *6*, 764-776.

Jaber, N., Dou, Z., Chen, J.S., Catanzaro, J., Jiang, Y.P., Ballou, L.M., Selinger, E., Ouyang, X., Lin, R.Z., Zhang, J.*, et al.* (2012). Class III PI3K Vps34 plays an essential role in autophagy and in heart and liver function. Proc Natl Acad Sci U S A *109*, 2003-2008.

Jahreiss, L., Menzies, F.M., and Rubinsztein, D.C. (2008). The itinerary of autophagosomes: from peripheral formation to kiss-and-run fusion with lysosomes. Traffic *9*, 574-587.

Janssens, V., Longin, S., and Goris, J. (2008). PP2A holoenzyme assembly: in cauda venenum (the sting is in the tail). Trends Biochem Sci *33*, 113-121.

Jewell, J.L., Kim, Y.C., Russell, R.C., Yu, F.X., Park, H.W., Plouffe, S.W., Tagliabracci, V.S., and Guan, K.L. (2015). Metabolism. Differential regulation of mTORC1 by leucine and glutamine. Science *347*, 194-198.

Jiang, L., Stanevich, V., Satyshur, K.A., Kong, M., Watkins, G.R., Wadzinski, B.E., Sengupta, R., and Xing, Y. (2013). Structural basis of protein phosphatase 2A stable latency. Nat Commun *4*, 1699.

Jiang, Y., and Broach, J.R. (1999). Tor proteins and protein phosphatase 2A reciprocally regulate Tap42 in controlling cell growth in yeast. EMBO J *18*, 2782-2792.

Johnson, E.E., Overmeyer, J.H., Gunning, W.T., and Maltese, W.A. (2006). Gene silencing reveals a specific function of hVps34 phosphatidylinositol 3-kinase in late versus early endosomes. J Cell Sci *119*, 1219-1232.

Johnson, S.A., and Hunter, T. (2005). Kinomics: methods for deciphering the kinome. Nat Methods *2*, 17-25.

Joo, J.H., Dorsey, F.C., Joshi, A., Hennessy-Walters, K.M., Rose, K.L., McCastlain, K., Zhang, J., Iyengar, R., Jung, C.H., Suen, D.F.*, et al.* (2011). Hsp90-Cdc37 chaperone complex regulates Ulk1- and Atg13-mediated mitophagy. Mol Cell *43*, 572-585.

Jung, C., Jun, C., Ro, S., Kim, Y., Otto, N., Cao, J., Kundu, M., and Kim, D. (2009). ULK-Atg13-FIP200 complexes mediate mTOR signaling to the autophagy machinery. Mol Biol Cell *20*, 1992-2003.

Junttila, M.R., Puustinen, P., Niemelä, M., Ahola, R., Arnold, H., Böttzauw, T., Ala-aho, R., Nielsen, C., Ivaska, J., Taya, Y.*, et al.* (2007). CIP2A inhibits PP2A in human malignancies. Cell *130*, 51-62.

Jäger, S., Bucci, C., Tanida, I., Ueno, T., Kominami, E., Saftig, P., and Eskelinen, E.L. (2004). Role for Rab7 in maturation of late autophagic vacuoles. J Cell Sci *117*, 4837-4848.

Kageyama, S., Omori, H., Saitoh, T., Sone, T., Guan, J.L., Akira, S., Imamoto, F., Noda, T., and Yoshimori, T. (2011). The LC3 recruitment mechanism is separate from Atg9L1-dependent membrane formation in the autophagic response against Salmonella. Mol Biol Cell *22*, 2290-2300.

Kanki, T., Wang, K., Cao, Y., Baba, M., and Klionsky, D. (2009). Atg32 is a mitochondrial protein that confers selectivity during mitophagy. Dev Cell *17*, 98-109.

Kim, J., Kim, Y.C., Fang, C., Russell, R.C., Kim, J.H., Fan, W., Liu, R., Zhong, Q., and Guan, K.L. (2013). Differential regulation of distinct Vps34 complexes by AMPK in nutrient stress and autophagy. Cell *152*, 290-303.

Kim, J., Kundu, M., Viollet, B., and Guan, K.L. (2011). AMPK and mTOR regulate autophagy through direct phosphorylation of Ulk1. Nat Cell Biol *13*, 132-141.

Kimmelman, A.C. (2011). The dynamic nature of autophagy in cancer. Genes Dev *25*, 1999-2010.

Kinchen, J.M., and Ravichandran, K.S. (2010). Identification of two evolutionarily conserved genes regulating processing of engulfed apoptotic cells. Nature *464*, 778-782.

Kirkin, V., Lamark, T., Sou, Y.S., Bjørkøy, G., Nunn, J.L., Bruun, J.A., Shvets, E., McEwan, D.G., Clausen, T.H., Wild, P.*, et al.* (2009). A role for NBR1 in autophagosomal degradation of ubiquitinated substrates. Mol Cell *33*, 505-516.

Klionsky, D.J. (2007). Autophagy: from phenomenology to molecular understanding in less than a decade. Nat Rev Mol Cell Biol *8*, 931-937.

Kolupaeva, V., Daempfling, L., and Basilico, C. (2013). The B55α regulatory subunit of protein phosphatase 2A mediates fibroblast growth factor-induced p107 dephosphorylation and growth arrest in chondrocytes. Mol Cell Biol *33*, 2865-2878.

Komander, D. (2009). The emerging complexity of protein ubiquitination. Biochem Soc Trans *37*, 937-953.

Komatsu, M., Waguri, S., Ueno, T., Iwata, J., Murata, S., Tanida, I., Ezaki, J., Mizushima, N., Ohsumi, Y., Uchiyama, Y.*, et al.* (2005). Impairment of starvation-induced and constitutive autophagy in Atg7-deficient mice. J Cell Biol *169*, 425-434.

Kong, M., Fox, C.J., Mu, J., Solt, L., Xu, A., Cinalli, R.M., Birnbaum, M.J., Lindsten, T., and Thompson, C.B. (2004). The PP2A-associated protein alpha4 is an essential inhibitor of apoptosis. Science *306*, 695-698.

Krebs, E.G., and Fischer, E.H. (1956). The phosphorylase b to a converting enzyme of rabbit skeletal muscle. Biochim Biophys Acta *20*, 150-157.

Krebs, E.G., Kent, A.B., and Fischer, E.H. (1958). The muscle phosphorylase b kinase reaction. the Journal of Biological Chemistry *231*, 73-84.

Kroemer, G., Mariño, G., and Levine, B. (2010). Autophagy and the integrated stress response. Mol Cell *40*, 280-293.

Kuma, A., Hatano, M., Matsui, M., Yamamoto, A., Nakaya, H., Yoshimori, T., Ohsumi, Y., Tokuhisa, T., and Mizushima, N. (2004). The role of autophagy during the early neonatal starvation period. Nature *432*, 1032-1036.

Kundu, M., Lindsten, T., Yang, C., Wu, J., Zhao, F., Zhang, J., Selak, M., Ney, P., and Thompson, C. (2008). Ulk1 plays a critical role in the autophagic clearance of mitochondria and ribosomes during reticulocyte maturation. Blood *112*, 1493-1502.

Kuo, Y.C., Huang, K.Y., Yang, C.H., Yang, Y.S., Lee, W.Y., and Chiang, C.W. (2008). Regulation of phosphorylation of Thr-308 of Akt, cell proliferation, and survival by the B55alpha regulatory subunit targeting of the protein phosphatase 2A holoenzyme to Akt. J Biol Chem *283*, 1882-1892.

Kuroyanagi, H., Yan, J., Seki, N., Yamanouchi, Y., Suzuki, Y., Takano, T., Muramatsu, M., and Shirasawa, T. (1998). Human ULK1, a novel serine/threonine kinase related to UNC-51 kinase of Caenorhabditis elegans: cDNA cloning, expression, and chromosomal assignment. Genomics *51*, 76-85.

Lawrence, B.P., and Brown, W.J. (1992). Autophagic vacuoles rapidly fuse with pre-existing lysosomes in cultured hepatocytes. J Cell Sci *102 (Pt 3)*, 515-526.

Lazarus, M.B., Novotny, C.J., and Shokat, K.M. (2015). Structure of the human autophagy initiating kinase ULK1 in complex with potent inhibitors. ACS Chem Biol *10*, 257-261.

Lee, E.J., and Tournier, C. (2011). The requirement of uncoordinated 51-like kinase 1 (ULK1) and ULK2 in the regulation of autophagy. Autophagy *7*, 689-695.

Lee, J.A., Beigneux, A., Ahmad, S.T., Young, S.G., and Gao, F.B. (2007). ESCRT-III dysfunction causes autophagosome accumulation and neurodegeneration. Curr Biol *17*, 1561-1567.

Lee, J.W., Park, S., Takahashi, Y., and Wang, H.G. (2010). The association of AMPK with ULK1 regulates autophagy. PLoS One *5*, e15394.

Leone, R.D., and Amaravadi, R.K. (2013). Autophagy: a targetable linchpin of cancer cell metabolism. Trends Endocrinol Metab *24*, 209-217.

Li, M., Guo, H., and Damuni, Z. (1995). Purification and characterization of two potent heat-stable protein inhibitors of protein phosphatase 2A from bovine kidney. Biochemistry *34*, 1988-1996.

Lim, J., Lachenmayer, M.L., Wu, S., Liu, W., Kundu, M., Wang, R., Komatsu, M., Oh, Y.J., Zhao, Y., and Yue, Z. (2015). Proteotoxic stress induces phosphorylation of p62/SQSTM1 by ULK1 to regulate selective autophagic clearance of protein aggregates. PLoS Genet *11*, e1004987.

Lin, S.Y., Li, T.Y., Liu, Q., Zhang, C., Li, X., Chen, Y., Zhang, S.M., Lian, G., Ruan, K., Wang, Z.*, et al.* (2012). GSK3-TIP60-ULK1 signaling pathway links growth factor deprivation to autophagy. Science *336*, 477-481.

Liou, W., Geuze, H.J., Geelen, M.J., and Slot, J.W. (1997). The autophagic and endocytic pathways converge at the nascent autophagic vacuoles. J Cell Biol *136*, 61-70.

Liu, L., Feng, D., Chen, G., Chen, M., Zheng, Q., Song, P., Ma, Q., Zhu, C., Wang, R., Qi, W.*, et al.* (2012). Mitochondrial outer-membrane protein FUNDC1 mediates hypoxia-induced mitophagy in mammalian cells. Nat Cell Biol *14*, 177-185.

Luzio, J.P., Parkinson, M.D., Gray, S.R., and Bright, N.A. (2009). The delivery of endocytosed cargo to lysosomes. Biochem Soc Trans *37*, 1019-1021.

Mack, H.I.D., Zheng, B., Asara, J., and Thomas, S.M. (2012). AMPK-dependent phosphorylation of ULK1 regulates ATG9 localization. Autophagy *8*.

Magnaudeix, A., Wilson, C.M., Page, G., Bauvy, C., Codogno, P., Lévêque, P., Labrousse, F., Corre-Delage, M., Yardin, C., and Terro, F. (2013). PP2A blockade inhibits autophagy and causes intraneuronal accumulation of ubiquitinated proteins. Neurobiol Aging *34*, 770-790.

Mancias, J.D., Wang, X., Gygi, S.P., Harper, J.W., and Kimmelman, A.C. (2014). Quantitative proteomics identifies NCOA4 as the cargo receptor mediating ferritinophagy. Nature *509*, 105-109.

Manning, G., Whyte, D.B., Martinez, R., Hunter, T., and Sudarsanam, S. (2002). The protein kinase complement of the human genome. Science *298*, 1912-1934.

Mari, M., Griffith, J., Rieter, E., Krishnappa, L., Klionsky, D.J., and Reggiori, F. (2010). An Atg9-containing compartment that functions in the early steps of autophagosome biogenesis. J Cell Biol *190*, 1005-1022.

Martin, K.R., Xu, Y., Looyenga, B.D., Davis, R.J., Wu, C.L., Tremblay, M.L., Xu, H.E., and MacKeigan, J.P. (2011). Identification of PTPsigma as an autophagic phosphatase. J Cell Sci *124*, 812-819.

Matsumoto, G., Wada, K., Okuno, M., Kurosawa, M., and Nukina, N. (2011). Serine 403 phosphorylation of p62/SQSTM1 regulates selective autophagic clearance of ubiquitinated proteins. Mol Cell *44*, 279-289.

Matsunaga, K., Morita, E., Saitoh, T., Akira, S., Ktistakis, N.T., Izumi, T., Noda, T., and Yoshimori, T. (2010). Autophagy requires endoplasmic reticulum targeting of the PI3-kinase complex via Atg14L. J Cell Biol *190*, 511-521.

Matsunaga, K., Saitoh, T., Tabata, K., Omori, H., Satoh, T., Kurotori, N., Maejima, I., Shirahama-Noda, K., Ichimura, T., Isobe, T.*, et al.* (2009). Two Beclin 1-binding proteins, Atg14L and Rubicon, reciprocally regulate autophagy at different stages. Nat Cell Biol *11*, 385-396.

Matsuura, A., Tsukada, M., Wada, Y., and Ohsumi, Y. (1997). Apg1p, a novel protein kinase required for the autophagic process in Saccharomyces cerevisiae. Gene *192*, 245-250.

McConnell, J.L., and Wadzinski, B.E. (2009). Targeting protein serine/threonine phosphatases for drug development. Mol Pharmacol *75*, 1249-1261.

McConnell, J.L., Watkins, G.R., Soss, S.E., Franz, H.S., McCorvey, L.R., Spiller, B.W., Chazin, W.J., and Wadzinski, B.E. (2010). Alpha4 is a ubiquitin-binding protein that regulates protein serine/threonine phosphatase 2A ubiquitination. Biochemistry *49*, 1713-1718.

McEwan, D.G., and Dikic, I. (2011). The Three Musketeers of Autophagy: phosphorylation, ubiquitylation and acetylation. Trends Cell Biol *21*, 195-201.

Mizushima, N., and Komatsu, M. (2011). Autophagy: renovation of cells and tissues. Cell *147*, 728-741.

Mizushima, N., Noda, T., Yoshimori, T., Tanaka, Y., Ishii, T., George, M.D., Klionsky, D.J., Ohsumi, M., and Ohsumi, Y. (1998). A protein conjugation system essential for autophagy. Nature *395*, 395-398.

Mizushima, N., Yoshimori, T., and Ohsumi, Y. (2011). The role of atg proteins in autophagosome formation. Annu Rev Cell Dev Biol *27*, 107-132.

Moreau, K., Renna, M., and Rubinsztein, D.C. (2013). Connections between SNAREs and autophagy. Trends Biochem Sci *38*, 57-63.

Mumby, M. (2004). Protein phosphatase 2A: A multifunctional regulator of cell signaling. In Protein Phosphatases, J.n. Ariño, and D.R. Alexander, eds. (Springer Berlin Heidelberg), pp. 45-72.

Mumby, M. (2007). The 3D structure of protein phosphatase 2A: new insights into a ubiquitous regulator of cell signaling. ACS Chem Biol *2*, 99-103.

Nair, U., Jotwani, A., Geng, J., Gammoh, N., Richerson, D., Yen, W.L., Griffith, J., Nag, S., Wang, K., Moss, T.*, et al.* (2011). SNARE proteins are required for macroautophagy. Cell *146*, 290-302.

Nakatogawa, H., Ohbayashi, S., Sakoh-Nakatogawa, M., Kakuta, S., Suzuki, S.W., Kirisako, H., Kondo-Kakuta, C., Noda, N.N., Yamamoto, H., and Ohsumi, Y. (2012). The Autophagy-Related Protein Kinase Atg1 Interacts with the Ubiquitin-Like Protein Atg8 via the Atg8 Family Interacting Motif to Facilitate Autophagosome Formation. J Biol Chem.

Nazio, F., Strappazzon, F., Antonioli, M., Bielli, P., Cianfanelli, V., Bordi, M., Gretzmeier, C., Dengjel, J., Piacentini, M., Fimia, G.M.*, et al.* (2013). mTOR inhibits autophagy by controlling ULK1 ubiquitylation, self-association and function through AMBRA1 and TRAF6. Nat Cell Biol *15*, 406-416.

Nishimura, T., Kaizuka, T., Cadwell, K., Sahani, M.H., Saitoh, T., Akira, S., Virgin, H.W., and Mizushima, N. (2013). FIP200 regulates targeting of Atg16L1 to the isolation membrane. EMBO Rep *14*, 284-291.

Ogata, M., Hino, S., Saito, A., Morikawa, K., Kondo, S., Kanemoto, S., Murakami, T., Taniguchi, M., Tanii, I., Yoshinaga, K.*, et al.* (2006). Autophagy is activated for cell survival after endoplasmic reticulum stress. Mol Cell Biol *26*, 9220-9231.

Ogris, E., Du, X., Nelson, K.C., Mak, E.K., Yu, X.X., Lane, W.S., and Pallas, D.C. (1999). A protein phosphatase methylesterase (PME-1) is one of several novel proteins stably associating with two inactive mutants of protein phosphatase 2A. J Biol Chem *274*, 14382-14391.

Okazaki, N., Yan, J., Yuasa, S., Ueno, T., Kominami, E., Masuho, Y., Koga, H., and Muramatsu, M. (2000). Interaction of the Unc-51-like kinase and microtubule-associated protein light chain 3 related proteins in the brain: possible role of vesicular transport in axonal elongation. Brain Res Mol Brain Res *85*, 1-12.

Orsi, A., Razi, M., Dooley, H., Robinson, D., Weston, A., Collinson, L., and Tooze, S. (2012). Dynamic and transient interactions of Atg9 with autophagosomes, but not membrane integration, is required for autophagy. Mol Biol Cell.

Ortega-Gutiérrez, S., Leung, D., Ficarro, S., Peters, E.C., and Cravatt, B.F. (2008). Targeted disruption of the PME-1 gene causes loss of demethylated PP2A and perinatal lethality in mice. PLoS One *3*, e2486.

Pankiv, S., Alemu, E.A., Brech, A., Bruun, J.A., Lamark, T., Overvatn, A., Bjørkøy, G., and Johansen, T. (2010). FYCO1 is a Rab7 effector that binds to LC3 and PI3P to mediate microtubule plus end-directed vesicle transport. J Cell Biol *188*, 253-269.

Pankiv, S., Clausen, T.H., Lamark, T., Brech, A., Bruun, J.A., Outzen, H., Øvervatn, A., Bjørkøy, G., and Johansen, T. (2007). p62/SQSTM1 binds directly to Atg8/LC3 to facilitate degradation of ubiquitinated protein aggregates by autophagy. J Biol Chem *282*, 24131-24145.

Papinski, D., Schuschnig, M., Reiter, W., Wilhelm, L., Barnes, C.A., Maiolica, A., Hansmann, I., Pfaffenwimmer, T., Kijanska, M., Stoffel, I.*, et al.* (2014). Early steps in autophagy depend on direct phosphorylation of Atg9 by the Atg1 kinase. Mol Cell *53*, 471-483.

Peterson, T.R., Laplante, M., Thoreen, C.C., Sancak, Y., Kang, S.A., Kuehl, W.M., Gray, N.S., and Sabatini, D.M. (2009). DEPTOR is an mTOR inhibitor frequently overexpressed in multiple myeloma cells and required for their survival. Cell *137*, 873-886.

Petherick, K.J., Conway, O.J., Mpamhanga, C., Osborne, S.A., Kamal, A., Saxty, B., and Ganley, I.G. (2015). Pharmacological Inhibition of ULK1 Kinase Blocks Mammalian Target of Rapamycin (mTOR)-dependent Autophagy. J Biol Chem *290*, 11376-11383.

Polson, H.E., de Lartigue, J., Rigden, D.J., Reedijk, M., Urbé, S., Clague, M.J., and Tooze, S.A. (2010). Mammalian Atg18 (WIPI2) localizes to omegasome-anchored phagophores and positively regulates LC3 lipidation. Autophagy *6*, 506-522.

Poteryaev, D., Datta, S., Ackema, K., Zerial, M., and Spang, A. (2010). Identification of the switch in early-to-late endosome transition. Cell *141*, 497-508.

Prickett, T.D., and Brautigan, D.L. (2004). Overlapping binding sites in protein phosphatase 2A for association with regulatory A and alpha-4 (mTap42) subunits. J Biol Chem *279*, 38912-38920.

Proikas-Cezanne, T., Ruckerbauer, S., Stierhof, Y.D., Berg, C., and Nordheim, A. (2007). Human WIPI-1 puncta-formation: a novel assay to assess mammalian autophagy. FEBS Lett *581*, 3396-3404.

Puustinen, P., Rytter, A., Mortensen, M., Kohonen, P., Moreira, J.M., and Jäättelä, M. (2014). CIP2A oncoprotein controls cell growth and autophagy through mTORC1 activation. J Cell Biol *204*, 713-727.

Rao, S., Tortola, L., Perlot, T., Wirnsberger, G., Novatchkova, M., Nitsch, R., Sykacek, P., Frank, L., Schramek, D., Komnenovic, V.*, et al.* (2014). A dual role for autophagy in a murine model of lung cancer. Nat Commun *5*, 3056.

Razi, M., Chan, E.Y., and Tooze, S.A. (2009). Early endosomes and endosomal coatomer are required for autophagy. J Cell Biol *185*, 305-321.

Reggiori, F., Tucker, K.A., Stromhaug, P.E., and Klionsky, D.J. (2004). The Atg1-Atg13 complex regulates Atg9 and Atg23 retrieval transport from the pre-autophagosomal structure. Dev Cell *6*, 79-90.

Reid, M.A., Wang, W.I., Rosales, K.R., Welliver, M.X., Pan, M., and Kong, M. (2013). The B55α subunit of PP2A drives a p53-dependent metabolic adaptation to glutamine deprivation. Mol Cell *50*, 200-211.

Rink, J., Ghigo, E., Kalaidzidis, Y., and Zerial, M. (2005). Rab conversion as a mechanism of progression from early to late endosomes. Cell *122*, 735-749.

Ronan, B., Flamand, O., Vescovi, L., Dureuil, C., Durand, L., Fassy, F., Bachelot, M.F., Lamberton, A., Mathieu, M., Bertrand, T.*, et al.* (2014). A highly potent and selective Vps34 inhibitor alters vesicle trafficking and autophagy. Nat Chem Biol *10*, 1013-1019.

Rosenberg, L.H., Lafitte, M., Grant, W., Chen, W., Cleveland, J.L., and Duckett, D.R. (2015). Development of an HTS-Compatible Assay for the Discovery of Ulk1 Inhibitors. J Biomol Screen.

Russell, R.C., Tian, Y., Yuan, H., Park, H.W., Chang, Y.Y., Kim, J., Kim, H., Neufeld, T.P., Dillin, A., and Guan, K.L. (2013). ULK1 induces autophagy by phosphorylating Beclin-1 and activating VPS34 lipid kinase. Nat Cell Biol *15*, 741-750.

Rusten, T.E., Vaccari, T., Lindmo, K., Rodahl, L.M., Nezis, I.P., Sem-Jacobsen, C., Wendler, F., Vincent, J.P., Brech, A., Bilder, D.*, et al.* (2007). ESCRTs and Fab1 regulate distinct steps of autophagy. Curr Biol *17*, 1817-1825.

Saitoh, T., Fujita, N., Hayashi, T., Takahara, K., Satoh, T., Lee, H., Matsunaga, K., Kageyama, S., Omori, H., Noda, T.*, et al.* (2009). Atg9a controls dsDNA-driven dynamic translocation of STING and the innate immune response. Proc Natl Acad Sci U S A *106*, 20842-20846.

Saitoh, T., Fujita, N., Jang, M.H., Uematsu, S., Yang, B.G., Satoh, T., Omori, H., Noda, T., Yamamoto, N., Komatsu, M.*, et al.* (2008). Loss of the autophagy protein Atg16L1 enhances endotoxin-induced IL-1beta production. Nature *456*, 264-268.

Sakaki, K., Wu, J., and Kaufman, R.J. (2008). Protein kinase Ctheta is required for autophagy in response to stress in the endoplasmic reticulum. J Biol Chem *283*, 15370-15380.

Sancak, Y., Bar-Peled, L., Zoncu, R., Markhard, A.L., Nada, S., and Sabatini, D.M. (2010). Ragulator-Rag complex targets mTORC1 to the lysosomal surface and is necessary for its activation by amino acids. Cell *141*, 290-303.

Sancak, Y., Peterson, T.R., Shaul, Y.D., Lindquist, R.A., Thoreen, C.C., Bar-Peled, L., and Sabatini, D.M. (2008). The Rag GTPases bind raptor and mediate amino acid signaling to mTORC1. Science *320*, 1496-1501.

Sancak, Y., and Sabatini, D. (2009). Rag proteins regulate amino-acid-induced mTORC1 signalling. Biochem Soc Trans *37*, 289-290.

Sarbassov, D.D., Ali, S.M., Sengupta, S., Sheen, J.H., Hsu, P.P., Bagley, A.F., Markhard, A.L., and Sabatini, D.M. (2006). Prolonged rapamycin treatment inhibits mTORC2 assembly and Akt/PKB. Mol Cell *22*, 159-168.

Sekito, T., Kawamata, T., Ichikawa, R., Suzuki, K., and Ohsumi, Y. (2009). Atg17 recruits Atg9 to organize the pre-autophagosomal structure. Genes Cells *14*, 525-538.

Sents, W., Ivanova, E., Lambrecht, C., Haesen, D., and Janssens, V. (2013). The biogenesis of active protein phosphatase 2A holoenzymes: a tightly regulated process creating phosphatase specificity. FEBS J *280*, 644-661.

Shang, L., Chen, S., Du, F., Li, S., Zhao, L., and Wang, X. (2011). Nutrient starvation elicits an acute autophagic response mediated by Ulk1 dephosphorylation and its subsequent dissociation from AMPK. Proc Natl Acad Sci U S A *108*, 4788-4793.

Shi, Y. (2009). Serine/threonine phosphatases: mechanism through structure. Cell *139*, 468-484.

Slupe, A.M., Merrill, R.A., and Strack, S. (2011). Determinants for Substrate Specificity of Protein Phosphatase 2A. Enzyme Res *2011*, 398751.

Strieter, E.R., and Korasick, D.A. (2012). Unraveling the complexity of ubiquitin signaling. ACS Chem Biol *7*, 52-63.

Swingle, M., Ni, L., and Honkanen, R.E. (2007). Small-molecule inhibitors of ser/thr protein phosphatases: specificity, use and common forms of abuse. Methods Mol Biol *365*, 23-38.

Szegezdi, E., Logue, S.E., Gorman, A.M., and Samali, A. (2006). Mediators of endoplasmic reticulum stress-induced apoptosis. EMBO Rep *7*, 880-885.

Thoreen, C.C., Kang, S.A., Chang, J.W., Liu, Q., Zhang, J., Gao, Y., Reichling, L.J., Sim, T., Sabatini, D.M., and Gray, N.S. (2009). An ATP-competitive mammalian target of rapamycin inhibitor reveals rapamycin-resistant functions of mTORC1. J Biol Chem *284*, 8023-8032.

Thumm, M., Egner, R., Koch, B., Schlumpberger, M., Straub, M., Veenhuis, M., and Wolf, D.H. (1994). Isolation of autophagocytosis mutants of Saccharomyces cerevisiae. FEBS Lett *349*, 275-280.

Todde, V., Veenhuis, M., and van der Klei, I.J. (2009). Autophagy: principles and significance in health and disease. Biochim Biophys Acta *1792*, 3-13.

Tsukada, M., and Ohsumi, Y. (1993). Isolation and characterization of autophagy-defective mutants of Saccharomyces cerevisiae. FEBS Lett *333*, 169-174.

Virshup, D.M., and Shenolikar, S. (2009). From promiscuity to precision: protein phosphatases get a makeover. Mol Cell *33*, 537-545.

Wang, C.W., Stromhaug, P.E., Shima, J., and Klionsky, D.J. (2002). The Ccz1-Mon1 protein complex is required for the late step of multiple vacuole delivery pathways. J Biol Chem *277*, 47917-47927.

Wang, R.C., Wei, Y., An, Z., Zou, Z., Xiao, G., Bhagat, G., White, M., Reichelt, J., and Levine, B. (2012). Akt-mediated regulation of autophagy and tumorigenesis through Beclin 1 phosphorylation. Science *338*, 956-959.

Wang, S., Tsun, Z.Y., Wolfson, R.L., Shen, K., Wyant, G.A., Plovanich, M.E., Yuan, E.D., Jones, T.D., Chantranupong, L., Comb, W.*, et al.* (2015). Metabolism. Lysosomal amino acid transporter SLC38A9 signals arginine sufficiency to mTORC1. Science *347*, 188-194.

Wei, H., Wei, S., Gan, B., Peng, X., Zou, W., and Guan, J.L. (2011). Suppression of autophagy by FIP200 deletion inhibits mammary tumorigenesis. Genes Dev *25*, 1510-1527.

Wei, Y., Zou, Z., Becker, N., Anderson, M., Sumpter, R., Xiao, G., Kinch, L., Koduru, P., Christudass, C.S., Veltri, R.W.*, et al.* (2013). EGFR-mediated Beclin 1 phosphorylation in autophagy suppression, tumor progression, and tumor chemoresistance. Cell *154*, 1269-1284.

Wilkinson, D.S., Jariwala, J.S., Anderson, E., Mitra, K., Meisenhelder, J., Chang, J.T., Ideker, T., Hunter, T., Nizet, V., Dillin, A.*, et al.* (2015). Phosphorylation of LC3 by the Hippo kinases STK3/STK4 is essential for autophagy. Mol Cell *57*, 55-68.

Wiseman, R.L., Zhang, Y., Lee, K.P., Harding, H.P., Haynes, C.M., Price, J., Sicheri, F., and Ron, D. (2010). Flavonol activation defines an unanticipated ligand-binding site in the kinase-RNase domain of IRE1. Mol Cell *38*, 291-304.

Wollert, T., Yang, D., Ren, X., Lee, H.H., Im, Y.J., and Hurley, J.H. (2009). The ESCRT machinery at a glance. J Cell Sci *122*, 2163-2166.

Wong, A.S., Cheung, Z.H., and Ip, N.Y. (2011). Molecular machinery of macroautophagy and its deregulation in diseases. Biochim Biophys Acta *1812*, 1490-1497.

Wong, P.M., Puente, C., Ganley, I.G., and Jiang, X. (2013). The ULK1 complex: sensing nutrient signals for autophagy activation. Autophagy *9*, 124-137.

Wu, W., Tian, W., Hu, Z., Chen, G., Huang, L., Li, W., Zhang, X., Xue, P., Zhou, C., Liu, L.*, et al.* (2014). ULK1 translocates to mitochondria and phosphorylates FUNDC1 to regulate mitophagy. EMBO Rep *15*, 566-575.

Xing, Y., Xu, Y., Chen, Y., Jeffrey, P.D., Chao, Y., Lin, Z., Li, Z., Strack, S., Stock, J.B., and Shi, Y. (2006). Structure of protein phosphatase 2A core enzyme bound to tumor-inducing toxins. Cell *127*, 341-353.

Xu, Y., Chen, Y., Zhang, P., Jeffrey, P.D., and Shi, Y. (2008). Structure of a protein phosphatase 2A holoenzyme: insights into B55-mediated Tau dephosphorylation. Mol Cell *31*, 873-885.

Xu, Y., Xing, Y., Chen, Y., Chao, Y., Lin, Z., Fan, E., Yu, J.W., Strack, S., Jeffrey, P.D., and Shi, Y. (2006). Structure of the protein phosphatase 2A holoenzyme. Cell *127*, 1239-1251.

Yan, J., Kuroyanagi, H., Tomemori, T., Okazaki, N., Asato, K., Matsuda, Y., Suzuki, Y., Ohshima, Y., Mitani, S., Masuho, Y.*, et al.* (1999). Mouse ULK2, a novel member

of the UNC-51-like protein kinases: unique features of functional domains. Oncogene *18*, 5850-5859.

Yan, L., Guo, S., Brault, M., Harmon, J., Robertson, R.P., Hamid, R., Stein, R., and Yang, E. (2012). The B55α-containing PP2A holoenzyme dephosphorylates FOXO1 in islet β-cells under oxidative stress. Biochem J *444*, 239-247.

Yang, S., Wang, X., Contino, G., Liesa, M., Sahin, E., Ying, H., Bause, A., Li, Y., Stommel, J.M., Dell'antonio, G.*, et al.* (2011). Pancreatic cancers require autophagy for tumor growth. Genes Dev *25*, 717-729.

Yang, Z., and Klionsky, D.J. (2010a). Eaten alive: a history of macroautophagy. Nat Cell Biol *12*, 814-822.

Yang, Z., and Klionsky, D.J. (2010b). Mammalian autophagy: core molecular machinery and signaling regulation. Curr Opin Cell Biol *22*, 124-131.

Yi, C., Ma, M., Ran, L., Zheng, J., Tong, J., Zhu, J., Ma, C., Sun, Y., Zhang, S., Feng, W.*, et al.* (2012). Function and molecular mechanism of acetylation in autophagy regulation. Science *336*, 474-477.

Young, A., Chan, E., Hu, X., Köchl, R., Crawshaw, S., High, S., Hailey, D., Lippincott-Schwartz, J., and Tooze, S. (2006). Starvation and ULK1-dependent cycling of mammalian Atg9 between the TGN and endosomes. J Cell Sci *119*, 3888-3900.

Young, A.R., Narita, M., Ferreira, M., Kirschner, K., Sadaie, M., Darot, J.F., Tavaré, S., Arakawa, S., Shimizu, S., and Watt, F.M. (2009). Autophagy mediates the mitotic senescence transition. Genes Dev *23*, 798-803.

Yu, L., McPhee, C.K., Zheng, L., Mardones, G.A., Rong, Y., Peng, J., Mi, N., Zhao, Y., Liu, Z., Wan, F.*, et al.* (2010). Termination of autophagy and reformation of lysosomes regulated by mTOR. Nature *465*, 942-946.

Zalckvar, E., Berissi, H., Mizrachy, L., Idelchuk, Y., Koren, I., Eisenstein, M., Sabanay, H., Pinkas-Kramarski, R., and Kimchi, A. (2009). DAP-kinase-mediated phosphorylation on the BH3 domain of beclin 1 promotes dissociation of beclin 1 from Bcl-XL and induction of autophagy. EMBO Rep *10*, 285-292.

Zhou, X., Babu, J.R., da Silva, S., Shu, Q., Graef, I.A., Oliver, T., Tomoda, T., Tani, T., Wooten, M.W., and Wang, F. (2007). Unc-51-like kinase 1/2-mediated endocytic

processes regulate filopodia extension and branching of sensory axons. Proc Natl Acad Sci U S A *104*, 5842-5847.